

DISSERTATION

*Submitted in partial fulfillment of the requirements
for the degree of*


**DOCTOR OF PHILOSOPHY
INDUSTRIAL ADMINISTRATION
(FINANCIAL ECONOMICS)**

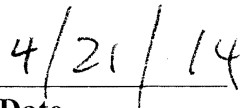
Titled
**"ESSAYS ON ASSET PRICING AND PORTFOLIO CHOICE
WITH TIME-VARYING UNCERTAINTY"**

Presented by

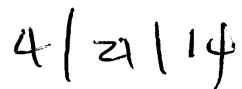
David Schreindorfer

Accepted by


Co-Chair: Prof. Lars-Alexander Kuehn

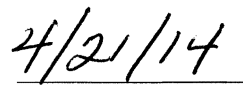

Date


Co-Chair: Prof. Bryan Routledge


Date

Approved by The Dean


Dean Robert M. Dammon


Date

DOCTORAL DISSERTATION

Essays on Asset Pricing and Portfolio Choice with Time-Varying Uncertainty

by

David SCHREINDORFER

*Submitted to the Tepper School of Business
in partial fulfilment of the requirements for the degree of*

Doctor of Philosophy

at

CARNEGIE MELLON UNIVERSITY

April 2014

Dissertation Committee:

Assistant Professor Lars-Alexander Kuehn

Associate Professor Bryan Routledge

Professor Duane Seppi

Assistant Professor Ariel Zetlin-Jones

Abstract

In the first essay, I present a parsimonious consumption-based asset pricing model that explains the pricing of equity index options. The model has two key ingredients, a recursive utility function that overweights left-tail outcomes and a process for endowment volatility that allows for shocks with different persistence levels. The utility function produces a high price for tail risks and allows the model to replicate the implied volatility smirk in times of high uncertainty, during which extreme events are more likely. In times of low uncertainty the smirk arises due to mean reversion in volatility, which results in substantial volatility feedback and a conditional return distribution that is strongly left-skewed. The presence of multiple shock frequencies gives the variance premium the ability to predict returns over short horizons and the price-dividend ratio the ability to predict returns over long horizons, as in the data. Consistent with recent empirical evidence, the equity and variance premiums in the model arise predominantly from a high price of tail risk.

The second essay (joint with Jan Schneemeier, University of Chicago) investigates the role of time-varying stock return volatility in a consumption and portfolio choice problem for a life-cycle investor facing short-selling and borrowing constraints. Faced with a benchmark investment strategy that conditions on age and wealth only, we find that an investor is willing to pay a fee of up to 1% - 1.5% of total life time consumption in order to optimally condition on volatility. Tilts in the optimal asset allocation in response to volatility shocks are considerably more pronounced than tilts in response to wealth shocks, and almost as important as life-cycle effects. Lastly, we find that the correlation between volatility and permanent labor income shocks may explain the low equity share of young households in the data.

The third essay analyzes whether cross-sectional differences in the variance premium and the implied volatility smirk are related to the underlying firms' exposure to market variance risk and common idiosyncratic variance (CIV) risk. Using both cross-sectional regressions and sorts based on firms' loadings, I find that firms whose variance co-moves more with market variance have steeper smirks and *larger* (less negative) variance premia. The latter finding is surprising in light of the fact that the variance premium of the market is believed to be negative. I show that the result persists in different sub-samples and that it is robust to various ways of estimating variance loadings. Exposure to CIV is not related to firm level option prices in a robust way.

Acknowledgements

I am grateful to my advisors, Lars Kuehn, Bryan Routledge, and Duane Seppi for their invaluable guidance, encouragement, and generosity of time. I am also indebted to Burton Hollifield, Emilio Osambela, Alex Schiller, and Fallaw Sowell for many helpful discussions that have significantly improved this work. For years of fun and help in many different ways, I thank my friends and fellow PhD students Steven Baker, Majid Bazarbash, Kevin Chung, Carlos Ramirez, Max Roy, Batchimeg Sambalaibat and Alex Schiller. I thank Lawrence Rapp for very professional help and much patience with many administrative issues, and Ariel Zetlin-Jones for serving on my committee.

Finally, I am indebted to my family, Courtney and Julian, for their love, support and patience and to my parents for their generosity and encouragement.

Contents

Abstract	i
Acknowledgements	ii
Contents	iii
List of Figures	v
List of Tables	vi
1 Tails, Fears, and Equilibrium Option Prices	1
1.1 Introduction	1
1.1.1 Related Literature	5
1.2 Stylized Facts of Equity Index Options	6
1.2.1 Data Sources	6
1.2.2 Variance Swap Rates	6
1.2.3 The Variance Premium	9
1.2.4 The Implied Volatility Smirk	10
1.3 Model	11
1.3.1 The Economy	11
1.3.2 Solution	14
1.3.3 Small Sample Statistics	17
1.4 Results	18
1.4.1 Calibration	18
1.4.2 Cash Flows	19
1.4.3 Basic Asset Prices	21
1.4.4 Variance Premium	22
1.4.5 Option Prices	23
1.4.6 The Term Structure of Variance Swap Rates	27
1.4.7 Return Predictability	29
1.5 Additional Results	33
1.5.1 The degree of tail sensitivity and option prices	33
1.5.2 The degree and nature of risk aversion of a GDA agent	36
1.6 Conclusion	38

2	Optimal Volatility Timing: A Life-Cycle Perspective	40
2.1	Introduction	40
2.1.1	Connections with Prior Literature	42
2.2	Model	43
2.3	Estimation	46
2.4	Results	50
2.4.1	Optimal Life-Cycle Portfolio Choice with Stochastic Volatility	50
2.4.2	The Economic Value of Volatility Timing	54
2.4.3	Household Heterogeneity and the Equity Share of Young Households	55
2.5	Discussion	58
2.5.1	The Degree of Return Predictability	58
2.6	Conclusion	59
3	Undiversifiable Variance Risk and Individual Equity Options	61
3.1	Introduction	61
3.1.1	Related Literature	62
3.2	Framework	63
3.3	Data	64
3.3.1	Option Data and Characteristics	64
3.3.2	Estimating Exposure to Sources of Systematic Variance Risk	68
3.4	Results	70
3.4.1	Fama-MacBeth Regressions	70
3.4.2	Sorts	72
3.4.3	Robustness: Alternative Loading Estimates	74
3.4.4	Comparison with Carr and Wu [2009]	76
3.5	Conclusion	77
A	Data	79
B	Model solution details	82
C	Proof of Lemma 1	91
	Bibliography	95

List of Figures

1.1	Equity Index Option Markets, 1990-2012	7
1.2	The volatility and persistence of variance swap rates	8
1.3	The Implied Volatility Smirk, 1990-2012	11
1.4	Returns and Disappointments	22
1.5	Implied Volatility Smirk	23
1.6	Conditional 1-Month Implied Volatility Smirk	24
1.7	Moments of variance swap rates	28
1.8	Shock Frequencies and Expected Returns	32
1.9	Tail Sensitivity of Preferences and Option Prices	35
1.10	Welfare measures	37
2.1	The Equity Share over the Life-Cycle	50
2.2	Tilts in the Optimal Equity Share	51
2.3	Impulse Response Functions	52
2.4	The Effect of Different Parameter Values on the Equity Share	56
2.5	The Effect of Changing χ^ξ	57
2.6	Return Predictability and Volatility Timing	58
3.1	Implied Volatility as a Function of Delta, Intel Corp.	65
3.2	Systematic Variance Factors, 1996-2012	68

List of Tables

1.1	The Variance Premium and Expected Returns	10
1.2	Calibrations	19
1.3	Quantities and Prices	20
1.4	Conditional Moments and Tail Probabilities	26
1.5	Return Predictability	30
2.1	Maximum Likelihood Estimates of the DGP	48
2.2	Volatility Shocks and the Optimal Equity Share	53
2.3	The Economic Value of Volatility Timing	54
3.1	Option Characteristics	66
3.2	Fama-MacBeth Regressions	71
3.3	Option characteristics of firms sorted by variance loadings	73
3.4	Characteristics of firms sorted by β^M	74
3.5	Option Characteristics of Firms Sorted by β^M: Alternative Loading Estimates	75

To my parents.

Chapter 1

Tails, Fears, and Equilibrium Option Prices

1.1 Introduction

Prices of equity index options provide significant information about the composition of risk premia in financial markets. A key observations is that deep out-of-the-money (OTM) index put options appear overpriced from the perspective of standard models. This suggests that investors are more concerned with large declines in the aggregate stock market than typically assumed. Indeed, recent nonparametric estimates in [Bollerslev and Todorov \[2011\]](#) show that about two thirds of the average equity premium represent compensation for extreme left tail events, defined as returns of -10% or less over the horizon of a few weeks. This finding is puzzling because such returns occur very infrequently in the data.

I show that investors' fear of extreme events can account for average option prices in a consumption-based asset pricing model with fundamentals that are conditionally Gaussian. The representative agent has Epstein-Zin ([1989](#)) utility with generalized disappointment aversion (GDA) risk preferences ([Routledge and Zin 2010](#)). Relative to the more commonly-used recursive utility function with expected utility (EU) risk aggregation, GDA can overweight lower-tail outcomes in the distribution over future aggregate wealth and produce a high price of tail risk. Cash flows (consumption and dividend growth) have constant means and time-varying volatility. Volatility follows the multifractal process of [Calvet and Fisher \[2001, 2004\]](#), which allows for shocks with different persistence levels and generates substantial volatility feedback in equilibrium, i.e. large endogenous return

jumps.¹ The combination of tail risk resulting from volatility feedback and the aversion to such risks implied by GDA preferences allows the model to replicate the steep implied volatility smirk implied by option prices.

The model successfully reproduces a number of additional stylized facts of asset markets and the equity index option market in particular, including (1) the high average equity premium, (2) the low risk-free rate, (3) the large excess volatility of returns relative to fundamentals, (4) the predictive ability of the price-dividend ratio for excess returns over long horizons, (5) the high excess kurtosis of monthly returns and the low excess kurtosis of annual returns (6) the high average variance premium² and its ability to predict excess returns over short horizons and (7) the time-series moments of option prices, which are reflected in the term structure of variance swap rates. At the same time, the model remains tightly parameterized.

In the model, the probability of disappointments increases in times of high macroeconomic uncertainty, during which extreme events are more likely. When disappointments occur, they tend to be accompanied by large negative returns that trigger payoffs to out-of-the-money put options. Puts thus provide a hedge against disappointments and the investor is willing to pay a large insurance premium for them in states of *high* uncertainty. In times of *low* uncertainty, disappointments are rare and insurance premia only account for a small part of put option prices. In these states the IV smirk instead arises from mean reversion in the conditional volatility of cash flows. Specifically, when volatility is low and therefore expected to increase, the price-dividend ratio is expected to *decrease* because volatility carries a negative price of risk in the model. As reductions in the price-dividend ratio translate into negative returns, the conditional return distribution is left-skewed when volatility is low.³ In these states, the model produces a steep implied volatility curve due to the relatively high likelihood of negative return jumps rather than due to high insurance premia.

¹Calvet and Fisher [2007] have previously shown that a model with recursive utility with EU risk preferences generates substantial volatility feedback. Different from the present paper, these authors focus on a model where multifractal volatility affects dividends but not consumption. In this case, volatility risks are not priced because they do not affect the pricing kernel.

²The variance premium equals the difference between the risk-neutral and statistical expectations of future market variance. Details are discussed in Section 3.3.

³For similar reasons, the conditional return distribution (under the statistical measure) is right-skewed when volatility is high. All else equal, this makes the IV curve flat or even upward sloping. However, I show that the effect of GDA preferences is strong enough to induce strong left-skewness in the *risk neutral* distribution when volatility is high.

I show that the magnitude of the conditional return skewness depends crucially on the nature of endowment volatility. When volatility is modeled as a persistent AR(1) process, mean reversion occurs too slowly to have a strong impact on the conditional skewness of short horizon returns. Instead, it affects the conditional skewness at longer horizons. A model with AR(1) volatility (and GDA preferences) therefore produces an IV curve that is steep at long maturities but too flat at short maturities. In contrast, multifractal volatility allows for mean reversion at different time scales. In particular, the shocks with low persistence levels mean revert quick enough to produce substantial return skewness at short horizons, and they allow the model to match the steep IV curve at both short and long maturities.

To summarize the *dynamics* of option prices I turn to variance swaps, i.e. forward contracts on realized stock market variance (see Section 3.3 for more details). These instruments can be replicated from portfolios of equity index options and they display some revealing patterns about the shocks that drive option prices. Specifically, swaps with a monthly maturity are considerably more volatile and less persistent than swaps with an annual maturity. Additionally, the autocorrelation functions of swap rates display pronounced long-memory behavior – a well-known feature of return volatility (Ding, Granger, and Engle 1993). The model is able to capture these complex time series features despite relying on a very parsimonious endowment specification. In particular, the multifractal volatility process depends on only four parameters, regardless of the number of volatility components. I show that these parameters can be calibrated such that the model provides almost an exact match for the term structure of variance swap rates. In contrast, the dynamics of option prices are counterfactual when cash flow volatility is modeled as a AR(1) process. The present model is the first, to my knowledge, to replicate the term structure of variance swap rates in an equilibrium setting.

Return predictability arises in the model from the interaction between time-varying risk (stochastic endowment volatility) and time-varying risk aversion. As previously emphasized by Routledge and Zin [2010], GDA preferences are capable of producing time-variation in effective risk aversion when combined with a persistent state variable. In the present economy, endowment volatility (the state variable) equals the product of several volatility components with different persistence levels. All else equal, when a component with a given frequency is currently in its high state, the conditional endowment volatility is higher and there is a greater chance of disappointing tail events. The overweighting of tail events in the GDA utility function raises the agent’s effective risk aversion when these outcomes are more likely to occur, which results in higher expected returns. However,

volatility components with different frequencies have a different effect on expected returns. Specifically, less persistent shocks alter expected returns over short horizons whereas more persistent shocks alter expected returns over long horizons. As time-variation in the price-dividend ratio is mainly driven by persistent shocks, it is a good predictor of long horizon returns. On the other hand, the (1-month) variance premium has considerably more exposure to transient shocks, making it a better predictor of short horizon returns. These implications for the term structure of risk premia agree with the empirical results of [Martin \[2013\]](#), who derives a lower bound on the equity premium from option prices and concludes that the equity premium has both a business cycle component and a higher-frequency component.

To assess the level of effective risk aversion implied by different risk preference calibrations, I conduct a welfare analysis in the spirit of [Lucas \[1987\]](#). Specifically, I hold the parameters controlling time preference and the endowment calibration constant, and consider various risk preference calibrations that all match the historical equity premium. The set of alternatives includes the (pure) disappointment aversion (DA) model of [Gul \[1991\]](#) as well as the EU model, i.e. the Epstein-Zin specification used by [Bansal and Yaron \[2004\]](#). For each economy, I then compute the welfare costs of heteroscedasticity risk as well as the welfare costs of total endowment risk. The results show that the GDA agent is less risk averse overall, but that he is considerably more averse to stochastic volatility than both EU and DA agents. The reason is that for a constant endowment variance, the extreme tail outcomes constituting a disappointment for the GDA agent are very rare and risk premia are close to zero. In line with the empirical findings of [Bollerslev and Todorov \[2011\]](#) discussed above, risk premia in the model therefore primarily arise from the aversion to extreme tail risks.

The rest of the paper is structured as follows. Section [2.1.1](#) points to connections with the existing literature. In Section [3.3](#), I discuss the option dataset, define option-related statistics, and present the set of stylized option market facts that serves as the empirical target. The model and the associated solution technique are shown in Section [2.2](#), whereas Section [3.4](#) shows calibration results and discusses the model mechanism. Section [1.5](#) illustrates how option pricing implications and effective risk aversion change for nested preference specifications, thereby shedding additional light on the mechanism. The appendix contains details on both the data and the model solution technique.

1.1.1 Related Literature

Rare disasters and option prices. An alternative mechanism for increasing the importance of tail risks is the rare disaster framework of [Rietz \[1988\]](#) and [Barro \[2006\]](#). While the assumption of a Peso problem greatly improves the asset pricing implications of simple representative agent models, [Backus, Chernov, and Martin \[2011\]](#) point out that the implied volatility smirk in these models is far steeper and lower than in the data. These authors argue that, contrary to the large and rare disasters assumed in Barro’s calibration, equity index options imply relatively small and frequent consumption disasters. A recent paper by [Seo and Wachter \[2013\]](#) shows that a model with *stochastic* disaster intensity and recursive preferences can reconcile this conflicting evidence and generate a more realistic smirk. [Du \[2011\]](#) shows that a combination of rare disasters and external habit formation in preferences also produces a smirk, but his results only focus on options on the consumption claim. In order to generate realistic prices of OTM puts, the above papers rely on the strong assumption that there is no default on option payoffs in the case of a macroeconomic disaster. In contrast, the current model increases the importance of tail risk by increasing its price rather than its quantity, i.e. it does not assume a Peso problem. As a consequence, the most severe drops in consumption are far less extreme and the no-default assumption is less restrictive.

Long run risks and option prices. A number of prior papers also build on [Bansal and Yaron \[2004\]](#) to study the implied volatility smirk or the variance premium. These studies extend the cash flow dynamics of the basic long run risks model by allowing for stochastic volatility-of-volatility ([Bollerslev, Tauchen, and Zhou \[2009\]](#)) or jumps in the conditional moments of consumption and dividend growth ([Benzoni, Collin-Dufresne, and Goldstein \[2011\]](#), [Drechsler and Yaron \[2011\]](#), [Drechsler \[2013\]](#)). Incorporating jumps into the state variable processes increases the quantity of tail risk because they map into endogenous jumps in returns. For example, a negative jump in the expected growth rate of dividends induces a discrete reduction in the price-dividend ratio and therefore a negative jump in returns. Additional extensions add time-varying risk aversion by incorporating jumps in investor confidence ([Shaliastovich \[2009\]](#)) or the degree of uncertainty aversion ([Drechsler \[2013\]](#)). In this line of work, jumps in returns result from jumps in risk aversion. The present model models endowment volatility as a Markov chain and therefore also allows for discrete changes in volatility that map into endogenous return jumps. Different from the long run risks model, I do not rely on persistent variation in the mean of consumption growth to generate high average risk premia, and I generate countercyclical effective risk aversion by specifying GDA preferences.

Nature and pricing of consumption volatility shocks. Nakamura, Sergeyev, and Steinsson [2012] estimate a long run risks model based on the international consumption data of Barro and Ursua [2008] (without using any asset market data) and find strong evidence in favor of priced consumption volatility shocks. Boguth and Kuehn [2013] find similar evidence based on the cross-section of U.S. consumption data alone and they do not assume a particular asset pricing model. Tamoni [2011] provides empirical evidence for the presence of consumption volatility shocks with highly heterogeneous persistence levels, and he shows that models with a single shock frequency have counterfactual implications for the long-run relationship between consumption growth volatility and expected returns in the data. In agreement with this empirical evidence, time-variation in risk premia in the present model is driven by consumption volatility shocks with different persistence levels.

1.2 Stylized Facts of Equity Index Options

This section discusses the option dataset and presents the set of stylized option market facts that serves as a target for the model. Specifically, I focus on moments of equity index options and variance swap rates with different maturities, as well as the variance premium and its predictive power for excess returns.

1.2.1 Data Sources

The option dataset, which spans the period from January 2, 1990 to December 31, 2012, was obtained from Market Data Express, a subsidiary of the Chicago Board Options Exchange (CBOE). It contains end-of-day information for all option contracts traded on the CBOE for which the S&P 500 index is the underlying asset. Variables include trading volume, open interest, and the daily open, high, low, and last sales prices. The exercise style of the options is European. On average, the dataset contains observations on 852 different option contracts per day, which amounts to approximately 5m total observations.⁴ I apply standard filters to the data (see Appendix A for details). For estimating the realized variance of market returns, I use tick-by-tick transaction prices of S&P500 futures for the same sample period, which were obtained from TICKDATA.

1.2.2 Variance Swap Rates

A variance swap is a forward contract on the underlying's future variance. At maturity, the seller (floating leg) pays the asset's realized variance, defined as the sum of squared

⁴The average number of daily observations increased from 270 in 1990 to 2600 in 2012.

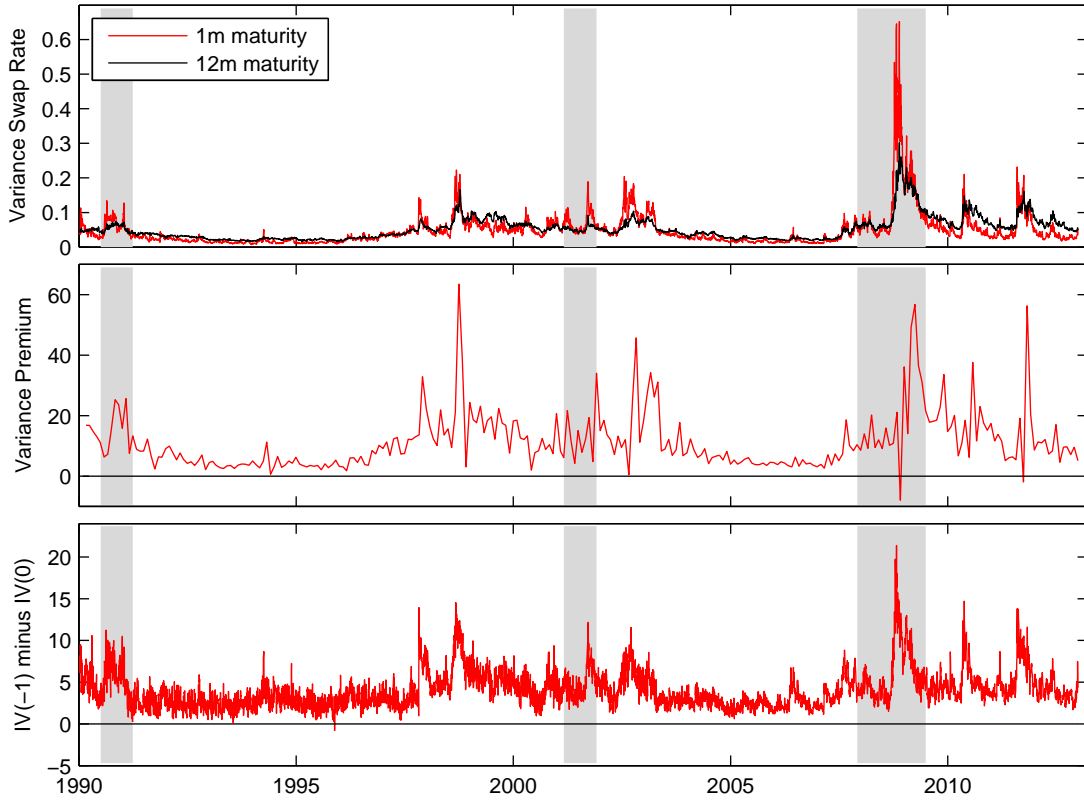


Figure 1.1: Equity Index Option Markets, 1990-2012

Figure 1.1 shows time series of option-related statistics. The top panel shows variance swap rates of maturities 1 and 12 months, expressed in annualized variance units. The middle panel shows the 1-month variance premium, expressed in monthly variance units. The lower panel shows the slope of the implied volatility (IV) curve, defined as the difference between the IV for a standardized moneyness of -1 and the IV for an at-the-money option. IVs are expressed in annualized standard deviation units. The time series for swaps and IVs are daily, whereas the time series for the variance premium is monthly. Shaded regions represent NBER recessions.

daily log returns over the term of the contract, i.e.

$$RV_{t:t+\tau} = \sum_{i=1}^{\tau} r_{t+i}^2, \quad (1.1)$$

where τ denotes the number of trading days. The buyer (fixed leg) pays the variance swap rate $\mathcal{S}_t(\tau)$, which is agreed upon at contract initiation.⁵ The variance swap rate can therefore be interpreted as the (forward) price of the underlying's realized variance. In the absence of arbitrage opportunities, the swap rate equals the risk neutral conditional expectation of future variance, i.e.

$$\mathcal{S}_t(\tau) = E_t^{\mathbb{Q}}[RV_{t:t+\tau}]. \quad (1.2)$$

⁵In reality, payments are netted. Also, the difference between RV and \mathcal{S} is typically multiplied by a factor that converts variances to annual units, as well as a notional. These details are irrelevant for the purposes of this paper.

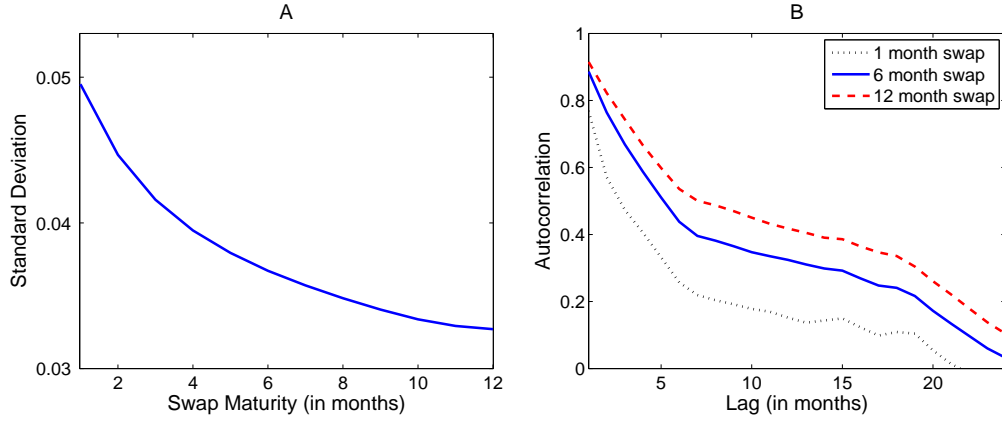


Figure 1.2: The volatility and persistence of variance swap rates

Figure 1.2 shows moments of variance swap rates, expressed in annualized variance units. The sample is daily and spans 1990-2012. Swap rates are expressed in annualized variance units. To compute the autocorrelation function, I create multiple overlapping monthly samples, compute the autocorrelation function for each sample, and then average across estimates.

The swap payoff can be replicated with a static portfolio of European options and a dynamic, self-financing position in the underlying and a bond. It follows that the price of the option portfolio equals the variance swap rate. The proof is an extension of the classic [Breedon and Litzenberger \[1978\]](#) result, which asserts that the second derivative of the call price with respect to the strike price X equals the risk neutral density evaluated at X and multiplied by the price of a risk-free bond⁶ (see [Britten-Jones and Neuberger \[2000\]](#), [Jiang and Tian \[2005\]](#) and [Carr and Wu \[2009\]](#)). Using this replication result, which also underlies the CBOE's volatility index VIX, I compute synthetic variance swap rates for various maturities (τ 's in the notation above). Specifically, for each day of the sample, I compute swap rates for all available option maturities and linearly interpolate them to constant maturities from 1 to 12 months. Further details of the implementation are discussed in Appendix A.

The top panel of Figure 1.1 shows the daily time series of variance swap rates of maturities of one and twelve months. Both series are very countercyclical and peak in the Fall of 2008 after the collapse of Lehman Brothers. Further, the one-month swap rate is both more volatile and less persistent than the 12-months swap rate. This feature is illustrated further in Figure 1.2. Panel A shows standard deviation of variance swap rates for maturities of 1, 2, ..., 12 months. The standard deviation falls monotonically in the swap horizon. The high volatility of short maturity swaps indicates the presence of some high-frequency shocks that partially average out at the longer horizons. Panel B shows the autocorrelation function for maturities 1, 6, and 12 months, and for monthly lags up

⁶ $\frac{\partial^2 C(k)}{\partial k^2} \big|_{k=X} = e^{-rT} f^Q(X)$, where $C(k)$ denotes the price of a call with strike k , r denotes the risk-free rate, and T denotes the maturity of the option.

to two years. The autocorrelation of all lags increases monotonically in the swap horizon.⁷ Further, the autocorrelation of all swap maturities declines very slowly with the lag length, which reflects the well-known long-memory property of return variances (Ding, Granger, and Engle [1993]). The slow decay indicates the presence of some low-frequency shocks with very long-lasting effects. The model presented in this paper captures the dynamics of variance swaps with a process for endowment variance that features shocks at different time-scales.

1.2.3 The Variance Premium

Using the Euler equation, the τ -period variance swap rate can be decomposed into the statistical expectation of realized variance and the variance premium⁸, i.e.

$$\mathcal{S}_t(\tau) = E_t[RV_{t:t+\tau}] + \underbrace{\frac{\text{Cov}_t[M_{t:t+\tau}, RV_{t:t+\tau}]}{E_t[M_{t:t+\tau}]}}_{\text{variance premium}}, \quad (1.3)$$

where $M_{t:t+\tau}$ denotes a τ -period pricing kernel. Measuring the (conditional) variance premium empirically requires an estimate of both the variance swap rate and the conditional expectation of realized variance. For the latter, I first compute a time series of monthly realized variance estimates from tick-by-tick transaction data, and then I estimate a simple time series model based on the realized variance series (see, e.g. Andersen, Bollerslev, Diebold, and Ebens [2001] and Andersen, Bollerslev, Diebold, and Labys [2003]). The difference between the one-month variance swap rate and the one-step-ahead forecast from the time-series model serves as a proxy for the 1-month variance premium. Details are contained in Appendix A. For comparability with previous studies, I express the variance premium in *monthly* variance units.

The middle panel of Figure 1.1 shows the monthly time series of the variance premium, which is positive in all but 2 out of 275 months in the sample. The mean variance premium equals 11.29, which amounts to almost 40% of the average realized variance. The large magnitude of the premium suggests that variance swaps provide a hedge for macroeconomic

⁷Using option data for 12 major international equity indices, Foresi and Wu [2005] document that short term option prices (expressed as IVs) are both more volatile and less persistent than long term option prices. These patterns are therefore a robust empirical feature of equity index options in that they hold for both (synthetic) variance swap rates and simple implied volatilities.

⁸Note that, while the equity premium equals the difference between the physical and risk neutral expectations of future returns, i.e. $E_t[R_{t+1}] - R_t^f = E_t[R_{t+1}] - E_t^Q[R_{t+1}]$, Equation 1.3 defines the variance premium as the difference between the risk neutral and the physical expectations of future realized variance, i.e. $\mathcal{S}_t(1) - E_t[RV_{t:t+1}] = E_t^Q[RV_{t:t+1}] - E_t[RV_{t:t+1}]$. I use this "reversed" definition because it makes the variance premium positive and because it corresponds to the convention in most of the previous literature.

Table 1.1: The Variance Premium and Expected Returns

Horizon (in m)	1	3	6
$\hat{\beta}$	0.89	0.88	0.65
t -statistic	2.10	4.10	3.29
R^2 (%)	2.53	6.49	6.52

Table 1.1 presents return predictability regressions. Excess returns of horizons 1, 3, and 6 months are regressed on the one-month variance premium. Regressions with horizons > 1 month use overlapping data. T-statistics are Newey and West [1987] (HAC) adjusted using $2 * (h - 1)$ lags.

risks. In other words, the market variance correlates positively with investors' marginal utility (see Equation 1.3).

Table 1.1 show predictability regressions for excess returns, which I measure as the difference between the value-weighted CRSP return and the yield of a 30 day Treasury bill. The variance premium can account for 2.5% of the return variation at the monthly horizon, and for about 6.5% at horizons of 3 and 6 months. Compared to other known predictors, these magnitudes are quite large for the short time horizons. Thus, the equity premium and the variance premium appear to share common factors. The model in this paper captures this co-movement via time-variation in effective risk aversion, which results from the interaction of GDA risk preferences and a persistent process for endowment variance.

1.2.4 The Implied Volatility Smirk

Throughout the paper, I express option prices in terms of Black-Scholes implied volatilities (IVs) and I graph them against standardized moneyness. I measure standardized moneyness as

$$\text{standardized moneyness} = \frac{\ln(X/S_t)}{\sqrt{\mathcal{S}_t(\tau)/\tau}},$$

where X denotes the option's strike price and S_t the underlying's price. The division by $\sqrt{\mathcal{S}_t(\tau)/\tau}$ converts moneyness ($\ln(X/S_t)$) to standard deviation units. This standardization allows for an easy comparison of the IV curve across option maturities.⁹ A standardized moneyness of -1 is equivalent to a one standard deviation drop in the stock price. I interpolate observed IVs to a fixed grid of standardized moneyness from -2 to 1 and maturities from 1 to 12 months. The bounds of the grids are chosen such that it is covered by liquid options on most days in the sample. As before, details are discussed in Appendix

⁹Many papers graph IVs against simple moneyness ($\ln(X/S_t)$). This is helpful for comparing the IV curve across different points in time. On the other hand, it makes it more challenging to compare it across option maturities. For example, if one considers a moneyness range of $[-10\%, +10\%]$, the endpoints of this range correspond to fairly extreme price moves at the monthly horizon, but to much more common moves at the annual horizon. I follow Carr and Wu [2003] and Foresi and Wu [2005] in using a standardized moneyness measure.

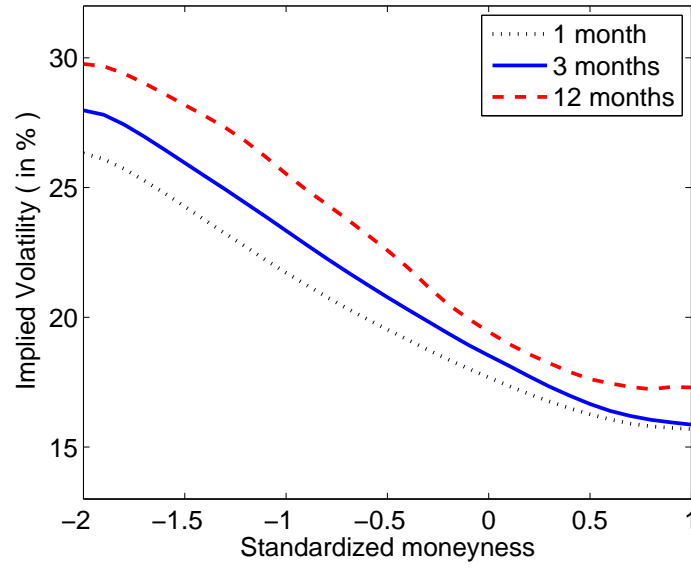


Figure 1.3: The Implied Volatility Smirk, 1990-2012

Figure 1.3 shows average (Black-Scholes) implied volatilities as a function of the options' relative moneyness. The sample is daily and spans 1990-2012.

A.

Figure 1.3 shows the IV curve for option maturities of 1, 6, and 12 months. According to the Black-Scholes model, IVs across all strikes and maturities should be equal to the volatility of the underlying asset. In the data, IVs are considerably higher for low strikes (for low values of standardized moneyness). Additionally, the figure shows that both the level and the slope of the IV smirk are increasing in maturity. This fact is well-known – see e.g. [Foresi and Wu \[2005\]](#), who show that the same pattern holds for 12 major international equity markets. Deviations from log-normality (in the risk-neutral distribution) are therefore more severe at longer horizons. The model presented in this paper captures the smirk via the interaction of GDA risk preferences and a multifractal process for cash flow volatility, which results in a high price for tail risks and large conditional return skewness.

1.3 Model

1.3.1 The Economy

Preferences. Following [Epstein and Zin \[1989\]](#), the representative agent's time t utility, V_t , is given by the constant elasticity of substitution recursion

$$V_t = [(1 - \beta)C_t^\rho + \beta\mu_t^\rho]^\frac{1}{\rho}. \quad (1.4)$$

The parameters β and ρ capture time preferences, whereas the function $\mu_t \equiv \mu_t(V_{t+1})$ captures risk preferences. μ_t equals the certainty equivalent of random future utility using the time t conditional probability distribution. I omit the argument for notational convenience. The certainty equivalent features Generalized Disappointment Aversion (GDA) as in [Routledge and Zin \[2010\]](#) (hereafter RZ), and it is defined by the implicit function

$$u(\mu_t) = E_t \left[u(V_{t+1}) \right] - \theta E_t \left[\left(u(\delta \mu_t) - u(V_{t+1}) \right) \mathbf{1}\{V_{t+1} \leq \delta \mu_t\} \right], \quad (1.5)$$

where

$$u(x) = \begin{cases} \frac{x^\alpha}{\alpha} & \text{for } \alpha \leq 1, \alpha \neq 0 \\ \log(x) & \text{for } \alpha = 0 \end{cases}, \quad (1.6)$$

and where $\mathbf{1}\{\cdot\}$ denotes the indicator function. Equation 1.5 nests two well-known preference specifications as special cases. First, for $\theta = 0$ the second term drops out and risk preferences simplify to expected utility (hereafter EU). In this case, the certainty equivalent is given by the *explicit* function $\mu_t = (E_t[V_{t+1}^\alpha])^{\frac{1}{\alpha}}$ (or $\mu_t = e^{\log(V_{t+1})}$ for $\alpha = 0$) and the utility function equals the Epstein-Zin specification used in [Bansal and Yaron \[2004\]](#). Second, for $\delta = 1$ and $\theta \neq 0$ risk preferences simplify to Gul's (1991) model of disappointment aversion (hereafter DA).¹⁰ In this case, all outcomes that fall below the certainty equivalent are considered disappointing and receive a penalty. The magnitude of the penalty is governed by the parameter θ . GDA preferences, which represent the most general version of Equation 1.5 ($\theta \neq 0$ and $\delta \neq 0$), place the disappointment threshold further into the tail of the (conditional) distribution of V_{t+1} . In particular, only realizations of V_{t+1} that fall below a fraction δ of the certainty equivalent μ_t are considered disappointing. In Sections 3.4 and 1.5, I use the nested cases to highlight why GDA is needed for realistic option prices.

RZ show that the solution to the representative agent's portfolio optimization problem yields the pricing kernel

$$M_{t+1} = \beta \left(\frac{C_{t+1}}{C_t} \right)^{\rho-1} \left(\frac{V_{t+1}}{\mu_t} \right)^{\alpha-\rho} \left(\frac{1 + \theta \mathbf{1}\{V_{t+1} \leq \delta \mu_t\}}{1 + \delta^\alpha \theta \mathbf{1} E_t[\mathbf{1}\{V_{t+1} \leq \delta \mu_t\}]} \right). \quad (1.7)$$

Notice that for $\theta = 0$, the last term cancels and the pricing kernel simplifies to EU, i.e. the most common form of Epstein-Zin. Relative to that simpler case, the GDA pricing kernel overweighs left tail outcomes. These outcomes (for which $V_{t+1} \leq \delta \mu_t$) receive a weight that is $(1+\theta)$ times as large as the weight for other outcomes (for which $V_{t+1} > \delta \mu_t$).

¹⁰The asset pricing implications of recursive utility with DA risk preferences have been analyzed by [Epstein and Zin \[2001\]](#) in an endowment economy and by [Campanale, Castro, and Clementi \[2010\]](#) in a production economy.

Cash Flows. The log growth rates of consumption and dividends are given by

$$\begin{aligned}\Delta c_{t+1} &= \mu + \sigma_t \varepsilon_{t+1}^c \\ \Delta d_{t+1} &= \mu + \sigma_t \varphi \varepsilon_{t+1}^d\end{aligned}\tag{1.8}$$

where μ is the mean growth rate, ε^c and ε^d are standard normals with correlation ϱ , and φ is a scaling factor that allows dividends to be more volatile than consumption. Endowment variance follows the Markov Switching Multifractal (MSM) process of [Calvet and Fisher \[2001, 2004\]](#), which allows for a large number of states while remaining tightly parameterized. Specifically, σ_t^2 equals the product of several variance components (and a constant), given by

$$\sigma_t^2 = \bar{\sigma}^2 \prod_{k=1}^K \mathcal{M}_{k,t}.\tag{1.9}$$

For tractability, components are assumed to be mutually independent. Each of the K variance components $\mathcal{M}_{k,t}$ (\mathcal{M} for multiplier) follows a two state Markov chain with state space $\{1 - \nu, 1 + \nu\}$, which is identical for all components. The parameter $\nu \in (0, 1)$ determines the high and low state. Since each component has two states, the Markov chain for σ_t^2 has $N = 2^K$ states. However, due to the fact that all components share the same state space, σ_t^2 can only take on $K + 1$ different values.¹¹ In the benchmark calibration I set $K = 6$, so that there are 64 states and 7 possible variance values.

The heterogeneity between components lies in their persistence levels. The transition matrix for the k^{th} component is given by

$$P_k = \begin{bmatrix} 1 - \gamma_k/2 & \gamma_k/2 \\ \gamma_k/2 & 1 - \gamma_k/2 \end{bmatrix},\tag{1.10}$$

i.e. it is completely characterized by one parameter. To prevent the number of parameters from growing with the number of variance components (K), the parameters are modeled via the recursion

$$\gamma_k = 1 - (1 - \gamma_{k-1})^b,\tag{1.11}$$

where $\gamma_1 \in (0, 1)$ and $b \in (1, \infty)$. Variance components with a higher index have higher γ 's and are therefore less persistent. The three parameters (ν, γ_1, b) control the volatility and persistence levels of all components, regardless of how many components there are.¹²

Since the transition matrices are symmetric, each component is equally likely to be in

¹¹The possible values of σ_t^2 are given by $\bar{\sigma}^2(1 - \nu)^0(1 + \nu)^K, \bar{\sigma}^2(1 - \nu)^1(1 + \nu)^{K-1}, \dots, \bar{\sigma}^2(1 - \nu)^K(1 + \nu)^0$, i.e. between 0 and K components in the low state and the others in the high state

¹²All else equal, increasing ν makes the high and low states more heterogeneous, which increases the volatility of σ_t^2 . Increasing γ_1 makes each component less persistent (by increasing γ_k for all k), thereby making σ_t^2 less persistent. Increasing b leads to a faster growth rate between γ_k 's, i.e. the persistence level

the high and low state in the long run, so that $E[\mathcal{M}_{k,t}] = \frac{1}{2}(1 - \nu) + \frac{1}{2}(1 + \nu) = 1$ for all k . The assumed independence between components therefore implies that $E[\sigma_t^2] = \bar{\sigma}^2 \prod_{k=1}^K E[\mathcal{M}_{k,t}] = \bar{\sigma}^2$, so that the parameter $\bar{\sigma}^2$ controls the mean of the process.

Discussion. I briefly discuss the determinants of a disappointing outcome. Note that the disappointment event $V_{t+1} \leq \delta\mu_t$ can be written as

$$\Delta c_{t+1} + \log \left(\frac{\lambda_{t+1}^V}{\lambda_t^V} \right) \leq \log \left(\frac{\delta\mu_t}{V_t} \right), \quad (1.12)$$

where $\lambda_t^V = V_t/C_t$ equals the utility-consumption ratio. The state of the volatility process affects the two terms on the LHS in opposite ways. All else equal, when volatility component $\mathcal{M}_{k,t}$ is currently in its high state, the conditional consumption growth volatility σ_t is also higher. This *increases* the disappointment probability because it increases the likelihood of low Δc_{t+1} -values. On the other hand, $\mathcal{M}_{k,t}$ being in its high state also implies the possibility that it switches to its low state, which in turn results in a positive jump in $\log \left(\frac{\lambda_{t+1}^V}{\lambda_t^V} \right)$ (volatility carries a negative price of risk). This possibility *decreases* the disappointment probability. Clearly, which effect dominates is a quantitative question. I show in Section 1.4.5 that the former channel prevails in my calibration, so that the conditional disappointment probability is increasing in the level of endowment volatility. Lastly, fluctuations in σ_t may also induce time-variation in the relative disappointment threshold on the RHS. However, I find that this variation is quantitatively negligible for a wide range of preference parameters and endowment processes.¹³

1.3.2 Solution

The model solution is exact, i.e. it does not rely on any log-linear approximations. It is characterized by a set of $N \times 1$ vectors that contain the values of the endogenous objects for each of the model's N states. All asset prices in the model can be expressed as simple matrix products, and the associated matrices can be computed in closed-form. Because these derivations are algebraically involved, I defer them to Appendices B and C. In the remainder of this section, I define asset prices and show the form of the associated matrix products.

declines faster when moving to a higher k . This makes components more heterogeneous, and it also makes σ_t^2 less persistent.

¹³In the benchmark calibration of Section 3.4, the RHS is equal to -0.0369 up to four decimals in all states. Numerically, I find that the relative threshold is also close to being constant for different calibrations of the model in Routledge and Zin [2010] (who model consumption growth as a 2-state Markov chain), as well as a version of the present model for which endowment variance is described by an AR(1) in logs.

Notation. Denote the transition matrix of the Markov chain for σ_t by P and the cumulative distribution function of a standard normal by $\Phi(\cdot)$. Let \odot denote the Hadamard (element-wise) matrix product and let ι_N and $\mathbf{1}_N$ denote a $N \times 1$ vector of ones and a $N \times N$ matrix of ones respectively.

Pricing Kernel. Denote the utility-consumption and certainty equivalent-consumption ratios by $\lambda_t^V \equiv V_t/C_t$ and $\lambda_t^\mu \equiv \mu_t/C_t$. Like all endogenous objects in the model, each of these ratios can take on N different values. The appendix shows how to express the value function (Equation 1.4) and the certainty equivalent (Equation 1.5) in terms of λ_t^V , λ_t^μ , and ε_{t+1}^c . Following the approach of [Bonomo, Garcia, Meddahi, and Tedongap \[2011\]](#), I integrate out ε_{t+1}^c , so that the remaining system consists of $2N$ (nonlinear) equations in $2N$ unknowns. The solution has to be found numerically. However, this is fast, even for large values of N ,¹⁴ and a solution is guaranteed to exist as long as the period utility function $u(\cdot)$ is continuous. The ratios λ_t^V and λ_t^μ can be used to re-write the disappointment event as

$$V_{t+1} \leq \delta \mu_t \Leftrightarrow \frac{\lambda_{t+1}^V}{\lambda_t^\mu} e^{\Delta c_{t+1}} \leq \delta \Leftrightarrow \varepsilon_{t+1}^c \leq \frac{\log\left(\frac{\delta \lambda_t^\mu}{\lambda_{t+1}^V}\right) - \mu}{\sigma_t^c} \equiv \phi_{t+1}^c, \quad (1.13)$$

where I have defined the disappointment threshold ϕ_{t+1}^c . After some simple algebra, M_{t+1} can be expressed as

$$M_{t+1} = \beta e^{(\alpha-1)\Delta c_{t+1}} \left(\frac{\lambda_{t+1}^V}{\lambda_t^\mu} \right)^{\alpha-\rho} \left(\frac{1 + \theta \mathbf{1}\{\varepsilon_{t+1}^c \leq \phi_{t+1}^c\}}{1 + \delta^\alpha \theta E_t[\Phi(\phi_{t+1}^c)]} \right), \quad (1.14)$$

which is a known function of the Markovian state (and ε_{t+1}^c). The pricing kernel can now be used to solve for asset prices via the Euler equation.

Risk-free Bonds. The price of a risk-free 1-period zero coupon bond, given by

$$\mathcal{B}_t(1) \equiv E_t[M_{t+1}],$$

can be computed in vector form as

$$\mathcal{B}(1) = (P \odot A^b) \cdot \iota_N,$$

where the $N \times N$ matrix A^b is defined in the appendix. To compute multi-period variance swap rates, one also needs the price of multi-period bonds. The price of a τ -period zero

¹⁴On a Windows machine with 12GB RAM and an Intel I7-X980 chip, computing the solution takes less than a second for $N = 2^6 = 64$ states and about 25 seconds for $N = 2^8 = 1024$ states.

can be computed recursively in vector form as

$$\mathcal{B}(\tau) = (P \odot A^b) \cdot \mathcal{B}(\tau - 1).$$

Equity. Denote the price of the dividend claim (equity) by S_t . The price-dividend ratio, given by

$$\lambda_t^d \equiv \frac{S_t}{D_t} = E_t \left[M_{t+1} \frac{S_{t+1} + D_{t+1}}{D_t} \right],$$

can be computed in vector form as

$$\lambda^d = (I_N - P \odot A^d)^{-1} \cdot (P \odot A^d) \cdot \iota_N,$$

where the $N \times N$ matrix A^d is defined in the appendix.

Variance Swap Rates and Variance Premium. Let $r_{t+1} = \log \left(\frac{S_{t+1}}{S_t} \right)$ denote the log ex-dividend return. The τ -period variance swap rate equals the risk-neutral expectation of future realized variance, i.e.

$$\mathcal{V}_t(\tau) \equiv E_t^Q \left[\sum_{h=1}^{\tau} r_{t+h}^2 \right] = E_t \left[M_{t+\tau} \sum_{h=1}^{\tau} r_{t+h}^2 \right] \mathcal{B}_t(\tau)^{-1}.$$

The 1-period swap rate can be computed in vector form as

$$\mathcal{V}(1) = (P \odot A^\nu) \cdot \iota_N,$$

where the $N \times N$ matrix A^ν is defined in the appendix. The τ -period swap rate can be computed in vector form as

$$\mathcal{V}(\tau) = \mathcal{B}(\tau)^{-1} \odot \sum_{h=1}^{\tau} \mathcal{V}(h, \tau),$$

where

- with a slight abuse of notation, $\mathcal{B}(\tau)^{-1}$ denotes the element-wise inverse of the vector containing τ -period bond prices.
- $\mathcal{V}(1, 1) \equiv \mathcal{V}(1)$ equals the 1-period swap rate.
- $\mathcal{V}(1, \tau) = (P \odot A^\nu) \cdot \mathcal{B}(\tau - 1)$ for $\tau > 1$.
- $\mathcal{V}(h, \tau) = (P \odot A^b) \cdot \mathcal{V}(h - 1, \tau - 1)$ for $h > 1$ and $\tau > 1$.

The (1-month) variance premium is defined as the difference between the one month variance swap rate and the analogous expectation under the physical measure, i.e. $VP_t = E_t^Q [\sum_{h=1}^{\tau} r_{t+h}^2] - E_t^P [\sum_{h=1}^{\tau} r_{t+h}^2]$.

Call Options. The (relative) price of a 1-period call option with strike price X and moneyness $K \equiv \frac{X}{S_t}$ is given by

$$\mathcal{C}_t(1, K) \equiv \frac{1}{S_t} \times E_t [M_{t+1} \max(0, S_{t+1} - X)] = E_t [M_{t+1} \max(0, e^{r_{t+1}} - K)].$$

It can be computed in vector form as

$$\mathcal{C}(1, K) = (P \odot A^c(K)) \cdot \iota_N,$$

where the $N \times N$ matrix $A^c(K)$, which is a function of the option's moneyness, is defined in the appendix. The price of a τ -period call equals

$$\mathcal{C}_t(\tau, K) \equiv E_t \left[\left(\prod_{h=1}^{\tau} M_{t+h} \right) \max \left(0, \exp \left(\sum_{h=1}^{\tau} r_{t+h} \right) - K \right) \right].$$

Because the max-operator cannot be factored into τ single-period terms, the expectation cannot be evaluated recursively. More importantly, the expectation for a τ -period option involves N^τ possible paths for the Markov chain, so that an analytical solution becomes quickly intractable as τ grows. I therefore compute multi-period option prices via Monte Carlo simulation. Specifically, starting from each of the N states, I simulate 100 million paths of both the Markov chain and $(\varepsilon^c, \varepsilon^d)$, use them to compute the pricing kernel and the option payoff, and evaluate the expectation in the associated Euler equation as the average across paths.¹⁵ To convert model-based option prices into Black-Scholes implied volatilities, I use the model-implied interest rate and dividend-yield.

1.3.3 Small Sample Statistics

In the remainder of the paper, I produce small sample statistics for different model calibrations and compare them to the data. Specifically, I simulate 100,000 samples of the same length as the data, compute the statistic of interest in each sample, and report the median value. For statistics that appear in tables (rather than figures), a model-based 90% confidence interval is reported in addition. The longest available dataset for cash flow and standard asset pricing moments is annual and spans 83 years (= 996 months).

¹⁵I repeated this procedure for different seeds of the random number generator to ensure that the Monte Carlo error is negligible given the number of paths.

The option data spans 23 years (= 276 months). All model-based calibration results are based on small samples whose lengths match these empirical counterparts.

In constructing annualized moments, I closely follow [Beeler and Campbell \[2012\]](#) and [Bansal, Kiku, and Yaron \[2012\]](#). Consumption and dividend growth rates are computed by adding twelve monthly consumption and dividend levels, and then taking the growth rate of the sum. Annual log stock returns are the sum of monthly values, while log price-dividend ratios use prices measured from the last month of the year. Because the price-dividend ratio in the data divides by the previous year's dividends, I multiply the price-dividend ratio in the model by the dividend in that month and divide by the dividends over the previous year. The annual risk-free rate is the sum of the four quarterly risk-free rates within a year.

1.4 Results

1.4.1 Calibration

I calibrate the model at the monthly frequency. All calibration targets equal small sample medians. The parameters μ and $\bar{\sigma}^2$ are chosen to match the mean and volatility of annual consumption growth, φ is set to match the volatility of annual dividend growth, and ϱ is set to match the correlation between the two endowments. The parameters governing the volatility and persistence of the endowment variance (ν, γ_K, b) naturally have a large effect on the dynamics of the conditional return variance, which are in turn reflected in the dynamics of variance swap rates. I calibrate them to match as good as possible the volatilities and autocorrelation functions of variance swaps with different maturities.¹⁶ I use $K = 6$ variance components in the MSM process. The calibration implies a first-order autocorrelation of 0.82 for σ_t , with persistence levels that range from 0.5 to 0.994 for the individual components. Given a time-discount factor of $\beta = 0.96^{1/12}$, I set ρ to match the mean risk-free rate. The implied elasticity of intertemporal substitution equals $\rho^{-1} = 0.49$. Lastly, the GDA parameters θ and δ are chosen jointly to match the equity premium and the variance premium. I refer to the full model as the GDA-MSM model.

¹⁶I find that preference parameters have a negligible effect on the autocorrelations of variance swap rates (see Section 1.4.6). This theoretical finding agrees with the empirical fact that both the physical return variance and variance swap rates (which represent a form of risk-neutral variance) display similar long-memory behavior.

Table 1.2: Calibrations

GDA-MSM	β	ρ	θ	δ	α		
	$0.96^{\frac{1}{12}}$	0.49^{-1}	43.2	0.9625	0		
	$\bar{\sigma}^2$	ν	γ_K	b	μ	ϱ	φ
	0.008 ²	0.33	0.5	2.6	0.015	0.53	5.2
EU-MSM	β	ρ	θ	δ	α		
	$0.96^{\frac{1}{12}}$	0.353^{-1}	0	—	−18.38		
	$\bar{\sigma}^2$	ν	γ_K	b	μ	ϱ	φ
	0.008 ²	0.33	0.5	2.6	0.015	0.53	5.2
GDA-AR1	β	ρ	θ	δ	α		
	$0.96^{\frac{1}{12}}$	0.687^{-1}	13.44	0.927	0		
	$E[\sigma_t^2]$	$std[\sigma_t^2]$	$AC1[\sigma_t^2]$		μ	ϱ	φ
	6.30×10^{-3}	5.78×10^{-3}	0.98		0.015	0.53	5.2

Table 1.2 reports the configuration of investors' preferences and the time-series parameters that describe the endowment process. The model is calibrated at a monthly decision interval.

In order to illustrate the role of the two main model components, I also show results for two alternative economies. First, The EU-MSM model consists of the MSM endowment (calibrated as in the benchmark model) and recursive utility with expected utility risk preferences. I set $\beta = 0.96^{1/12}$ and choose ρ to match the mean risk-free rate. The curvature parameter α is chosen to match the average equity premium. Second, the GDA-AR1 model combines GDA preferences with an AR(1) process for log endowment variance¹⁷. To fit the process into the Markov switching environment, I discretize it with the method of Rouwenhorst [1995]. I use 51 states and calibrate the process to a first-order autocorrelation of 0.98. The mean of σ_t^2 is chosen to match the mean volatility of annual consumption growth and the volatility of σ_t^2 is set to the same value as in the other two economies. All three calibrations are summarized in Table 1.2.

1.4.2 Cash Flows

The top panel of Table 1.3 shows moments of annual cash flows. Except for the mean of dividend growth, the models are calibrated to match the first two endowment moments

¹⁷Note that the long run risks literature typically models cash flow volatility as an AR(1) in levels rather than in logs. The log specification has the advantage that volatility cannot become negative. Additionally, it allows for a cleaner comparison with the multifractal process, whose unconditional distribution is right-skewed and resembles that of a log normal distribution.

Table 1.3: Quantities and Prices

	Data	GDA-MSM			EU-MSM			GDA-ARI		
		5%	50%	95%	5%	50%	95%	5%	50%	95%
Cash Flows	$E[\Delta c]$	1.82	1.30	1.80	2.30	1.30	1.80	1.30	1.80	2.30
	$\sigma[\Delta c]$	2.18	1.69	2.21	2.84	1.69	2.21	1.62	2.17	2.92
	$AC1[\Delta c]$	0.51	0.04	0.23	0.41	0.04	0.23	0.03	0.23	0.42
	$E[\Delta d]$	1.26	-0.81	1.80	4.40	-0.81	1.80	-0.78	1.80	4.39
	$\sigma[\Delta d]$	11.32	8.81	11.50	14.78	8.81	11.50	8.43	11.28	15.21
	$AC1[\Delta d]$	0.20	0.04	0.23	0.41	0.04	0.23	0.03	0.23	0.41
	$corr[\Delta c, \Delta d]$	0.53	0.35	0.53	0.68	0.35	0.53	0.34	0.53	0.68
Prices and Returns	$E[r - r^f]$	5.24	2.53	5.26	8.38	2.61	5.23	1.63	5.30	11.56
	$\sigma[r]$	19.85	13.17	17.03	21.32	11.97	15.55	13.77	20.33	27.84
	$AC1[r]$	-0.01	-0.25	-0.06	0.14	-0.22	-0.03	-0.28	-0.06	0.16
	$kurt[r]$	3.54	2.74	3.77	6.33	2.71	3.73	3.12	4.65	8.61
	$kurt[r](\text{monthly})$	9.45	5.90	8.37	13.29	4.93	6.98	5.40	7.41	11.62
	$E[r^f]$	0.49	-0.39	0.52	1.69	0.23	0.49	-4.32	0.51	2.72
	$\sigma[r^f]$	2.87	1.23	1.88	3.47	0.14	0.36	1.49	5.61	11.79
	$AC1[r^f]$	0.70	0.36	0.55	0.74	0.49	0.75	0.44	0.74	0.89
	$E[p - d]$	3.39	3.09	3.20	3.32	3.11	3.22	3.08	3.24	3.35
	$\sigma[p - d]$	0.45	0.10	0.14	0.18	0.06	0.12	0.11	0.21	0.34
	$AC1[p - d]$	0.88	0.73	0.86	0.93	0.78	0.90	0.70	0.83	0.92
Variance Premium	$E[VP]$	11.29	4.45	11.30	20.67	-1.49	1.79	0.14	10.98	45.55
	$\sigma[VP]$	9.65	7.04	15.27	21.45	0.65	1.61	0.63	22.42	37.75
	$AC1[VP]$	0.46	0.60	0.79	0.91	0.90	0.96	0.69	0.93	0.98

Table 1.3 presents moments for annual cash flows and asset prices. Also shown is the kurtosis of monthly returns and the (monthly) variance premium. r denotes the log cum dividend return on the market, r^f the log risk-free rate, $p - d$ the log price-dividend ratio, and VP the variance premium. Model equivalents are computed from 100,000 samples of the same length as the data as described in Section 1.3.3. Details on the data are contained in Appendix A. The sample for moments in the first two panels spans 1930-2012, whereas the sample for the variance premium spans 1990-2012.

exactly. I follow the convention in the previous literature of assuming that consumption and dividend growth have the same mean. The fact that cash flows are modeled without time-variation in conditional means implies that their first-order autocorrelations are close to the ones of a time-aggregated continuous-time random walk, which equals 0.25 (see [Working \[1960\]](#)). The Table shows this is a good approximation for dividend growth rates, whose empirical autocorrelation of 0.2 is close to the median model estimate of 0.23 in all three economies. Only the autocorrelation of consumption growth falls slightly out of the model-implied 90% confidence interval.

1.4.3 Basic Asset Prices

The middle panel of Table [1.3](#) presents the model implications for annual asset pricing moments. All three models are calibrated to match the equity premium and the risk-free rate exactly. For both GDA models, the volatility of returns falls inside the model-implied 90% confidence interval, whereas the volatility is too low in the EU model. The reason is that the time-varying risk aversion generated by GDA results in more variability in the equity premium and therefore more volatile returns. The effect of GDA shows up even stronger in the volatility of the risk-free rate. With EU preferences, there is little time-variation in the conditional mean of the pricing kernel and r_t^f displays much less volatility than in the data. The upper end of the EU-MSM confidence interval equals 0.51, which is less than a fifth of the data value. In contrast, the risk free rate volatility of 1.88% in the benchmark model is close to its data counterpart, which comfortably falls in the model-based confidence interval. In the GDA-AR1 model, the risk-free rate is twice as volatile as in the data, which shows that the slow-moving nature of the AR(1) process results in too much time-variation in the conditional mean of M_t when combined with GDA preferences. Lastly, all three models are successful at replicating the high mean and persistence of the log price-dividend ratio, but fall somewhat short of matching its volatility.

Because the main goal of my paper is to explain features of index options, it appears important to ensure that the model's implications for the quantity of tail risk are not counterfactual. The Table shows that the kurtosis of both annual and monthly returns in the GDA-MSM model are very close to their data counterparts. At the 1 month horizon, the kurtosis equals 8.37 in the model and 9.45 in the data. At the 12 month horizon, the value falls to 3.77 in the model and 3.54 in the data. The model therefore successfully replicates the non-normality of short-horizon returns and the fact that this feature considerably weakens at longer horizons. A comparison with the EU-MSM model shows that part of the kurtosis in monthly returns stems from the large weight that GDA places on tail outcomes. In particular, GDA generates larger price jumps in response to changes in endowment volatility, i.e. more volatility feedback. I discuss this channel in more detail in Section [1.4.5](#), where I explicitly compute tail probabilities in all three models.

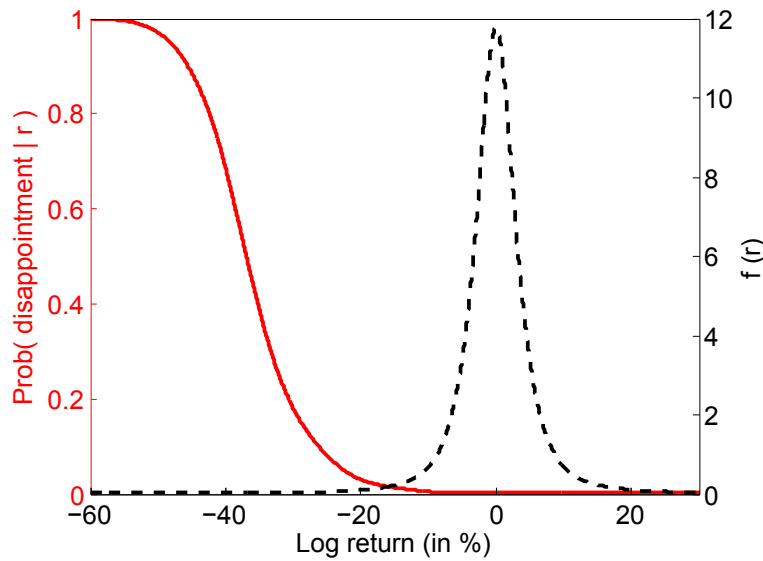


Figure 1.4: Returns and Disappointments

Figure 1.4 shows the unconditional density of monthly ex-dividend log returns (dashed line, right axis), as well as the probability of disappointment conditional on a given return (solid line, left axis).

1.4.4 Variance Premium

The bottom panel of Table 1.3 shows moments of the 1-month variance premium. Both GDA models are calibrated to match the average variance premium exactly. The same is not possible for the EU model¹⁸, whose sole risk preference parameter (α) was chosen to match the equity premium. To illustrate the source of the variance premium in the GDA models, it is helpful to consider the relationship between returns and the probability of disappointments. Equation 1.12 showed that disappointments are caused by a combination of negative innovations in consumption growth and positive innovations in endowment volatility. Because consumption and dividend growth share the same volatility process as well as (imperfectly) correlated innovations, disappointments tend to coincide with negative returns. This is illustrated in Figure 1.4, which shows the unconditional return distribution (dashed line, right axis) along with the probability of a disappointment conditional on a given return (solid line, left axis), both for the GDA-MSM model¹⁹. It is clear that the lower a given return, the higher the chance that it is associated with a disappointment. Because strongly negative returns also result in a large realized variance (large payoffs to variance swaps), variance swaps embed a large insurance premium.

¹⁸Drechsler and Yaron [2011] present a model with EU risk preferences that *does* match both the equity premium and the variance premium. Whereas the present model features jumps in the conditional variances of cash flows (due to the discrete nature of the Markov chain), their model additionally assumes jumps in the conditional means of cash flows. Jumps have a larger effect on the variance premium than on the equity premium because the return variance is convex in returns. Drechsler and Yaron are thus able to match both risk premia by assuming a lower curvature parameter of $\alpha = -8.5$ (vs. -18.38 in the present EU model) and considerably more jump risk.

¹⁹The plot looks very similar for the GDA-AR1 model.

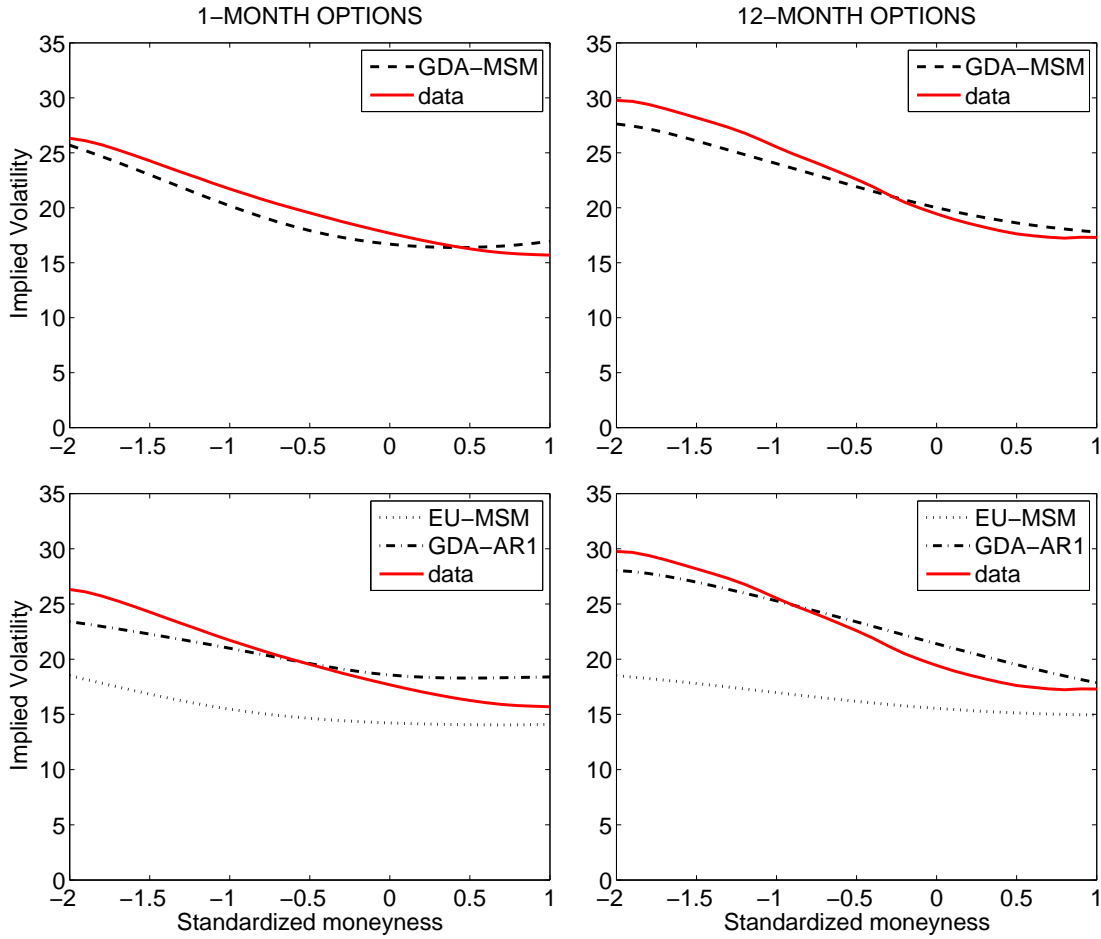


Figure 1.5: Implied Volatility Smirk

Figure 3.1 shows average (Black-Scholes) implied volatilities for option maturities of 1 and 12 months, and relative moneyness of -2 to 1. Volatilities are expressed in annualized percentage units. The top row shows results for the benchmark model (GDA-MSM), whereas the bottom panel shows results for the EU-MSM and GDA-AR1 models. Small-sample model statistics are computed from 100,000 samples whose length equals that of the data – see Section 1.3.3. The sample spans 1990-2012.

1.4.5 Option Prices

Figure 3.1 shows the empirical and model-based implied volatility (IV) curve for 1-month (left column) and 12-month (right column) maturities. The full model (top rows) provides a very good match for the empirical IV curve. At the 1-month maturity, options with a relative moneyness of -2 have an IV of about 26.0%, both in the model and in the data. At-the-money options have an IV of 17% in the model, close to the data value of 18%. At the 12-month maturity, the GDA-MSM model provides a similarly good match for the data, replicating the higher level of the curve relative to the shorter maturity. It is worth emphasizing that the IV curve did not serve as a calibration target for the model.

The bottom row of Figure 3.1 shows the IV curve for the two alternative economies. The

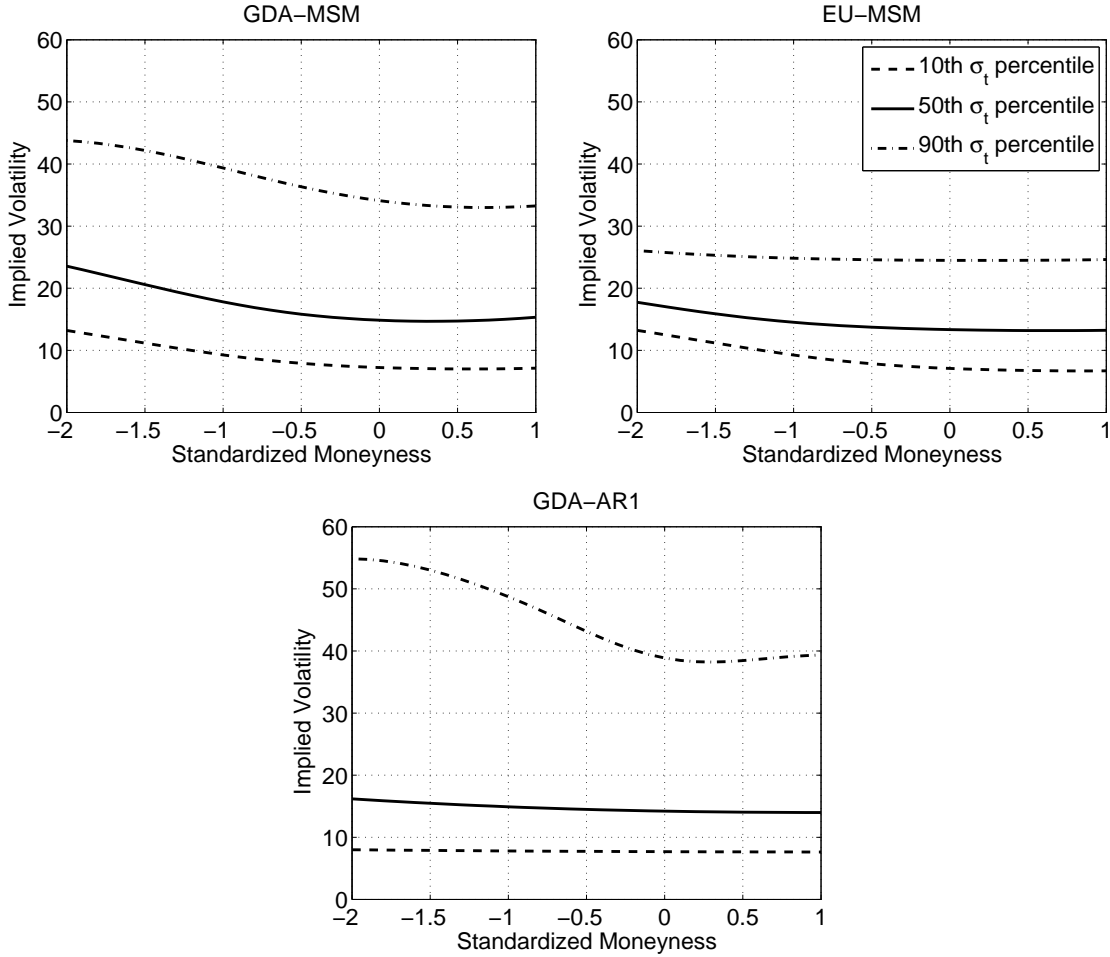


Figure 1.6: Conditional 1-Month Implied Volatility Smirk

Figure 1.6 shows the implied volatility smirk conditional on values of the endowment variance σ_t . Volatilities are expressed in annualized percentage units. Each plot shows the IV curve at the 10th, 50th, and 90th percentile of σ_t for a different model.

EU-MSM model (dotted lines) implies a slight smirk, but its level and slope fall short of the data counterparts for both maturities. Nevertheless, it is noteworthy that the EU model can produce a smirk at all because [Benzoni, Collin-Dufresne, and Goldstein \[2011\]](#) have shown that the IV curve is almost exactly horizontal in the basic long run risks (LRR) model. The LRR model is based on the same utility function but an autoregressive process for endowment variance. Average option prices therefore seem to support the presence of multifractal variance risks in cash flows. The GDA-AR1 model (dash-dotted lines) provides a good match for the level of the IV curve at both maturities, which was expected from the fact that the model matches the average variance premium. The model is further capable of matching the steep slope of the IV curve at the annual maturity, but it produces a curve that is too flat at the 1-month maturity.

To understand why the full model is able to replicate the smirk, I plot conditional IV curves. Figure 1.6 shows 1-month implied volatilities, conditional on different percentiles

of the endowment volatility σ_t .²⁰ In the GDA-MSM model (top-left panel), the curve has a noticeably negative slope at the 10th, 50th, and 90th percentiles of σ_t . The steep unconditional IV curve therefore results from the fact that the curve is relatively steep in most states. This is an attractive feature of the model because the slope of the curve is nearly always significantly positive in the data (see Figure 1.1). In contrast to the benchmark model, the slope of the IV curve becomes flat for certain regions of σ_t in both alternative economies. In the EU-MSM model (top-right panel), the slope is negative when endowment volatility is low but close to zero when it is high. In the GDA-AR1 model (bottom panel), the conditional slopes behave in the exact opposite way, being strongly negative when endowment volatility is high but close to zero when it is low. These differences can be explained by time-variation in the conditional disappointment probability as well as time-variation in the distribution of (endogenous) return jumps, which in turn result from changes in σ_t .

In what follows, I show that (1) in the two models with GDA preferences, the smirk is steep for high values of σ_t due to a high conditional disappointment probability and (2) in the two models with MSM volatility, the smirk is steep when volatility is low due to a high probability of large negative returns. To quantify the effect of the two channels, Table 1.4 shows conditional return moments and conditional tail probabilities under both the statistical measure (\mathbb{P}) and the risk-neutral measure (\mathbb{Q}).²¹ As in Figure 1.6, all numbers are conditional on percentiles of σ_t (I omit the 50th percentile to save space). For comparability with the IV plots, I express tail thresholds in standard deviation units.

States of low endowment volatility. Notice from Table 1.4 that when volatility is at its 10th percentile, the return distribution in the two MSM models is strongly left-skewed and leptokurtic under \mathbb{P} . In the benchmark model, the conditional skewness (kurtosis) equals -2.57 (23.51) whereas it equals -2.05 (23.39) in the EU-MSM model. The higher moments are also reflected in a considerably larger probability of left tail outcomes relative to right tail outcomes in both models. For example, in the GDA-MSM (EU-MSM) model, there is a chance of 1.78% (1.22%) of observing a return of less than *minus* two standard deviations but only a chance of 0.34% (0.28%) of observing a return of more than *plus* two standard deviations. In contrast, the conditional return distribution in the GDA-AR1 model is close to normal with a skewness of -0.08 and a kurtosis of 3.13. The left-skewness in the MSM models results from mean reversion in endowment volatility:

²⁰In the MSM models, σ_t only takes on $K + 1 = 7$ different values (with different probabilities). The 10th percentile is given by the states in which exactly one component is in its high state. The IV curve at the 10th percentile of σ_t equals the mean curve across these states. The curve is computed similarly at the other two percentiles.

²¹The risk neutral density can be computed from call prices using the result of Breeden and Litzenberger [1978], who show that it equals the second derivative of the call price with respect to the strike price, divided by the price of a risk-free bond of equal maturity. I compute call prices on a fine grid of strikes and compute the second derivative via finite differences.

Table 1.4: Conditional Moments and Tail Probabilities

Model	σ_t -pct	Dist.	Moments			Tail Probabilities			
			std	skew	kurt	< -3	< -2	> 2	> 3
GDA-MSM	10	\mathbb{P}	2.63	-2.57	23.51	1.29	1.78	0.34	0.17
		\mathbb{Q}	2.91	-3.57	34.25	1.61	2.13	0.30	0.15
	90	\mathbb{P}	8.31	0.16	4.05	0.04	0.60	1.48	0.20
		\mathbb{Q}	11.12	-0.51	3.68	1.35	6.94	0.96	0.11
EU-MSM	10	\mathbb{P}	2.33	-2.05	23.39	0.75	1.22	0.28	0.11
		\mathbb{Q}	2.93	-3.43	25.40	1.79	2.44	0.18	0.05
	90	\mathbb{P}	7.39	0.12	3.64	0.14	1.68	2.90	0.44
		\mathbb{Q}	7.43	-0.11	3.64	0.49	3.18	1.52	0.14
GDA-AR1	10	\mathbb{P}	2.23	-0.08	3.13	0.22	2.56	1.92	0.13
		\mathbb{Q}	2.23	-0.08	3.14	0.24	2.74	1.82	0.12
	90	\mathbb{P}	9.93	-0.05	3.90	0.06	0.80	0.89	0.02
		\mathbb{Q}	13.57	-0.74	3.70	1.34	9.43	0.58	0.01

Table 1.4 shows conditional moments and tail probabilities of 1-month ex-dividend log returns for the physical (\mathbb{P}) and risk-neutral (\mathbb{Q}) distributions. All quantities condition on a given percentile of the endowment volatility σ_t . Returns are expressed in monthly percent, i.e. a standard deviation of 2.63 represents 2.63% per month. Return thresholds are measured in standard deviation units, where the square root of the 1-month variance swap rate is used to measure the conditional standard deviation. Probabilities are expressed in percent, i.e. 1.29 stands for 1.29%.

When σ_t increases as expected, it induces a decrease in the price dividend ratio and therefore a negative return. In particular, the less persistent volatility components in the MSM models mean-revert fast enough to induce large negative return jumps and a conditional return distribution that is strongly left-skewed at the 1-month horizon. In contrast, mean reversion occurs too slowly in the GDA-AR1 model to have a significant effect on returns over short horizons.²²

For the risk neutral distribution (\mathbb{Q}), the moments and tail probabilities at the 10th percentile of σ_t are similar to those under \mathbb{P} in both GDA models. As one may guess from this result, disappointment aversions plays a minor role in states with low endowment volatility. The conditional disappointment probability only equals 0.0001% in the GDA-MSM model and it essentially equals zero in the GDA-AR1 model. The fact that the two MSM models produce a large smirk in the low volatility states is therefore primarily a consequence of the MSM process rather than the preference specification. Put differently, OTM puts are expensive because there is relatively more left tail risk than right tail risk when volatility is low. Insurance premia play a minor role in these states.

²²At the *annual* return horizon, mean reversion has a stronger effect in the GDA-AR1 model, resulting in conditional return skewness (kurtosis) of -0.44 (3.95). The higher skewness contributes to the model's ability to produce a reasonable IV curve for options with a 12-month maturity (see Figure 3.1). For comparison, the skewness (kurtosis) of annual returns equals -0.79 (5.02) in the GDA-MSM model and -0.58 (4.64) in the EU-MSM model, both conditional on σ_t being at its 10th percentile.

States of high endowment volatility. Mean-reversion in volatility has the opposite effect when σ_t is at its 90th percentile, resulting in positive rather than negative return jumps on average. In both MSM models, the conditional return distribution is therefore slightly right-skewed under \mathbb{P} . All else equal, right-skewness makes the smirk flat or even increasing. However, in the two models with GDA preferences, high volatility states are also associated with an increased disappointment probability. This probability equals 0.33% in the GDA-MSM model and 0.51% in the GDA-AR1 model.²³ As a consequence, the conditional return distribution is significantly left-skewed under the risk-neutral measure in both GDA models. Table 1.4 shows that the amplification of left tail probabilities under \mathbb{Q} is especially pronounced for the most extreme tails. For example, returns of -3 standard deviations or less are $\frac{1.35}{0.04} \approx 34$ times as likely under \mathbb{Q} than under \mathbb{P} in the GDA-MSM model and $\frac{1.34}{0.06} \approx 22$ times as likely in the GDA-AR1 model. In contrast, the ratio only equals $\frac{0.49}{0.14} \approx 4$ in the EU-MSM model because an EU investor is much less focused on tail events. The fact that the two GDA models produce a large smirk in the high volatility states is therefore a consequence of the utility function rather than the process for endowment variance. In other words, OTM puts are expensive because they embed a large insurance premium when volatility is high.

Lastly, it is interesting to note that the results in Table 1.4 are broadly consistent with the empirical findings of [Bollerslev and Todorov \[2011\]](#). These authors look at nonparametric estimates of tail probabilities under both measures and find that large negative returns have a much higher probability under the risk neutral measure. GDA preferences represent a possible explanation for this finding.

1.4.6 The Term Structure of Variance Swap Rates

Figure 1.7 presents moments of variance swap rates for maturities from 1 to 12 months. Panel A shows the mean of swap rates as a function of the swap maturity. Longer-term swaps have a slightly higher mean compared to short-term swaps, indicating the presence of a term premium in swap rates.²⁴ All three models can replicate this increasing pattern in mean swap rates, but only the GDA models matches their level. The level is too low in the EU-MSM model because both the variance premium (see Section 1.4.4) and the return volatility (see Table 1.3) fall below their respective data counterparts, whereas these moments are matched well in the other two models.

²³A comparison with the disappointment probabilities at the low σ_t percentile shows that the conditional disappointment probability is increasing in the endowment variance. Recall from the discussion following Equation 1.12 on page 14 that this conclusion was not clear ex ante because endowment volatility has two opposing effects on the conditional disappointment probability.

²⁴The (annualized) variance of realized returns is very close to constant across return horizons, both in the data and in the two models. The term premium in swap rates therefore arises due to higher variance premia at longer return horizons.

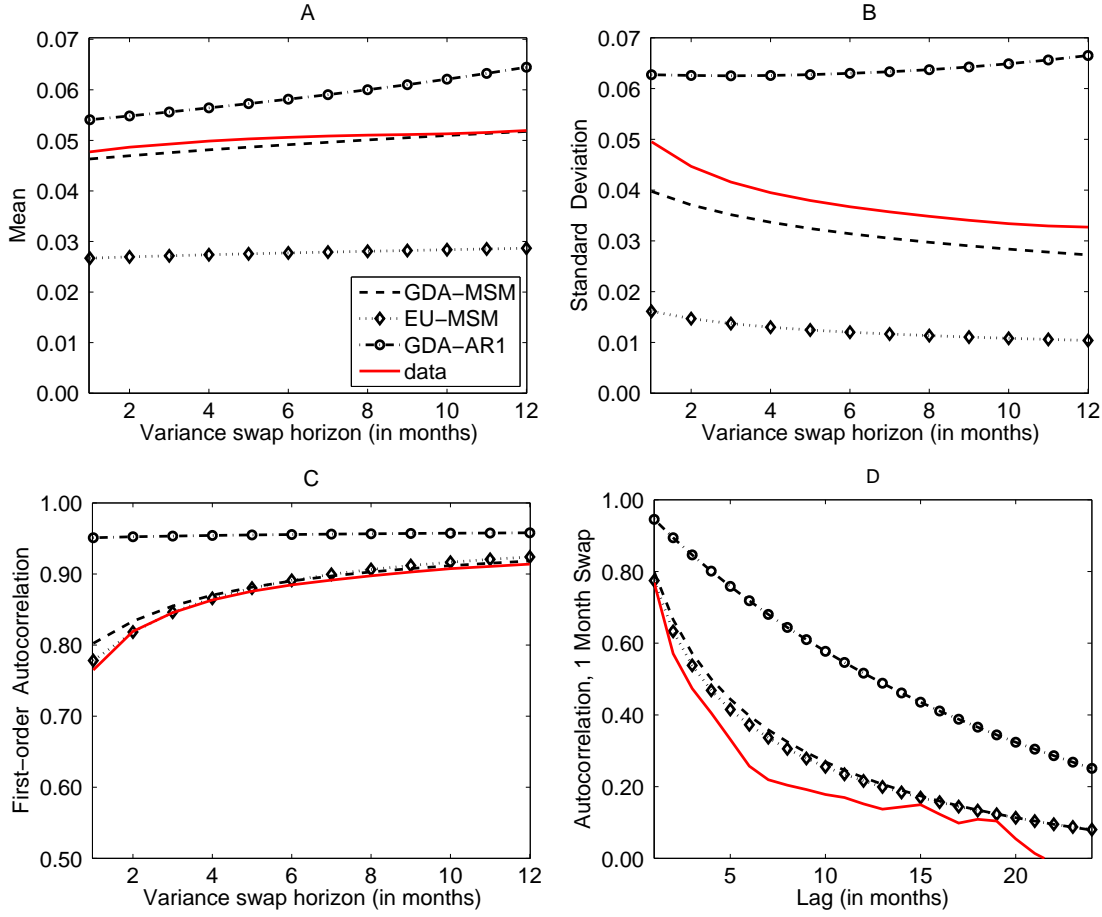


Figure 1.7: Moments of variance swap rates

Figure 1.7 shows moments of variance swap rates with maturities between 1 to 12 months. Small-sample model statistics are computed as discussed in Section 1.3.3. The sample spans 1990-2012.

The remaining panels of Figure 1.7 illustrate the volatility and persistence of swaps with different maturities. Panels B and C show the volatility and first-order autocorrelation of swap rates as a function of the swap maturity, whereas Panel D shows the autocorrelation function of 1-month swap rates. These moments served as a calibration target for the parameters controlling the volatility and persistence of the MSM endowment variance, i.e. (ν, γ_K, b) . Both MSM models are able to replicate the higher volatility and lower persistence of short term swaps, as well as the long-memory behavior reflected in the autocorrelation function. The GDA-MSM model is additionally able to replicate the high level of the volatility because its state-dependent risk aversion induces time-variation in the variance premium, which makes swap rates more volatile. The same is not true for the EU model. As I will discuss in the next section, this feature of the GDA model also endows the variance premium with large predictive power for excess returns.

The success of the MSM models in replicating moments of the term structure of swap rates is due to the presence of both high-frequency and low-frequency shocks in the variance process. The less persistent shocks increase the volatility of variance over short horizons

but they average out over longer horizons, making the long end of the term structure less volatile and more persistent. [Calvet and Fisher \[2004\]](#) have previously shown that the MSM process exhibits an autocorrelation structure that mimics the one of a long memory process. While this is a feature of the endowment variance, it is inherited by the endogenously determined variance swap rates in the present model. In contrast, the GDA-AR1 model relies on a single shock frequency and therefore it cannot match the dynamics of variance swap rates.

1.4.7 Return Predictability

The data section highlighted that the variance premium has high predictive power for excess returns over horizons of a few month. The top panel of Table 1.5 shows the results of running the same regressions on simulated model data. I report the slope coefficients and R^2 s for predictive regressions of log excess returns on the (one-month) variance premium for return horizons of one, three and six months. As in the data, the GDA-MSM model-based slope coefficients are falling in the return horizon and the R^2 s are quite large for the short horizons. Further, all median model estimates are close to their data counterparts. In the EU-MSM model, the median slope estimates and R^2 s fall considerably below the data values because the model does not generate time-variation in effective risk aversion. On the other hand, the GDA-AR1 model implies considerably too much predictability, producing R^2 s that exceed their data counterparts by a factor of 3 to 5. The large degree of predictability results from too much time-variation in the conditional disappointment probability, which also showed up in the very high volatility of the risk-free rate (see Table 1.3) and the an IV smirk that is extremely steep in high volatility states but essentially flat in low volatility states (see Figure 1.6).

In addition to the short-horizon predictive power of the variance premium, it is well-known that the price-dividend ratio has high predictive power over horizons that span several years. In the bottom panel of Table 1.5, I report the results of regressing excess returns of horizons one, three and five years on the log price-dividend ratio. As in the data, the price dividend ratio in the GDA-MSM model has large predictive power for excess returns. The median R^2 s in the model rise from 6.3% at the annual horizon to 14.5% at the 5-year horizon. The EU-MSM model produces substantially less predictability. In particular, the median R^2 equals 1.5% at the 1-year horizon and it only rises to 5.2% at the 5-year horizon. These numbers are very similar to the ones implied by the long run risks model of [Bansal, Kiku, and Yaron \[2012\]](#), which is based on the same utility function. On the other hand, the GDA-AR1 model once again produces considerably too much predictability. For example, the median R^2 of 21.82% at the 1-year horizon exceeds its data counterpart by a factor of six.

Table 1.5: Return Predictability

	Data	GDA-MSM			EU-MSM			GDA-AR1		
		5%	50%	95%	5%	50%	95%	5%	50%	95%
Regressor: VP										
$\hat{\beta}(1m)$	0.89	0.16	0.72	1.48	-4.13	0.55	5.70	0.54	1.03	7.27
$R^2(1m)$	2.53	0.18	3.04	9.03	0.00	0.40	3.76	0.66	7.72	16.18
$\hat{\beta}(3m)$	0.88	0.13	0.60	1.19	-4.39	0.36	4.93	0.52	0.98	5.73
$R^2(3m)$	6.49	0.03	6.40	19.16	0.01	1.13	9.58	1.46	19.63	36.97
$\hat{\beta}(6m)$	0.65	0.09	0.49	0.96	-4.45	0.24	4.40	0.46	0.91	4.43
$R^2(6m)$	6.52	0.04	8.67	27.40	0.02	2.13	16.22	1.93	31.65	54.74
Regressor: p-d										
$\hat{\beta}(1y)$	-0.08	-0.59	-0.31	1.48	-0.48	-0.16	0.10	-0.69	-0.48	-0.26
$R^2(1y)$	3.67	0.58	6.31	17.01	0.02	1.53	9.18	5.56	21.82	41.69
$\hat{\beta}(3y)$	-0.27	-1.36	-0.71	1.19	-1.23	-0.40	0.32	-1.59	-1.10	-0.54
$R^2(3y)$	17.90	0.58	12.24	33.20	0.04	3.70	21.54	8.44	37.88	64.99
$\hat{\beta}(5y)$	-0.42	-1.89	-0.96	0.96	-1.81	-0.59	0.56	-2.18	-1.43	-0.61
$R^2(5y)$	29.87	0.42	14.50	40.99	0.05	5.24	29.71	7.37	39.21	68.38

Table 1.5 shows predictive regressions for excess log returns. The regressions take the form $r_{t:t+h} - r_t^f = \alpha(h) + \beta(h)x_t + \varepsilon_{t+h}(h)$, where h stands for the predictive horizon and x_t for the predictor. The top panel shows the results of regressing excess returns of horizons 1, 3, and 6 months on the one month variance premium. The regression is run on overlapping monthly data. The bottom panel shows the results of regressing excess returns of horizons 1, 3, and 5 years on the log price dividend ratio. The regression is run on overlapping annual data. In each case, I report the slope coefficient as well as the R^2 . Small-sample model statistics are computed as discussed in Section 1.3.3. The sample for the first set of regressions spans 1990-2012, whereas the sample for the second set of regressions spans 1930-2012.

An interesting aspect of the results in Table 1.5 is that the variance premium and the price-dividend ratio differ in terms of their ability to predict returns over different horizons. The variance premium is a successful predictor over short horizons (it produces a R^2 of 6.4% at the *quarterly* horizon in the GDA-MSM model), whereas the price-dividend ratio works better at longer horizon (it produces a R^2 of 6.3% at the *annual* horizon). The model successfully captures this challenging dimension of the data because it incorporates variance shocks with different persistence levels. As discussed above, an increase in endowment variance leads to an increase in the probability of disappointments and higher expected returns. However, the nature of this effect differs substantially across variance components. This is illustrated in Figure 1.8, which shows expected 1-month returns at different horizons conditional on one of the multipliers being in its high state. The panels differ in terms of the multipliers being considered. Conditional on the most persistent component being in its high state, returns are expected to be high over a long horizon (top-left panel). On the other hand, expected returns only increase over a short horizon conditional on the least persistent component being in its high state (bottom-right panel).

How do these differences help in reconciling the differences in the predictive ability of the variance premium and the price-dividend ratio? Because the price-dividend ratio reflects the riskiness of cash flows over the long-run, it is strongly affected by persistent shocks and much less strongly affected by transient shocks. Specifically, the log price-dividend ratio equals 3.11 conditional on component 1 being high and 3.33 conditional on component 1 being low. On the contrary, it only changes from 3.22 to 3.23 when conditioning on the most transient component (component 6) being high rather than low. Because changes in the price dividend ratio are mostly associated with changes in persistent variance components, it is a better predictor over long horizons than over short horizons.

As the (one-month) variance premium equals the conditional covariance between realized return volatility and the pricing kernel over the next month (see Equation 1.3), its value depends more strongly on transient shocks than on persistent shocks. Specifically, the variance premium equals 11.99 conditional on component 1 being high and 11.53 conditional on component 1 being low. In contrast, it changes from 15.70 to 7.82 when conditioning on the most transient component (component 6) being high rather than low. The variance premium is therefore a better predictor over short horizons than over long horizons.

Lastly, Figure 1.8 shows that GDA risk preferences increase the importance of transient shocks relative to EU. For example, the intercept in the bottom-right panel (the expected 1-month return conditional on component 6 being in its high state) equals 6.87% the GDA model but only 6.36% in the EU model. Relative to the unconditional expected return of about 5.8%, transient shocks therefore increase the expected return by twice as much in

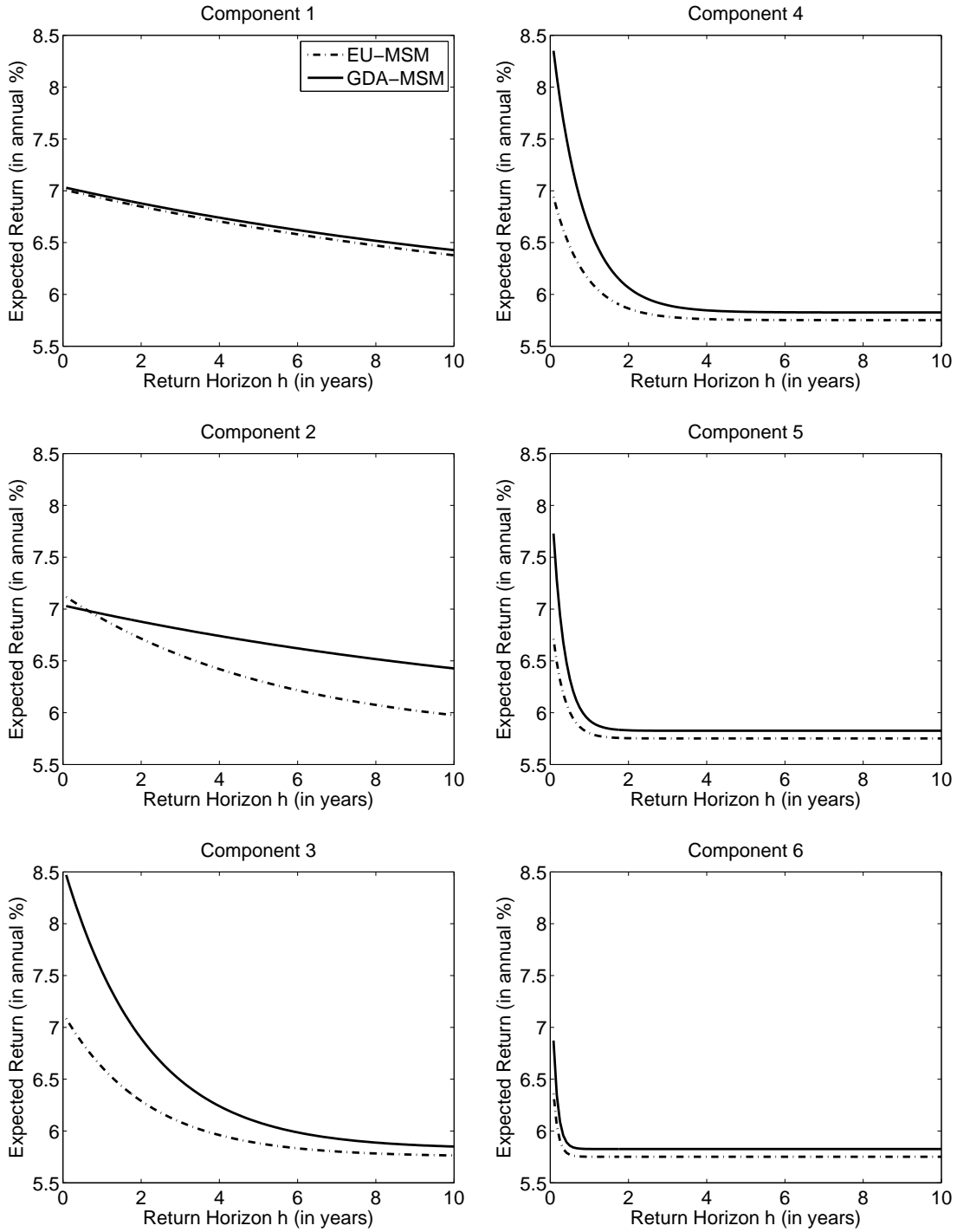


Figure 1.8: Shock Frequencies and Expected Returns

Figure 1.8 shows the expectation of the (annualized) 1-month log return at time $t+h$ conditional on the k^{th} variance component being in the high state at time t (not conditioning on values of the other components). Component 1 has the highest persistence and component 6 has the lowest persistence. Dash-dotted lines refer to the EU model whereas solid lines refer to the GDA model.

The unconditional mean return equals about 5.8% in both models.

the GDA model than in the EU model. On the other hand, the most persistent variance component affects expected returns equally for both preference specifications (top-left panel).²⁵

1.5 Additional Results

This section illustrates additional details about the model mechanism. First, I contrast the option pricing implications of the GDA model with those of the two nested cases, i.e. DA and EU risk preferences. Next, I quantify the risk aversion implied by different preference specifications and show explicitly that risk premia in the GDA-MSM model arise predominantly from aversion against tail risk. The analysis further shows that GDA preferences imply less risk aversion than both nested preference specifications when calibrated to match the equity premium.

1.5.1 The degree of tail sensitivity and option prices

The main mechanism for matching option prices in the present model is the high aversion toward tail risk implied by GDA preferences. In particular, risk aversion in the benchmark calibration is almost entirely determined by disappointment aversion because the period utility function, $u(x) = \log(x)$ has very little curvature. Furthermore, the disappointment threshold is set to a relatively low value of $\delta = 0.9625$, which implies an unconditional disappointment probability of 0.075% or about once per century.²⁶ This section investigates the importance of these choices for quantitatively matching option prices.

I begin by considering the role of the low disappointment *threshold*. Relative to the nested case of (pure) disappointment aversion (DA) risk preference, the GDA model shifts the disappointment threshold further into the left tail of the distribution, thereby lowering the probability of disappointment.²⁷ In the first experiment, I show how the variance premium and the implied volatility curve change as one gradually moves from a GDA calibration with a low threshold parameter ($\delta = 0.95$) to pure DA ($\delta = 1$). I keep the curvature parameter α fixed at the benchmark value of 0. To make the comparisons meaningful, I

²⁵A recent paper by [Dew-Becker, Giglio, Le, and Rodriguez \[2013\]](#) shows that recursive utility with EU risk preferences imply risk prices for low persistence shocks that are too low relative to what is implied by variance swap rates. The higher price for such shocks under GDA preferences represents a potential solution for this problem, and it likely contributes to the present model's ability to capture the dynamics of swap rates.

²⁶It should be noted that, while disappointing outcomes are overweighted in the utility computation ex-ante, the fact that an outcome is disappointing has no effect ex-post. In other words, events that fall just below and just above the disappointment threshold are not associated with systematically different changes in the price-dividend ratio or systematically different returns.

²⁷DA preferences imply an unconditional disappointment probability of 39.7%, or about once per quarter when calibrated to match the equity premium.

simultaneously adjust the disappointment magnitude θ so that the model-implied equity premium remains unchanged. In other words, I consider a set of economies that differ in terms of their risk preference calibrations, but not in their ability to match the historically observed equity premium. The left panel of Figure 1.9 shows the results. In all LHS panels, the horizontal axis is identical and scaled to be in units of δ . The MSM endowment calibration as well as the parameters controlling time preference are kept unchanged.

Panel A of Figure 1.9 shows that the average variance premium equals zero with DA preferences ($\delta = 1$). As δ is lowered, the variance premium increases and reaches the data value of 11.29 at the benchmark disappointment threshold of 0.9625. The reason for this effect is that the return variance is a convex function of the return itself, which implies that it is predominantly determined by extreme values. As the disappointment threshold is lowered, the utility function puts increasingly more weight on a smaller set of left-tail events, which are associated with large negative returns (see Section 1.4.4). Because variance swaps have high payoffs in these states, lowering δ increases the risk premium associated with them. Similar to the effect on the variance premium, both the level of the 1-month implied volatility curve (Panel C) and its slope (Panel E) are much too low for the DA model, increase as δ is lowered, and are close to their data counterparts for the benchmark calibration.²⁸ The level shift can be explained by the higher variance premium as well as the fact that lower δ values lead to more volatility feedback and therefore a higher return volatility. For example, the standard deviation of annual returns equals 14.7% for $\delta = 1$ and it increases to 18.2% for $\delta = 0.95$. The slope of the IV curve changes with the disappointment threshold for a similar reason as the variance premium, i.e. as δ is lowered, the agent's focus shifts toward more extreme returns, which makes put options with low strike prices particularly valuable.

In the second experiment, I illustrate the effect of changing the disappointment magnitude θ , and I adjust the curvature parameter α to hold the equity premium constant. The disappointment threshold δ is held fixed at the benchmark value of 0.9625. The results are shown in the right column of Figure 1.9, where the horizontal axis is scaled to be in units of θ . For $\alpha < 0$, the period utility function equals $u(x) = x^\alpha/\alpha$. The value $\theta = 0$, shown at the left end of the plots, corresponds to expected utility (EU) risk preferences, i.e. the most popular version of Epstein-Zin.²⁹ EU preferences imply a very low variance premium (Panel B), as well as an implied volatility curve that is both too low (Panel D) and too flat (Panel F) relative to the data. These results agree with those of previous studies that investigate option prices in the long run risks framework. As the disappointment magnitude is increased (and the curvature parameter lowered), risk aversion is increasingly

²⁸I define the slope as the IV with a relative moneyness of -2 minus the at-the-money IV.

²⁹The calibration is slightly different from the EU model in Section 3.4 because ρ is held fixed at the benchmark GDA calibration rather than that of the EU model. This is done to ensure that the benchmark GDA calibration appears among the considered cases.

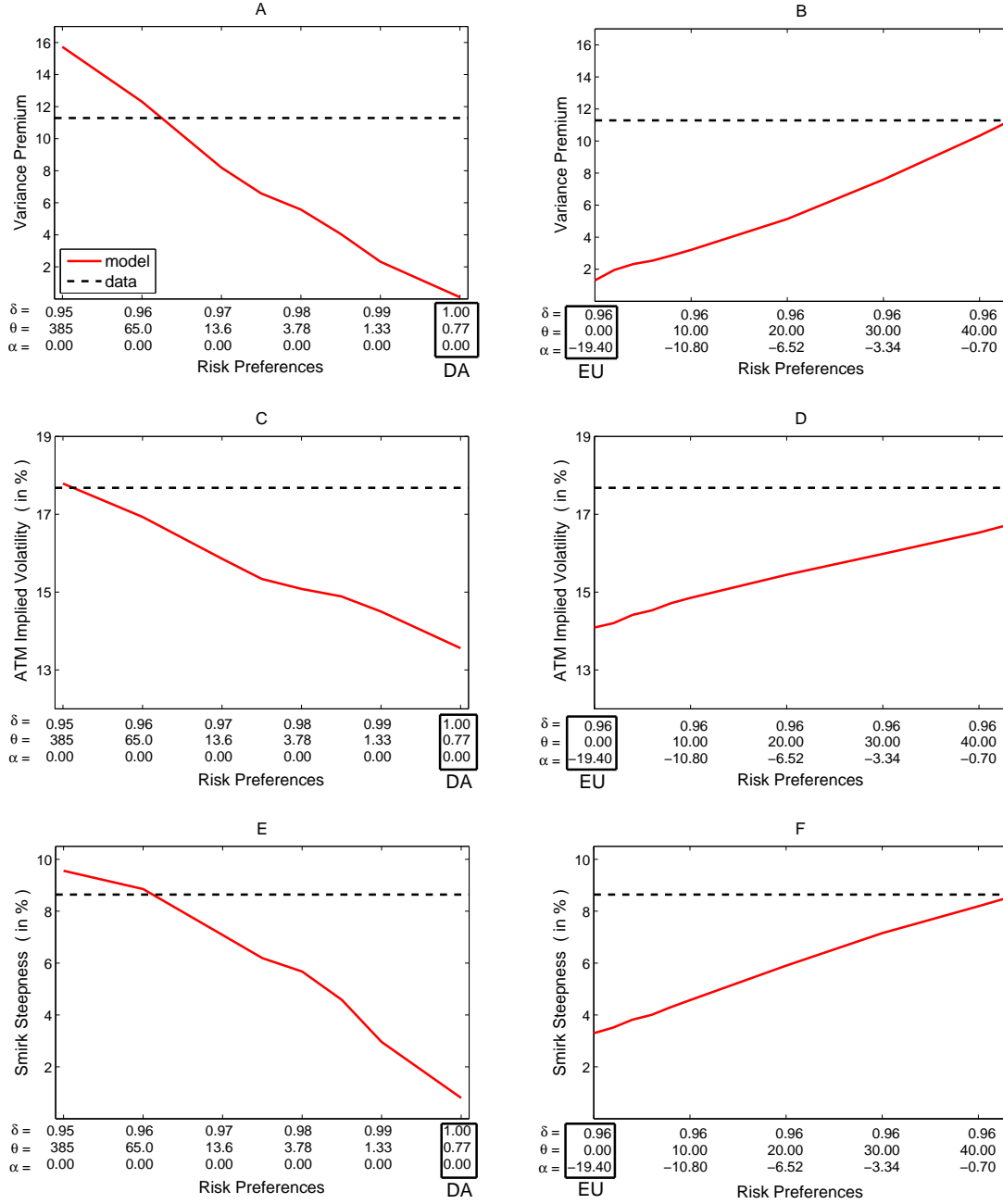


Figure 1.9: Tail Sensitivity of Preferences and Option Prices

Figure 1.9 shows how option-related moments change for different preference calibrations. All considered parameter combinations (shown on the horizontal axis) imply a mean annual equity premium equal to the historical average from 1930-2012. The graphs on the left consider changes in the disappointment threshold δ and include pure disappointment aversion ($\delta = 1$) as a special case. The graphs on the right consider changes in the disappointment magnitude θ and include expected utility risk preferences ($\theta = 0$) as a special case. Solid (red) lines show model-implied quantities, while dashed (black) lines show data equivalents. Panels A and B show the mean variance premium, Panels C and D show the at-the-money implied volatility, and Panels E and F show the steepness of the IV smirk, defined as the mean IV for options with a relative moneyness of -2 minus the mean IV for at-the-money options. Model-implied statistics equal small sample medians, computed as described in Section 1.3.3.

determined by aversion to tail outcomes, which moves all three statistics closer to their data counterparts. Taken together, the results in this section illustrate that matching average option prices clearly requires GDA preferences ($\delta < 1$ and $\theta > 0$).

1.5.2 The degree and nature of risk aversion of a GDA agent

What is the degree of effective risk aversion implied by the benchmark GDA calibration? How does the answer compare to the one for the nested risk preference specifications of pure disappointment aversion (DA) and expected utility (EU)? To answer these questions, I conduct a welfare analysis in the spirit of Lucas [1987]. Consider the following thought experiment. You are facing the consumption process described in Section 2.2 for $t, t+1, \dots$. Parameter values are calibrated as shown in Table 1.2. How much would you pay to eliminate the risk inherent in the consumption process? More precisely, suppose you were offered to trade your current endowment for a consumption stream with the same current level of consumption but no future shocks (so that $\Delta c_s = \mu$ for $s = t+1, t+2, \dots$). What is the maximum fraction of the mean consumption level that you would give up for this trade? Denote this fraction by Δ_t , and denote the value function evaluated at the alternative endowment by \bar{V}_t . Then Δ_t is defined by

$$\Delta_t = 1 - \frac{V_t}{\bar{V}_t} = 1 - \frac{\lambda_t^V}{\bar{\lambda}_t^V}, \quad (1.15)$$

where $\lambda_t^V = V_t/C_t$ and $\bar{\lambda}_t^V = \bar{V}_t/C_t$. For the deterministic endowment, there is no time-variation in the state, \bar{V}_t and $\bar{\mu}_t$ grow at a constant rate of e^μ , and nothing is disappointing. Using these facts, the value function can be computed in closed form³⁰, which allows me to write Equation 1.15 as

$$\Delta_t = 1 - \lambda_t^V \left(\frac{1 - \beta}{1 - \beta e^{\mu\rho}} \right)^{-\frac{1}{\rho}}. \quad (1.16)$$

Note that Δ_t depends on the state via λ_t^V . Similarly, Δ_t depends on risk preferences via λ_t^V . This latter fact allows me to use Δ_t to compare the degree of risk aversion across different risk preference calibrations. The results of this exercise are illustrated in Figure 1.10, where solid lines show the unconditional mean of Δ_t (the dashed lines will be discussed shortly). As in Section 1.5.1, all considered risk preference calibrations imply a mean equity premium equal to the historical mean.

The left panel considers changes in the disappointment threshold (δ) in order to contrast GDA with DA. The horizontal axis, which is identical to the one for the comparative

³⁰Dividing the certainty equivalent (Equation 1.5) by C_t implies that $\bar{\lambda}^\mu = \bar{\lambda}^V e^\mu$, which can be substituted into the value function (Equation 1.4) to yield $\bar{\lambda}^V = \left(\frac{1 - \beta}{1 - \beta e^{\mu\rho}} \right)^{\frac{1}{\rho}}$. Note that the value function is time-invariant in this case because there is no time-variation in the state.

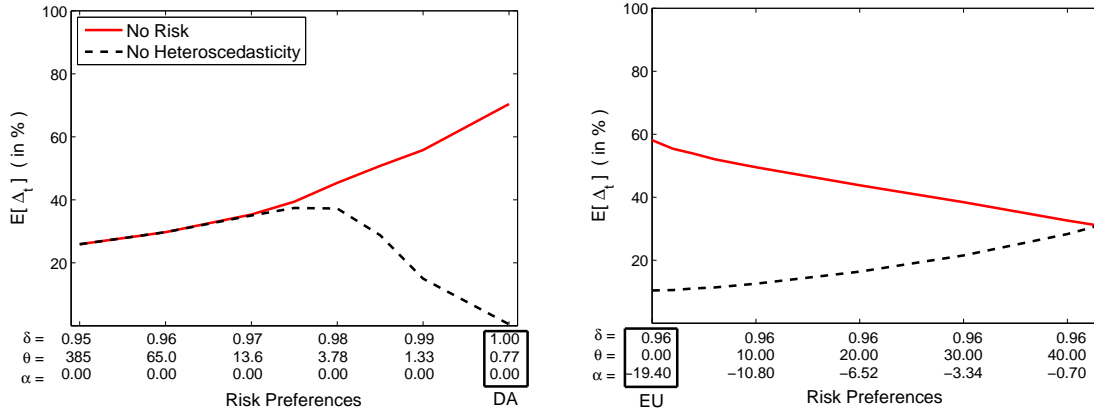
**Figure 1.10: Welfare measures**

Figure 1.10 shows welfare measures for different risk preference calibrations. All considered parameter combinations (shown on the horizontal axis) imply a mean annual equity premium equal to the historical average from 1930-2012. The endowment and time-preference parameters equal those of the benchmark GDA model calibration.

statics results in Figure 1.9, is scaled to be in units of δ . The equity premium is held constant by adjusting the disappointment magnitude (θ) for each value of δ (the curvature parameter α is held constant at the benchmark value of $\alpha = 0$). The figure shows that the degree of risk aversion, as measured by $E[\Delta_t]$, is monotonically and nearly linearly increasing in δ . GDA thus implies less risk aversion than DA.

The right panel considers changes in the disappointment magnitude (θ) in order to contrast GDA with EU risk preferences. The horizontal axis is scaled to be in units of θ . The equity premium is held constant by adjusting the curvature parameter, α , for each value of θ (the disappointment threshold δ is held constant at the benchmark value of $\delta = 0.9625$). In this case risk aversion is linearly decreasing in θ , which implies that a GDA agent is less risk averse than an agent with EU preferences. To the extent that a low level of risk aversion is preferred because it corresponds more closely to estimates commonly found in Microeconomic studies, GDA risk preferences appear preferable compared to either DA or EU preferences.

To gain a clearer understanding about the interaction between risk preferences and stochastic endowment volatility in determining effective risk aversion, I compute a second, related welfare measure. Specifically, I consider an alternative endowment that sets volatility constant, so that $\Delta c_{t+1} = \mu + \bar{\sigma} \varepsilon_{t+1}^c$. As above, I ask how much the agent would give up in order to trade the benchmark endowment for this alternative endowment.³¹ The results

³¹Different from the previous case, no closed-form solution exists for the value function for this alternative endowment, so that $\bar{\lambda}^V$ has to be computed numerically. The computation mimics the one for the benchmark model discussed in Section 1.3.2.

are shown with dashed lines in Figure 1.10. The following three features of the plot are helpful for understanding the mechanism of the GDA model:

1. (Left panel) The DA agent ($\delta = 1$) would give up close to nothing to eliminate the heteroscedasticity of his endowment (the dashed line is close to zero). The reason is that the disappointment threshold for DA equals the certainty equivalent, which implies that even outcomes close to the center of the distribution (of V_{t+1}) are considered disappointing. Shifting probability mass from the tails of the endowment distribution toward the center by removing stochastic volatility leads to no reduction in risk because these outcomes continue to be disappointing.
2. (Left panel) For sufficiently low disappointment thresholds (δ less than about 0.975), the GDA agent would give up just as much for eliminating stochastic volatility as he would give up for eliminating endowment risk all together (the two lines overlap for low δ 's). This is due to the fact that without stochastic volatility, the probability of extreme tail outcomes becomes very small, so that nearly no outcomes are disappointing. Specifically, the i.i.d. endowment implies an unconditional disappointment probability of less than once per 100,000 years and risk premia that are very close to zero. Eliminating stochastic volatility is therefore just as valuable as eliminating all risk.
3. (Right panel) Starting from EU ($\theta = 0$), increasing the disappointment magnitude increases the amount the GDA agent would give up for eliminating stochastic volatility. This holds true despite the fact that his overall degree of risk aversion (solid line) is decreasing in θ , which shows that tail risks account for a larger fraction of overall risk premia under GDA.

Overall, the results in this section illustrate that GDA implies somewhat less risk aversion than both DA and EU risk preferences. At the same time, the GDA agent is more averse to tail outcomes, generating a higher price of tail risk.

1.6 Conclusion

The model presented in this paper provides a parsimonious explanation for a broad set of stylized facts in equity and equity index option markets, including the implied volatility smirk. In times of low macroeconomic uncertainty, volatility feedback leads to substantial left-skewness in the conditional return distribution and the smirk arises from a relatively high probability of (endogenous) negative return jumps. In these states, the conditional disappointment probability is low and insurance premia play a minor role for option prices. In times of high uncertainty, the probability of disappointing tail events increases. Because

these events tend to coincide with negative returns, OTM put options provide a hedge against disappointments and a steep implied volatility smirk arises from the insurance premium in puts. In line with the empirical evidence in [Bollerslev and Todorov \[2011\]](#), equity and variance premia in the model arise primarily from the representative agent's aversion to tail risk. In particular, the model is able to increase the importance of tail risks without assuming a Peso problem. Lastly, model solutions for one-period options and variance swaps of arbitrary horizons can be obtained in closed form, which makes the framework suitable for structural estimation based on derivative data. This avenue will be explored in future work.

Chapter 2

Optimal Volatility Timing: A Life-Cycle Perspective

2.1 Introduction

Stock market volatility varies over time. How should investors use this fact in their asset allocation decisions? To what extent does the optimal allocation of savings to risky and riskless assets change over time to reflect changes in volatility? What is the economic value of “volatility timing”? In this paper, we study these questions in a life-cycle portfolio choice model.

We base our analysis on a fairly streamlined life-cycle framework which is extended to allow for heteroscedasticity in stock returns. In each period, a household with Epstein and Zin (1989) preferences receives stochastic labor income and chooses optimal consumption and portfolio shares subject to borrowing and short-selling constraints. Labor income includes both an individual-specific and an aggregate component where the latter is allowed to covary with the stock market (i.e. stock returns and volatility). The household can invest in a risk-free bond as well as in a risky stock. We estimate a joint process for returns, return volatility, and the aggregate component of labor income based on annual U.S. data from 1930 to 2012. Based on the estimated data generating process and a wide range of preference parameters, there are three main results: (a) Households are willing to give up as much as 1% - 1.5% of total life-time consumption to optimally condition on volatility.¹ (b) Variation in return volatility leads to strong reactions in investors’ optimal equity holdings. For instance, a negative one standard deviation volatility shock reduces the equity share by up to 17 percentage points. (c) A small increase in the correlation

¹This fee is relative to a benchmark strategy that conditions on age and wealth only.

between volatility and labor income (relative to the estimated value) can explain the low equity share by young households observed in the data.

Relative to the previous literature (reviewed in detail in the next section), one of our main contributions is to explicitly estimate a (significant) joint process for returns, volatility, and (aggregate) labor income. In addition to the well known negative return/volatility correlation², the interplay between stochastic volatility and labor income is particularly important for our results. Return volatility affects labor income growth both via the contemporaneous correlation in innovations and through its effect on the conditional mean. Both channels lead to a negative relationship between the investment opportunity set and the return on human capital.³ As returns become more volatile, current and future labor income tends to decrease. This renders human capital less bond-like and reduces households' equity holdings.⁴

We analyze the impact of stochastic volatility on households' optimal portfolio choices. We make three main findings with respect to the equity share. First, relative to conventional life-cycle models without stochastic volatility, investors' equity holdings decrease more rapidly over the early stages of the life cycle. This is due to the stronger (negative) relationship between returns and changes in human capital. Second, volatility is an important determinant of optimal portfolio shares. Whereas age is known to be a significant determinant for the optimal equity share, we show that volatility is almost equally important. Lastly, households reduce their equity share strongly in response to (positive) volatility shocks for two reasons. On the one hand and not surprisingly, stocks are now riskier and hence less attractive.⁵ On the other hand, a rise in volatility also reduces agents' human capital, which in turn amplifies the negative effect on stock holdings.

To judge the economic importance of stochastic volatility, we compute the dynamic consumption fee a household would be willing to pay to implement the optimal policies. We find that this fee lies between 0.95% and 1.58% of total life-time consumption. Interestingly, the fee tends to decline with higher values of both the investor's elasticity of intertemporal substitution (EIS) and the risk aversion coefficient. Even though the EIS does not impact optimal equity holdings, it plays an important role for the *economic value* of volatility timing. As low EIS investors have a high preference for smooth consumption,

²The fact is well known, and it is usually ascribed to either the leverage effect (Black [1976]) or the volatility feedback effect (see, e.g. French, Schwert, and Stambaugh [1987] and Campbell and Hentschel [1992]).

³Human capital is defined as the present discounted stream of future labor income.

⁴The bond-like behavior of human capital is a well known feature of conventional life-cycle models. See e.g. Cocco, Gomes, and Maenhout [2005].

⁵It is economically plausible to expect changes in risk (volatility) to be associated with changes in expected returns. This implies that stocks need not be less attractive when volatility is high. In the estimation we allow for this risk/return trade-off.

they are willing to sacrifice a lot to implement volatility timing.

The rest of the paper is organized as follows: In Section 2.1.1 we review the related literature. We set up the life-cycle framework in Section 2.2 and discuss the estimation results in Section 2.3. Section 3.4 shows the effects of stochastic volatility on portfolio decisions and welfare. Section 2.6 concludes.

2.1.1 Connections with Prior Literature

A small literature analyzes the implications of stochastic volatility for *asset allocation* decisions. Fleming, Kirby, and Ostdiek [2001] consider a short-horizon investor who allocates funds on a daily basis across stocks, bonds, gold, and cash. A mean-variance strategy based on a rolling window estimate of the conditional covariance matrix is shown to produce a higher Sharpe ratio than a strategy based on the unconditional covariance matrix. Fleming, Kirby, and Ostdiek [2003] show that the performance of this trading rule improves further when intra-daily return data is used in the estimation of the conditional covariance matrix. The mean-variance preference specification implies that the higher Sharpe ratio maps one-to-one into higher utility gains. Our paper also studies the economic value of volatility timing, but our framework considers the *dynamic* problem of a *long-horizon* (life-cycle) investor. Chacko and Viceira [2005] and Liu [2007] both analyze the effect of stochastic volatility in the portfolio choice problem of (unconstrained) long horizon investors in a continuous-time setting. Chacko and Viceira show that the intertemporal hedging demand resulting from stochastic volatility is quantitatively small for a recursive utility investor and a wide range of preference parameters. Liu [2007] studies a power utility investor and different processes for stochastic volatility and also finds modest hedging demands. Different from the latter two papers, we focus on the economic value of volatility timing rather than the magnitude of the intertemporal hedging demand.

Similar to Chacko and Viceira [2005], we estimate a data generating process based on low-frequency return data. However, in the spirit of Fleming, Kirby, and Ostdiek [2003], our estimation strategy additionally utilizes the information contained in high-frequency returns. Relative to Chacko and Viceira [2005], this results in a more precise estimate of the conditional return variance, which is reflected in (a) highly significant parameter estimates and (b) higher values for the estimated vol-of-vol and the correlation between return and volatility innovations. Chacko and Viceira [2005] show that higher values for these parameters increase the intertemporal hedging demand.

Our article also relates to the vast life-cycle literature (e.g. Cocco, Gomes, and Maenhout [2005], Gomes and Michaelides [2005], Gourinchas and Parker [2002], and Viceira [2001]),

which analyzes the optimal consumption and portfolio choice of households that are subject to non-insurable labor income shocks. These papers arrive at two main conclusions. First, optimal stock holdings heavily depend on age. Younger households optimally invest a lot in stocks because they hold large positions in human capital, which is perceived as relatively risk-free. As retirement approaches, human capital gradually diminishes and households reallocate funds from stocks to bonds. Second, the optimal equity allocation is highly sensitive to the correlation between income and stock returns. When this correlation is high, human capital is very similar to stocks and optimal portfolios incorporate a lower equity share. Our paper sheds additional light on these two main findings. First, we show that tilts in the optimal portfolio share induced by stochastic volatility are as pronounced as tilts induced by the life cycle. Second, we show that the correlation between return *volatility* and labor income is much larger than the one between returns and labor income. Reductions in labor income are therefore associated with a deterioration of the investment opportunity set, which makes labor income riskier than assumed in previous models.

Two recent papers investigate the implications of time-variation in the macroeconomic environment in a life-cycle framework. [Kojien, Nijman, and Werker \[2010\]](#) study the welfare gains a household can realize by exploiting bond return predictability and [Lynch and Tan \[2011\]](#) analyze optimal portfolios in the presence of business-cycle variation in the volatility of households' labor income shocks. Similarly, we contribute to the life-cycle literature by analyzing the effects of time-varying investment opportunities in the form of heteroscedasticity in stock returns.

2.2 Model

Environment

We consider a life-cycle investor who starts working at age 0, retires at age K , and lives for T periods. As is common, we interpret the modeled age as true age minus 20. Preferences are defined over a single consumption good and have the standard [Epstein and Zin \[1989\]](#) form,

$$V_t = [(1 - \beta)C_t^\rho + \beta\mu_t^\rho]^\frac{1}{\rho}, \quad (2.1)$$

where the certainty equivalent function

$$\mu_t = E_t [V_{t+1}^\alpha]^\frac{1}{\alpha} \quad (2.2)$$

is defined over random future utility using the time t conditional probability distribution. The conventional interpretation is that $\rho < 1$ captures time preference (the intertemporal elasticity of substitution is $1/(1 - \rho)$) and $\alpha < 1$ captures risk aversion (the coefficient of

relative risk aversion is $1 - \alpha$). Time-additive expected utility is a special case with $\alpha = \rho$. Log labor income is modeled as

$$y_t = \begin{cases} f_t + p_t & \text{if } t \leq K \\ \lambda + f_K + p_K & \text{if } t > K \end{cases} \quad (2.3)$$

$$p_t = p_{t-1} + e_t \quad (2.4)$$

where f_t is a deterministic function of age that captures the hump-shaped pattern in labor income over the life-cycle, $e_t \sim N(-\frac{1}{2}\sigma_p^2, \sigma_p^2)$ represents a shock to permanent labor income, and λ equals the (log) replacement ratio. The functional form implies that retired households receive a constant fraction of their last pre-retirement income. Following the previous life-cycle literature, we calibrate f_t to the average income of households in the Panel Study of Income Dynamics (PSID). It is common in the life-cycle literature to additionally include a transitory shock in the labor income process, but we omit this for parsimony because we find it to be quantitatively unimportant for our results.⁶

The agent can invest in two assets, a risk-free asset with constant log return r^f , and a risky asset whose excess log return and variance are given by

$$r_{t+1} - r^f = m_t + \sqrt{v_t} \varepsilon_{t+1}^r \quad (2.5)$$

$$\ln v_{t+1} = \gamma_0 + \gamma_1 \ln v_t + \sigma_v \varepsilon_{t+1}^v \quad (2.6)$$

where ε_t^r and ε_t^v denote standard normal innovations and m_t denotes the conditional expected excess return.⁷ Volatility is modeled as an AR(1) in logs rather than levels to allow for positive skewness, which results in occasional volatility spikes, as in the data. We allow for correlation between the innovations in p_t , r_t , and $\ln v_t$. Correlation between ε_t^r and ε_t^v captures the well-known leverage effect, i.e. the empirical regularity that market returns are negatively correlated with innovations in volatility. Correlation between ε_t^v and e_t captures business cycle variation in individual labor income.

The investor's (financial) wealth at age t , which we denote by X_t , evolves according to

$$X_{t+1} = S_t e^{r_{t+1}} + B_t e^{r^f} + e^{y_{t+1}}, \quad (2.7)$$

⁶We have solved a version of the model with idiosyncratic shocks, calibrated as in Cocco, Gomes, and Maenhout (2005). The addition of this shock has almost no effect on any of our quantitative results.

⁷In the estimation we allow the conditional mean to vary with return volatility.

where S_t and B_t denote the time t position in the risky asset and the risk-free asset respectively. The budget constraint is given by

$$X_t = C_t + S_t + B_t. \quad (2.8)$$

Finally, we impose the short selling restrictions

$$S_t \geq 0 \quad (2.9)$$

$$B_t \geq 0 \quad (2.10)$$

to prevent the agent to borrow against his future labor income.

Individual-Specific Parameters

The model is calibrated at an annual horizon. To parameterize the function f_t , we use the estimates for a “high-school individual” in [Cocco, Gomes, and Maenhout \[2005\]](#) which are based on PSID data. The deterministic income profile is modeled as:

$$f_t = \alpha_0 + \alpha_1 \tau + \alpha_2 \frac{\tau^2}{10} + \alpha_3 \frac{\tau^3}{100} \quad (2.11)$$

where $\tau = t + 20$ the household’s (true) age. The parameters are set to $\alpha_0 = -2.1700$, $\alpha_1 = 0.1682$, $\alpha_2 = -0.0323$, and $\alpha_3 = 0.0020$. Households retire at age $K = 65$ and receive a fraction $\lambda = 0.68212$ of their (last) pre-retirement income after that. For all quantitative results, we set the subjective discount rate to $\beta = 0.96$ and the standard deviation of the permanent labor shock to $\sigma_p = 0.15$.

We show most of our numerical results for a broad range for the coefficient of relative risk aversion γ and the EIS ψ . This is done to better understand the role of stochastic volatility for different preference specifications.⁸

Maximization Problem and Solution Method

The investor’s consumption savings problem is to maximize life-time utility (equations 2.1 and 2.2) subject to the laws of motion for labor income, stock returns, stock return volatility, and wealth (equations 2.3-2.7), as well as the budget constraint (equation 2.8) and the short selling and borrowing constraints (equations 2.9 and 2.10). Because the value function is linearly homogeneous, we can normalize V_t , e^{y_t} , X_t , S_t , and B_t by e^{p_t} , which reduces the number of state variables by one. The remaining state variables are age (t), return volatility (v_t), and normalized wealth ($X_t e^{-p_t}$). Because the agent dies with certainty after age T , we have $V_{T+1} = 0$. We can now use this value function to compute

⁸In few cases, we focus on the results for $\gamma = 10$ and $\psi = 0.5$ to make qualitative statements.

the policy rules for the previous period, and given these, obtain the corresponding value function. This procedure is then iterated backwards.

The model solution is based on a discretized state space with 50 grid points for normalized financial wealth ($X_t e^{p_t}$) and 21 grid points for $\ln v_t$. We confirmed that using a higher number of points has only a marginal effect on the solution. The grid for X_t is constructed so that points are denser for lower values, where the value function has more curvature. The grid for $\ln v_t$ consists of Gaussian quadrature nodes. Cubic spline interpolation is used to evaluate the value function at off-grid values. Expectations over $(e_t, \varepsilon_t^r, \varepsilon_t^v)$ are evaluated using a trivariate Gaussian quadrature with 5 nodes for each e_t and ε_t^r and 11 points for ε_t^v . Once again, increasing the number of nodes has a very small effect on the solution. While the agent has to choose consumption as well as his holdings of both the risk-free asset and the risky asset, the budget constraint (equation 2.8) implies that there are only two independent choices. We maximize over consumption and the equity share $E_t \equiv \frac{S_t}{S_t + B_t}$, which has the advantage that it is bounded between 0 and 1. To carry out the maximization, we use an iterated grid search method that starts with a relatively rough grid and then moves to subsequently finer grids in determining the utility maximizing choices for C_t^* and E_t^* .

Model Simulation

To illustrate the quantitative implication of the model, we simulate a cross-section of 1 million households and compute “population” moments by averaging across households. We follow Wachter and Yogo [2010] in drawing an initial level of wealth (relative to permanent income) from a lognormal distribution for each household. Based on Wachter and Yogo’s estimates for the subsample of stockholders in the Survey of Consumer Finances, we set the mean of normalized wealth to 0.988 and the standard deviation of its logarithm to 1.370. Given draws for initial normalized wealth ($X_t e^{-p_t}$) and log return variance ($\ln v_t$), we then iterate through the life-cycle, draw a set of shocks $(e_t, \varepsilon_t^r, \varepsilon_t^v)$ at each age, and use linear interpolation to evaluate policies at off-grid values for wealth and variance. After the simulation, we reverse the normalization of all variables by using the simulated paths for p_t .

2.3 Estimation

We estimate the joint process for the shock to permanent labor income (equation 2.4), stock returns (equation 2.5), and return variance (equation 2.6) based on annual U.S. data from 1930-2012. Labor data is taken from the BEA, and our definition of aggregate labor income is identical to the one in Lettau and Ludvigson [2001]. We use value-weighted returns on the CRSP portfolio to measure the return on the risky asset and the 90 day

Treasury yield to measure the risk-free rate.

Following [Campbell, Cocco, Gomes, and Maenhout \[2001\]](#), we decompose the permanent labor income shock (in equation 2.4) as

$$e_{it} = -\frac{1}{2}\sigma_p^2 + \xi_t + \omega_{it},$$

where $\omega_{it} \sim N(0, \sigma_\omega^2)$ represents an idiosyncratic component and $\xi_t \sim N(0, \sigma_\xi^2)$ represents an aggregate component.⁹ We assume that individual labor income covaries with aggregate variables (stock returns and stock return volatility) only through its aggregate component, and we estimate the covariance structure based on (de-meaned) aggregate labor income growth. Our estimates can therefore be interpreted as the average covariances across the U.S. workforce.¹⁰

An important issue in estimating the data generating process is that most stochastic volatility models – including ours – yield insignificant parameter estimates when estimated based on low-frequency return data alone.¹¹ To overcome this problem, we adopt an estimation strategy that utilizes the information contained in *daily* returns. In particular, we incorporate a “measurement equation” that relates the conditional variance of annual returns to the annual realized variance.¹² The measurement equation is given by

$$\log(RV_{t+1}) = \theta + \log(v_t) + \sigma_{RV}\varepsilon_{t+1}^v, \quad (2.12)$$

where RV_t denotes the realized variance in year t , defined as the sample variance of daily returns. The assumption underlying equation 2.12 is that the conditional variance of the annual return also determines the conditional mean of realized variance over the year.¹³

⁹Note that $\sigma_p^2 \equiv \text{Var}(e_{it}) = \text{Var}(\xi_t + \omega_{it}) = \sigma_\xi^2 + \sigma_\omega^2$. We set $E[e_{it}] = -\frac{1}{2}\sigma_p^2$ to ensure that $E[\exp(e_{it})] = 1$.

¹⁰An alternative would be to estimate the average covariance structure based on a panel data set. For example, [Campbell, Cocco, Gomes, and Maenhout \[2001\]](#) regress the average income growth rate across households in the Panel Study of Income Dynamics (PSID) data on the (de-meaned) excess stock returns in order to estimate the correlation between individual labor income and returns. By averaging across households, idiosyncratic shocks “wash out”, so that the resulting estimate can be interpreted as the average correlation across households. Compared to this approach, aggregate data has the advantage that it reflects a larger population and that it is available for a longer sample. A disadvantage is that we are not able to compute the correlations for different educational groups, which is possible in the PSID data.

¹¹As an example of this problem for monthly and annual data, see the estimation results in Table 1 of [Chacko and Viceira \[2005\]](#).

¹²A number of recent papers have used a similar approach for estimating stochastic volatility models based on daily data (see [Hansen, Huang, and Shek \[2012\]](#), [Koopman and Scharth \[2013\]](#), and [Christoffersen, Feunou, Jacobs, and Meddahi \[2013\]](#)). This literature computes the daily realized variance from intra daily data, and incorporates it into a measurement equation for the conditional variance of daily returns. We apply the same idea to low frequency data and augment the model with a third equation for labor income.

¹³We include an intercept because the average realized variance of daily returns differs noticeably from the standard deviation of annual returns in our sample. Without a constant, the average value of v_t would be forced to equal the average realized variance.

Table 2.1: Maximum Likelihood Estimates of the DGP

$$\begin{aligned}
r_{t+1} - r^f &= \bar{r} + \chi^r \left(\log(v_t) - \frac{\gamma_0}{1 - \gamma_1} \right) + \sqrt{v_t} \varepsilon_{t+1}^r \\
\log(v_{t+1}) &= \gamma_0 + \gamma_1 \log(v_t) + \sigma_v \varepsilon_{t+1}^v \\
\xi_{t+1} &= \chi^\xi \left(\log(v_t) - \frac{\gamma_0}{1 - \gamma_1} \right) + \sigma_\xi \varepsilon_{t+1}^\xi \\
\log(RV_{t+1}) &= \theta + \log(v_t) + \sigma_{RV} \varepsilon_{t+1}^v
\end{aligned}$$

Parameter	\bar{r}	χ^r	γ_0	γ_1	χ^ξ	θ
Estimate	0.053	0.009	-1.639	0.512	-0.021	-0.635
t-statistic	[2.107]	[0.120]	[-3.297]	[3.666]	[-1.910]	[-3.203]
Parameter	σ_v	σ_ξ	σ_{RV}	$\text{corr}[\varepsilon^r, \varepsilon^v]$	$\text{corr}[\varepsilon^r, \varepsilon^\xi]$	$\text{corr}[\varepsilon^v, \varepsilon^\xi]$
Estimate	0.460	0.059	0.697	-0.537	0.130	-0.329
t-statistic	[7.119]	[21.161]	[10.472]	[-6.090]	[1.222]	[-2.395]

Table 2.1 shows maximum likelihood parameter estimates and t-statistics based on asymptotic standard errors for the process driving stock returns, volatility, and the aggregate component of labor income. Innovations are assumed to be normally distributed, correlated with each other within a period, and serially uncorrelated. Annual and daily returns are value-weighted CRSP returns. Realized variance is computed as the sample variance of daily returns within each year. Annual labor income, which is defined as in [Lettau and Ludvigson \[2001\]](#), is taken from the BEA, it is deflated using the CPI, and log growth rates are de-meant before the estimation. The sample spans 1930-2012.

Realized variance – which is observable – can therefore be used to estimate the current value of the latent variance. Instead of describing variance as a weighted average of past squared returns – as in standard GARCH models – our model implies that variance equals a weighted average of past realized variance.¹⁴ Because the realized variance of daily returns is a better proxy for the latent return variance than the squared annual return, we obtain a more accurate estimate of the latent variance. As we show next, this results in highly significant estimates of the parameters that govern volatility dynamics.

As in [Lynch and Tan \[2011\]](#), we allow the conditional means of both returns and the aggregate component of permanent labor income growth to change over the business cycle. While Lynch and Tan specify that these conditional means depend on the dividend yield, we model them as varying with volatility. The first channel captures the risk-return trade-off whereas second channel captures countercyclicality in expected labor income growth. The functional forms for both conditional means are shown in table 2.1.

¹⁴To see this, note that we can write $\log(v_t) = \gamma_0 + \gamma_1 \log(v_{t-1}) + \sigma_v \left[\frac{\log(RV_t) - \theta - \log(v_{t-1})}{\sigma_{RV}} \right] = \left[\gamma_0 - \theta \frac{\sigma_v}{\sigma_{RV}} \right] + \left[\gamma_1 - \frac{\sigma_v}{\sigma_{RV}} \right] \log(v_{t-1}) + \frac{\sigma_v}{\sigma_{RV}} \log(RV_t) = \dots = \text{const.} + \frac{\sigma_v}{\sigma_{RV}} \sum_{i=0}^{\infty} \left[\gamma_1 - \frac{\sigma_v}{\sigma_{RV}} \right]^i \log(RV_{t-i})$.

Maximum likelihood estimates for the joint process are shown in Table 2.1. The estimates of the unconditional mean of excess returns (\bar{r}) and the parameters governing the volatility dynamics ($\gamma_0, \gamma_1, \sigma_v$) are all statistically significant. Furthermore, the mean effect of volatility on labor income growth (χ^ξ) is negative and significant at the 10% level. As in much of the existing literature, the risk-return tradeoff (χ^r) is insignificant. The estimates imply a mean equity premium of 5.3%, an unconditional excess return volatility of 20.0%, and a first-order autocorrelation of 47.7% for the *conditional* return volatility. For comparison, the historical equity premium in our sample equals 5.4%, the excess return volatility equals 19.9%, and the first-order autocorrelation of annual *realized* volatility equals 67.5%.

Like many previous studies, we find the correlation between innovations in volatility and innovations in returns to be negative. Interestingly, despite the low annual frequency of our model, the coefficient is highly statistically significant with a t -statistic of -6.090 . This results from the fact that we incorporated information from daily return data, which leads to a much more precise volatility estimate compared to estimates that are filtered from annual data alone. Because negative returns are associated with a deterioration of the investment opportunity set (higher volatility), equity in our model is riskier than in models without stochastic volatility.

Innovations in volatility are also significantly negatively correlated with innovations in the aggregate component of labor income, with a point estimate of -0.329 and a t -statistic of -2.395 . Labor income is therefore riskier than in models without stochastic volatility. Lastly, we find the correlation between innovations in returns and innovations in the aggregate component of labor income to be positive but insignificant. We calibrate the standard deviation of the total innovation in labor income, $\text{std}(\xi_t + \omega_{it})$, to 0.15, the value used in Gomes and Michaelides [2005]. Together with the estimate of $\text{corr}[\varepsilon^r, \varepsilon^\xi]$, this implies a correlation of 0.051 between the innovation in returns and the total innovation in labor income.¹⁵ The value of this correlation is very important for the model's implications for the equity share, because it determines how “stock like” labor income behaves. A higher correlation implies that household prefer to hold less equity. Because estimates in previous papers span a fairly wide range of values, we investigate the robustness of our main results with respect to this number in Section 2.4.3.

¹⁵ $\text{corr}[\xi_t + \omega_{it}, r_t] = \frac{\text{cov}[\xi_t + \omega_{it}, r_t]}{\text{std}[\xi_t + \omega_{it}] \times \text{std}[r_t]} = \frac{\text{cov}[\xi_t, r_t]}{\text{std}[\xi_t + \omega_{it}] \times \text{std}[r_t]} = \frac{\text{corr}[\xi_t, r_t] \times \text{std}[\xi_t] \times \cancel{\text{std}[r_t]}}{\text{std}[\xi_t + \omega_{it}] \times \cancel{\text{std}[r_t]}} = \frac{0.130 \times 0.059}{0.150} = 0.051.$

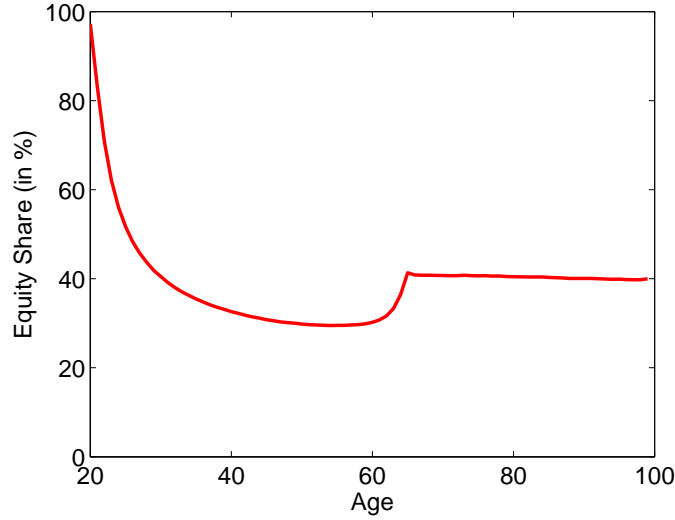


Figure 2.1: The Equity Share over the Life-Cycle

Figure 2.1 shows the life cycle profile of average equity holdings for $\gamma = 10$ and $\psi = 0.5$.

2.4 Results

In Section 2.4.1, we characterize optimal portfolio shares in the presence of stochastic volatility. Section 2.4.2 shows the utility gains an investor can achieve by optimally conditioning on volatility. We discuss the effects of cross-sectional heterogeneity (in labor income) on equity holdings for young households in Section 2.4.3.

2.4.1 Optimal Life-Cycle Portfolio Choice with Stochastic Volatility

Figure 2.1 displays the optimal allocation to stocks and bonds over the life cycle. To construct the plot, the equity share, $S_t/(S_t + B_t)$, is averaged over different values of wealth, volatility, and permanent income at each age. The graph shows that the optimal equity share decreases over the life cycle. Early in life, most agents invest fully in stocks and hit the borrowing constraint. This is explained by their large position in human capital, which is a closer substitute for bonds than for stocks. As human capital is gradually depleted over time, agents start investing in bonds. Relative to many previous life-cycle models (e.g. Cocco, Gomes, and Maenhout [2005] and Gomes and Michaelides [2005]), the equity decreases earlier and at a higher rate in our model. This indicates that the presence of stochastic volatility leads to a faster depletion of investors' human capital. As a result, their *implicit* bond position decays quickly so that they shift more funds away from stocks towards bonds.

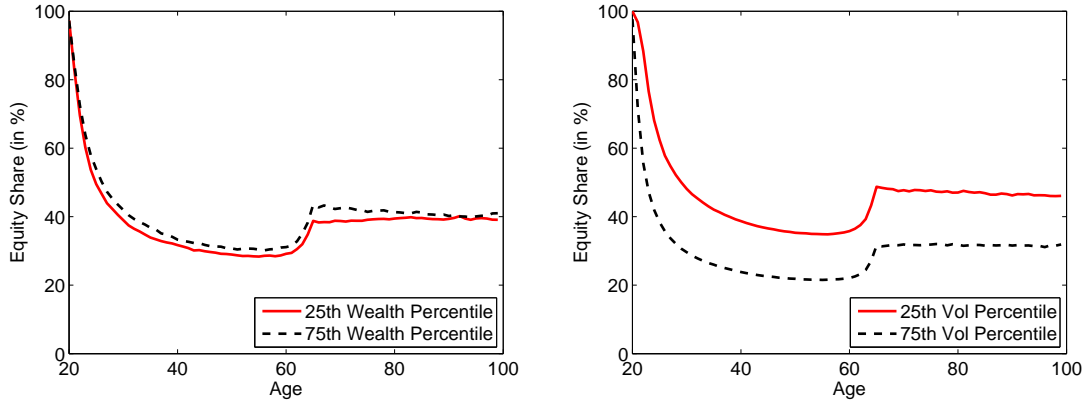


Figure 2.2: Tilts in the Optimal Equity Share

Figure 2.2 shows tilts in the optimal equity share for $\gamma = 10$ and $\psi = 0.5$. Wealth and volatility percentiles are age-specific.

Figure 2.2 shows the response of the optimal *conditional* asset allocation to changes in financial wealth and conditional volatility. The left panel shows the equity share for investors in the 25th and 75th (age-specific) wealth percentile, respectively. It is apparent that wealth has very little effect on the optimal portfolios. For example, a 40-year-old investor in the 25th wealth percentile optimally holds 32% in equity, and the fraction increases only to 34% in the 75th wealth percentile. The right panel shows the optimal equity share in the 25th and 75th percentiles of volatility. In contrast to wealth, volatility is a very important state variable for optimal portfolios. A 40-year-old investor optimally holds 39% in equity when volatility is at its 25th percentile and 24% when volatility is at its 75th percentile. Interestingly, this inter-quartile spread is relatively constant over the life cycle.

To better understand the dynamic response of households' optimal choices to different types of shocks, we plot impulse response functions for a 40-year-old household. Figure 2.3 shows the results for the equity share (first row), the consumption-wealth ratio (second row), and the ratio of human capital to total wealth (third row). We study the dynamics of these quantities in response to orthogonal one standard deviation shocks to returns (first column), permanent labor income (second column), and log-volatility (third column).

We observe that a positive return shock leads to negative responses for all three variables. In particular, the equity share decreases by about 0.5% on impact and returns slowly to its pre-shock level. The response in the consumption-wealth ratio is weaker, but more persistent. The economic mechanism can be best understood by looking at the last figure in the first column. As mentioned earlier, the human capital share measures the households' implicit holding of a risk-free asset. Since a positive return shock decreases only the

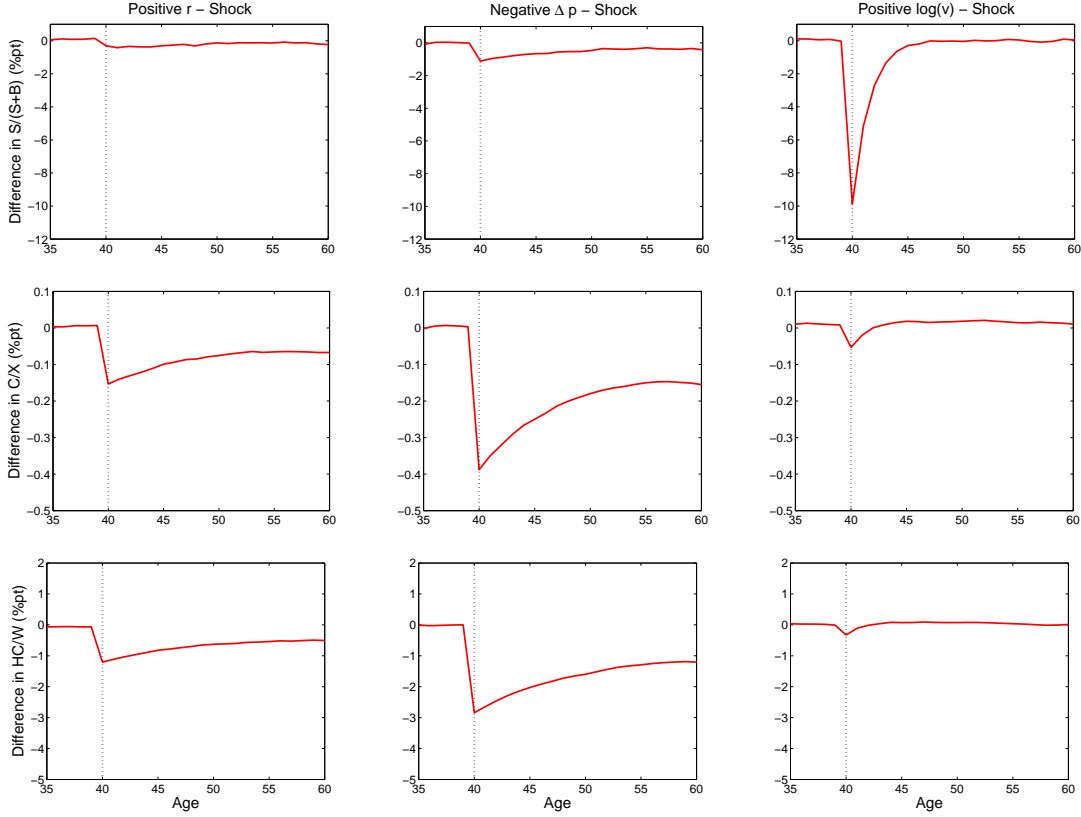


Figure 2.3: Impulse Response Functions

Figure 2.3 shows how the equity share (first row), the consumption-wealth ratio (second row), and the human capital share (third row) react to a one standard deviation shock in the innovation to returns (ε^r), the innovation in permanent labor income (ε^p), and the innovation in log-volatility (ε^v), respectively. The left column considers return shocks, the middle column considers labor income shocks, and the right column considers volatility shocks. The plots show the impact of the shocks at age 40. We computed the average difference in the two series (shocked and un-shocked) across all sample paths. We used $\gamma = 10$ and $\psi = 0.5$ for all plots.

denominator (expected future labor income remains unaffected¹⁶), this ratio goes down. Consequently, investors hold a lower implicit position in the risk-free asset. This, in turn, increases their demand for bonds which leads to a decline in the equity share. As human capital slowly returns to its stationary value, the (negative) impact on equity holdings diminishes as well. Interestingly, the consumption-wealth ratio falls only by about 0.15%. Thus, households use a small part of the growth in wealth, to increase consumption. The remainder is used as precautionary savings.

Turning to the second column, we observe that a *negative* income shock leads to the same patterns as a *positive* return shock. Thus, both equity holdings and the consumption-wealth ratio decrease persistently. Again, the first is affected more strongly than the latter. Again, the human capital share is key to understanding these responses. A negative shock to *permanent* income reduces households' expected future income stream and

¹⁶Note that there is also a “discount rate” effect on human capital as household's consumption stream is affected by the shock. However, this effect is (numerically) relatively small in our setup.

Table 2.2: Volatility Shocks and the Optimal Equity Share

$\psi \backslash \gamma$	Age = 25		Age = 40		Age = 55		Age = 70	
	5	10	5	10	5	10	5	10
$1/\gamma$	-0.40	-15.60	-16.08	-9.79	-16.85	-8.59	-15.59	-10.40
0.5	-0.60	-15.67	-16.08	-9.94	-16.82	-8.87	-15.61	-11.42
1.5	-1.42	-15.32	-16.55	-10.29	-16.82	-9.38	-15.28	-13.60

Table 2.2 shows the impact of a one standard deviation shock to log volatility on the equity share for different preference specifications and different stages of the life cycle.

therefore their human capital. As a result, the human capital share drops by almost 3% on impact. Similar to before, this implies a lower implicit holding of debt through human capital which reduces investors' demand for equity. In anticipation of lower future income, agents reduce the consumption share and increase precautionary savings.

The third column shows the responses to a positive volatility shock. There are two main differences compared to the return and income shock discussed before. First, the equity share drops dramatically by about 10% as the shock is realized. Second, the effect on the both the consumption-wealth and the human capital ratio are only modest. Hence, the unexpected rise in volatility mainly affects the bond/equity trade-off. There are two economic mechanisms behind this result. On the one hand, higher volatility renders equity riskier and hence less attractive. On the other hand, the last figure in the third column shows that a volatility shock also negatively affects households' human capital share. Intuitively, higher volatility today (and in future periods) raises investors' marginal utility and therefore leads to a lower value of discounted labor income (human capital). Consequently, households implicitly hold less of the risk-free asset. Both channels imply less demand for stocks and thus a lower equity share.

Figure 2.3 illustrated that, for a particular preference calibration, the optimal equity share is reduced significantly after a positive shock to volatility. In Table 2.2, we show that the same conclusion continues to hold for a broad set of alternative preference parameters. Here we present the response in the equity share as volatility is shocked by one standard deviation for three ages, two levels of risk aversion (γ), and three levels of elasticity of intertemporal substitution (ψ). We can observe that changes in ψ only imply minor changes in the optimal equity share. A change in γ , however, leads to strongly different responses. At age 25 investors with low risk aversion ($\gamma = 5$) are mostly borrowing constrained, i.e. their actual unconstrained equity share greatly exceeds 100%. Therefore, only a small group of agents is unconstrained which enables them to respond to changes in volatility. For $\gamma = 10$ most agents are not constrained and hence an increase in volatility leads to a large response in the equity share. At higher ages when more or less all agents

Table 2.3: The Economic Value of Volatility Timing

$\gamma \backslash \psi$	$1/\gamma$	0.5	1.5
5.0	1.58	1.50	1.38
10.0	1.43	1.21	0.95

Table 2.3 shows the consumption fee (defined in equation (2.13)) as a percentage of life-time consumption.

are unconstrained, less risk averse investors reduce their equity holdings more. This can be explained by the fact that these investors have a weaker desire to build up a buffer stock against negative future shocks.

2.4.2 The Economic Value of Volatility Timing

In the previous section we showed that changes in the conditional stock market volatility have a strong effect on households' optimal asset allocation. We next examine the economic benefit of following this “volatility-timing” strategy. Specifically, we consider a benchmark strategy that conditions on age and wealth (as, e.g. in Cocco, Gomes, and Maenhout [2005] and Gomes and Michaelides [2005]), and we compute the utility gain a household can realize by additionally conditioning on volatility.

Denote the value function corresponding to the optimal policies by $V(X, t, v)$ and the value function corresponding to the benchmark policies by $\tilde{V}(X, t, v)$.¹⁷ We define the utility gain as

$$\chi(X, v) \equiv 1 - \frac{\tilde{V}(X, 0, v)}{V(X, 0, v)}, \quad (2.13)$$

which equals the maximum proportional consumption fee that a 20-year-old household is willing to pay in order to implement the optimal policies over his life time. Stated differently, if a household is allowed to condition on volatility but simultaneously has to relinquish the fraction χ of his current and future consumption (in every state), he would be indifferent to following the benchmark strategy.¹⁸

Table 2.3 presents the consumption fee for different combinations of relative risk aversion (γ) and EIS (ψ). Results are averaged over both wealth and volatility. The table shows that for $\gamma \in \{5, 10\}$ and $\psi \in \{\frac{1}{\gamma}, 0.5, 1.5\}$, households would give up between 0.95% and

¹⁷Note that, even though the suboptimal policies are independent of volatility, \tilde{V} does in general depend on v_t . This is due to the dependence of the conditional expectation on $\ln v_t$.

¹⁸An equivalent interpretation is that the fee represents the maximum fraction of total wealth (present discounted value of future consumption) that the household would pay in order to optimally condition on volatility.

1.58% of their total wealth in order to optimally condition on volatility. We observe two basic patterns: fees are decreasing in both γ and ψ . The decrease in γ can be explained by the fact that less risk-averse agents react more strongly to changes in volatility (see Table 2.2). As a result, the welfare gain from conditioning on volatility is larger for agents with a smaller γ . In contrast, the results presented in Table 2.2 indicate that changes in ψ do not lead to different responses in investors' portfolios. Nonetheless, Table 2.3 shows a large spread in fees across different values for ψ . This can be reconciled by the fact that agents with a low ψ coefficient are very reluctant to substitute consumption over time. Volatility timing allows agents to reduce the variance of total financial wealth (and hence consumption) by changing the equity share as volatility changes. Therefore, volatility timing is more valuable for households with a low EIS.

To put the magnitude of the consumption fee into perspective, we compare it to the results in Cocco, Gomes, and Maenhout [2005]. These authors construct a life-cycle model similar to ours but with time-additive power utility and homoscedastic returns. They compute the consumption fee for optimally conditioning on age and wealth relative to a benchmark that utilizes the popular practitioner portfolio allocation rule “equity share = 100 – age”. For a coefficient of relative risk aversion of 10 and various perturbations of the economic environment, Cocco, Gomes, and Maenhout find fees between 0.28% and 1.07%. Our finding for the same value of γ exceeds the upper end of this range. Ignoring time-variation in volatility can therefore be considered more costly than following a rule of thumb in an environment without stochastic volatility.

2.4.3 Household Heterogeneity and the Equity Share of Young Households

Identifying the empirical relationship between age and average equity holdings is difficult because age, time, and cohort effects cannot be separately identified. Nevertheless, existing evidence suggests that the equity share is approximately constant among different age groups (see Gomes and Michaelides [2005]). Contrary to this finding, standard life-cycle models predict that young households should hold close to 100% of their investments in equities.¹⁹ In this section, we analyze whether cross-sectional differences in the correlation between individual labor income and aggregate variables (returns and volatility) may be

¹⁹It is not clear whether this is a result of suboptimal behavior or model-misspecification. Nevertheless, one focus of the more recent life-cycle literature has been to find model mechanisms to explain the low average equity holdings of young households. In particular, Gomes and Michaelides [2005] achieve low equity holdings at young ages through the combination of (fixed) stock market participation costs and investor heterogeneity. Lynch and Tan [2011] get a similar result by introducing counter-cyclical labor income volatility and predictability in stock returns. On the other hand, Benzoni, Collin-Dufresne, and Goldstein [2007] assume a cointegrating relationship between labor income and dividends in order to increase the correlation between stock returns and changes in human capital. This makes human capital more stock-like, especially for young households.

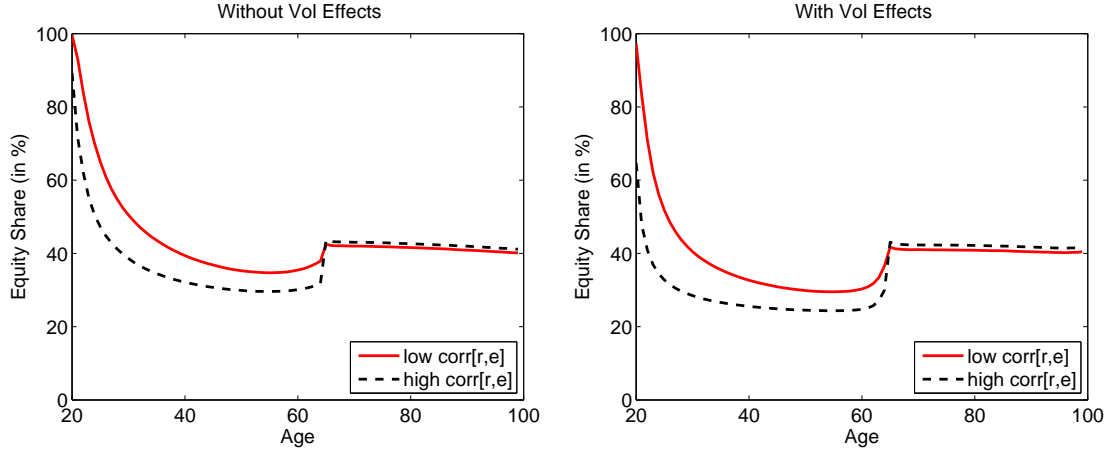


Figure 2.4: The Effect of Different Parameter Values on the Equity Share

Figure 2.4 shows the average equity share (as a function of age) for different values of $\text{corr}[\varepsilon_t^r, e_t]$. The first value equals our estimate (based on aggregate labor data). The second value of 0.15 equals the value considered in Gomes and Michaelides [2005]. In the left panel, we show a calibration with $\text{corr}[v, r] = \text{corr}[v, e] = \chi^r = \chi^e = 0$, so that volatility is independent of both labor income and returns. The right panel shows the benchmark model. We used $\gamma = 10$ and $\psi = 0.5$ for both plots.

able to account for the low equity share of young households.

In our first experiment, we examine how the optimal equity share responds to perturbations in the correlation between innovations in returns and labor income ($\text{corr}[\varepsilon_t^r, e_t]$). As discussed in Section 2.3, we estimate a value of about 0.05 for this correlation based on aggregate labor data. However, it is well-known that there exists large cross-sectional heterogeneity in the data. For example, Davis and Willen [2000a,b] find that the correlation increases with education and ranges from about -0.25 to 0.25 . Because our model focuses on stockholders, and because stock-ownership is strongly positively correlated with education, it appears reasonable to consider a value that exceeds our empirical estimate. In Figure 2.4, we set $\text{corr}[\varepsilon_t^r, e_t]$ to 0.15, the value used in Gomes and Michaelides [2005]. The left panel shows the effect for a model in which volatility is independent of both returns and labor income.²⁰ Confirming results in the prior literature, the increase in $\text{corr}[\varepsilon_t^r, e_t]$ has a negative but small effect on the equity share.²¹ In particular, the effect is very similar at different stages of the life-cycle. The right panel of Figure 2.4 shows how the increase in $\text{corr}[\varepsilon_t^r, e_t]$ effects the equity share in the benchmark model (for which volatility is correlated with labor income and returns). We find that it has a considerably larger effect on young households than in the model with independent volatility. For example, while equity share decreases from 99.6% to 89.3% in the later model, it drops from 97.2%

²⁰Specifically, we set $\text{corr}[v, r] = \text{corr}[v, e] = \chi^r = \chi^e = 0$ in the alternative model. Note that this model still features heteroscedastic stock returns.

²¹Benzoni, Collin-Dufresne, and Goldstein [2007] show that this is due to the fact that the long-run correlation between stock returns and changes in human capital are too low.

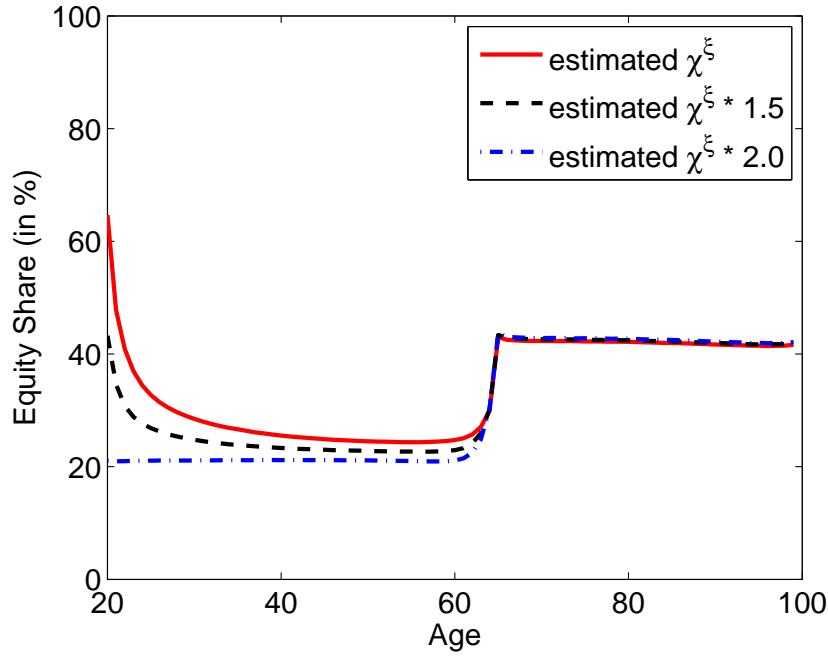


Figure 2.5: The Effect of Changing χ^ξ

Figure 2.5 shows the average equity share (as a function of age) for different values of χ^ξ . The value of $\text{corr}[r, e]$ is set to 0.15 in all three scenarios. We used $\gamma = 10$ and $\psi = 0.5$.

to 64.7% in the benchmark model.

Encouraged by the previous results, our second experiment examines the effect of a perturbation in the correlation between labor income and return *volatility*. Because labor income of stockholders is known to have an above-average correlation with returns, it is reasonable to assume that it is also more correlated with return volatility. In Figure 2.5, we continue to use a value of 0.15 for $\text{corr}[\varepsilon_t^r, e_t]$, and we simultaneously increase the effect of volatility on the conditional mean of labor income growth (χ^ξ) by either 50% or 100%. We observe that increases in χ^ξ result in a flatter life-cycle profile, i.e. they have a larger effect on the equity share of young households than on the equity share of middle-aged households.

The results presented in this section show that heteroscedasticity in stock returns represents a potential explanation for the low equity share of young households. However, the findings are only suggestive because we have not explicitly estimated the correlation between individual labor income and volatility based on household level income data. We leave a more detailed examination of this issue for future research.

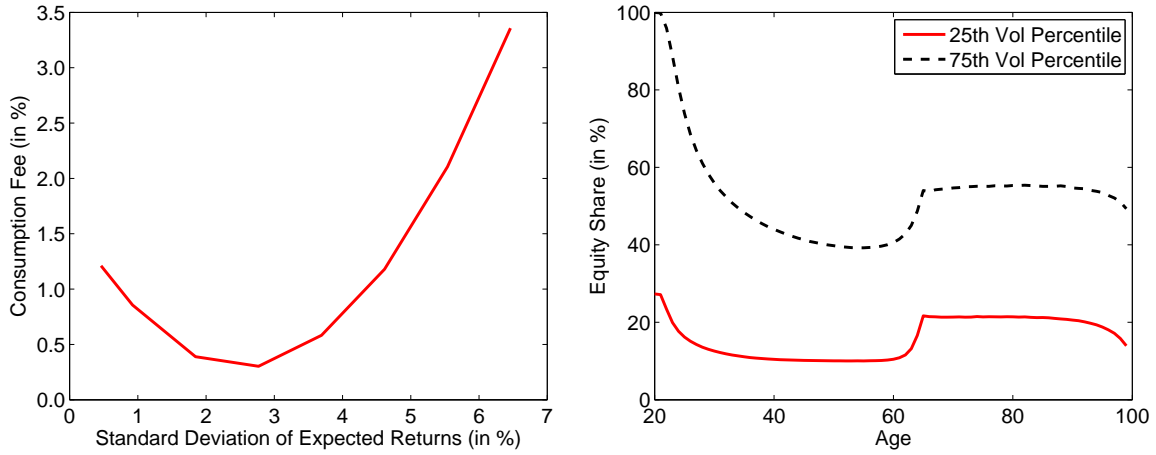


Figure 2.6: Return Predictability and Volatility Timing

Figure 2.6 shows the effect of an increased degree of return predictability. The left panel shows the economic value of volatility timing (defined in Equation 2.13) as a function of the standard deviation of expected returns. The right panel shows the optimal equity share as a function of age for different volatility percentiles for the highest considered degree of return predictability. Preference parameters are set to $\gamma = 10$ and $\psi = 0.5$.

2.5 Discussion

2.5.1 The Degree of Return Predictability

The estimation results in Section 2.3 imply a negligible risk-return trade-off, i.e. expected returns do not fluctuate significantly with the conditional return volatility. While this finding is in line with much of the prior empirical literature, it is conceivable that predictability is simply hard to detect in small samples due to a large degree of noise in realized returns. In this section, we therefore evaluate how the economic value of volatility timing changes when one allows for a tighter relationship between risk and return, as it is implied by many leading asset pricing models.²²

Note that the degree of return predictability in our model is controlled by the parameter χ^r . The estimated parameter value implies that expected excess returns have a standard deviation of 0.46%.²³ We consider increases in χ^r (and therefore the standard deviation of expected returns) up to a factor of fifteen. Values at the upper end of this range imply that the volatility of the equity premium is about as large as its mean, which corresponds to typical estimates (Cochrane [2011]).²⁴ All other parameters are held fixed at our estimates, i.e. we alter the degree of return predictability without changing the dynamics of

²²For example, in the class of Long Run Risk models (Bansal and Yaron [2004]), expected returns and expected return volatility both depend positively on endowment volatility. Consequentially, these models suggest that the conditional return volatility is a good predictor of excess returns.

²³ $\text{std}[E_t[r_{t+1} - r^f]] = \chi^r \times \text{std}[\log(v_t)] = \chi^r \times \frac{\sigma_v}{\sqrt{1-\gamma_1^2}} = 0.009 \times \frac{0.460}{\sqrt{1-0.512^2}} = 0.0046$

²⁴Note that, in the data, this time-variation is largely orthogonal to the conditional return volatility and rather associated with the price-dividend ratio.

return volatility. The left panel of Figure 2.6 illustrates the value of volatility timing as a function of the standard deviation of expected returns.

The leftmost point on the graph, corresponding to our estimate, implies a consumption fee of about 1.2%. In this case, agents reduce their equity share in response to positive shocks to volatility to avoid the increased risk of stock market investments. As we begin moving to the right on the graph, such increases in volatility are accompanied by larger increases in expected returns. Initially, the increased reward of stock investments has an offsetting effect on the increased risk, so that volatility timing is less beneficial. However, for large degrees of return predictability (towards the right end of the graph), changes in expected returns more than offset changes in volatility and conditioning becomes more valuable again. In this region, agents effectively conduct market timing rather than volatility timing. This is illustrated in the right panel of Figure 2.6, which shows the equivalent of the benchmark results in 2.2, i.e. the equity share as a function of age for different volatility percentiles. For high values of return volatility (dashed line) households hold more rather than less equity, which is the opposite of the benchmark result illustrated in Figure 2.2.

The above analysis shows that it is not clear whether an increase in return predictability relative to our estimation results in a higher or lower value of volatility timing. The effect depends on the *relative* predictability of volatility and expected returns.

2.6 Conclusion

We solve a life-cycle model with idiosyncratic labor income shocks and stochastic volatility. First, we look at the effects on quantities and find that shocks to stochastic volatility lead to significant responses in equity holdings. Subsequently, we measure the economic importance of volatility timing. Relative to a benchmark strategy that conditions only on wealth and age, investors are willing to give up as much as 1.58% of life-time consumption to time volatility. Lastly, we explore the sensitivity of our findings with respect to two variables: the correlation between returns and labor and the correlation between volatility and labor. Figure 2.4 and Figure 2.5 suggest that optimal equity holdings are highly sensitive to these three channels. In particular, the combination of a higher return/labor correlation and a higher effect of volatility on expected labor income leads to low and flat equity share during working age.

Recent empirical evidence in Guvenen, Ozkan, and Song [2013] shows that persistent labor income shocks feature counter-cyclical skewness. It would be interesting to add this feature to the present model and analyze how it interacts with stochastic volatility in returns.

Because counter-cyclical skewness would make labor income riskier in times of high stock market volatility, we suspect that it would increase the economic value of volatility timing and the model's ability to replicate the low equity share of young households in the data.

Chapter 3

Undiversifiable Variance Risk and Individual Equity Options

3.1 Introduction

Index options imply a steeper implied volatility smirk and more negative variance premia than equity options, and there exist large cross-sectional differences in these features across firms ([Bakshi, Kapadia, and Madan \[2003\]](#) and [Carr and Wu \[2009\]](#)). In this paper, I investigate the relationship between the observed cross-sectional differences and the underlying firms' exposure to systematic variance risk.

The analysis is motivated by the fact that option prices depend strongly on the underlying's variance dynamics, and the observation that part of individual firms' variance is systematic. A natural conjecture is therefore that firm-level variance premia represent compensation for bearing systematic variance risk. Similarly, the implied volatility smirk could depend on exposure to systematic risk to the extent that it arises from risk premia rather than simply higher (co-)moments of returns (see, e.g. [Drechsler \[2013\]](#) and [Schreindorfer \[2013\]](#)). I distinguish between two sources of systematic variance risk. First, in the presence of a factor structure in returns (e.g., [Fama and French \[1993\]](#)), time-variation in factor variances results in time-variation in individual firms' return variances. Second, it has been shown that the variances of idiosyncratic returns (factor model residuals) share a common component (e.g., [Campbell, Lettau, Malkiel, and Xu \[2001\]](#) and [Herskovic, Kelly, Lustig, and Van Nieuwerburgh \[2014\]](#)). While the variance of idiosyncratic returns is diversifiable in large equity portfolios, its common component is non-diversifiable in option portfolios. Financial intermediaries may therefore demand a risk premium for bearing common idiosyncratic variance (CIV) risk.

My empirical analysis is based on fifty-five S&P 100 components that have continuous option quotes over 1996-2012. I begin by computing holding period returns of synthetic variance swaps as a measure of firms' variance premia, as well as a measure of the slope of each firm's implied volatility smirk. Next, I estimate each firm's exposure to the two sources of variance risk by regressing its realized variance on the realized variance of the market and a CIV factor. To do so, I compute daily realized variances for the individual stocks and for the market from intra-daily price quotes, and I construct a novel daily CIV factor. The fact that the new CIV measure is observable at the daily frequency allows me to estimate conditional loadings based on relatively short windows of daily data.

Evidence from both Fama-MacBeth regressions and sorts based on the estimated loadings suggest that firms' exposure to market variance has a significant effect on their option prices. First, firms with higher loadings have steeper smirks. This finding is consistent with the leverage effect in market returns and a factor structure in individual stock returns, and it confirms simple unconditional results in [Christoffersen, Fournier, and Jacobs \[2013\]](#). Second, larger loadings on market variance are associated with larger (less negative) variance premia. This finding is very surprising because it is well-known that market variance carries a negative price of risk (see, e.g. [Bakshi and Kapadia \[2003\]](#) and [Carr and Wu \[2009\]](#)). I show that the result is robust in subsamples and to different specifications and data frequencies for estimating loadings. Firms' exposure to CIV is not significantly related to their variance premia, and the evidence regarding the smirk is mixed.

3.1.1 Related Literature

A few papers have previously investigated the empirical relationship between systematic risk and individual equity option prices. The closest paper is Carr and Wu (2009), who document a significantly *negative* relationship between firms' loadings on market variance and their variance premia for a set of 35 stocks and 5 stock indices over 1996-2003. I replicate their result in Section 3.4.4 and show that it is not robust to excluding the indices or to measuring loadings from variances rather than log variances. Measuring loadings from level variances results in a significantly *positive* relationship in their sample, which agrees with my finding. [Duan and Wei \[2008\]](#) focus on a set of 30 stocks over 1991-1995 and show that firms with a larger systematic risk proportion, defined as systematic variance over total variance, have steeper IV smirks and larger differences between option-implied and historical volatilities. An auxiliary result in Duan and Wei's paper shows a negative (but insignificant) relationship between CAPM betas and the differences between option-implied and historical volatilities. While the authors interpret this finding as indicating that beta is not suited as a measure of systematic risk, I note that the negative sign is consistent with the relationship documented in the present paper. [Driessen, Maenhout, and Vilkov \[2009\]](#) investigate the differential pricing of equity and index options and conclude

that the former carry smaller risk premia because they are less exposed to market-wide correlation risk. Different from their paper, I focus on cross-sectional differences across firms rather than a comparison between equity and index options.

A related literature documents patterns in equity option returns that are puzzling because they appear to be unrelated to known risk factors. [Cao and Han \[2013\]](#) show that delta-hedged option returns are negatively related to the level of idiosyncratic volatility of the underlying stocks, while [Goyal and Saretto \[2009\]](#) show that options on stocks with a large difference between historical realized volatility and at-the-money implied volatility earn significantly higher returns than options on stocks with a small difference. In contrast, the finding documented in my paper is puzzling because differences in variance premia *are* related to the underlyings firms' exposure to systematic variance risk.

Lastly, my paper relates to a large literature on CIV (see, e.g. [Campbell, Lettau, Malkiel, and Xu \[2001\]](#), [Brandt, Brav, Graham, and Kumar \[2009\]](#), and [Bekaert, Hodrick, and Zhang \[2012\]](#)) and the relationship between idiosyncratic volatility and stock returns (see, e.g. [Ang, Hodrick, Xing, and Zhang \[2006, 2009\]](#) and [Fu \[2009\]](#)). Complimentary to this literature, I investigate whether firms' exposure to CIV affects risk premia embedded in their equity options.

3.2 Framework

This section presents a simple factor model for returns and return variances to motivate the empirical analysis. Assume that the cross-section of excess stock returns has a linear factor structure,

$$r_{it} = \beta_i' F_t + \varepsilon_{it}, \quad (3.1)$$

where F_t denotes a set of return factors and ε_{it} is a firm-specific shock that is uncorrelated with F_t and across firms. The conditional variance is given by

$$Var_{t-1}[r_{it}] = \beta_i' Var_{t-1}[F_t] \beta_i + Var_{t-1}[\varepsilon_{it}], \quad (3.2)$$

which shows that any heteroscedasticity in the return factors gets inherited by individual firm returns. Because there is strong evidence for a negative price of market variance ([Coval and Shumway \[2001\]](#), [Bakshi and Kapadia \[2003\]](#), and [Carr and Wu \[2009\]](#)), Equation 3.2 suggests that firms with higher market betas have variance premia that are smaller (more negative). In Section 3.4, I document the puzzling fact that the opposite is true for 17-year sample of fifty-three large firms with liquid option markets.

Assume further that there is a common factor in the variance of idiosyncratic returns,

$$Var_{t-1}[\varepsilon_{it}] = \gamma_i G_{t-1} + \eta_{it-1} \quad (3.3)$$

Firm i 's total variance is given by

$$Var_{t-1}[r_{it}] = \beta_i' Var_{t-1}[F_t] \beta_i + \gamma_i' G_{t-1} + \eta_{it-1}. \quad (3.4)$$

The first two terms result in co-movement between the variances of individual firms while the third term is purely idiosyncratic. The rest of the paper analyzes the pricing of the two systematic components.

For the empirical analysis, I focus on the pricing of the variance of a single return factor (the excess return on the market) and a single common idiosyncratic variance (CIV) factor. However, as is common, I allow for the possibility that there are additional return factors by computing CIV based on the residuals from a multi-factor model.

3.3 Data

In Section 3.3.1, I discuss data sources as well as the measures for the implied volatility smirk and the variance premium. Section 3.3.2 discusses the construction of the common idiosyncratic variance (CIV) factor and the estimation of firms' loadings on CIV and market variance.

3.3.1 Option Data and Characteristics

End-of-day implied volatility (IV) surface data is taken from OptionMetrics.¹ The sample spans 1996-2012 and it contains data for 53 firms that (i) were part of the S&P 100 for at least consecutive 10 years during 1996-2012 and (b) have continuous option observations over 1996-2012. Variables include the option's implied volatility, price, strike, maturity and delta.

To measure the slope of the IV curve, for each day (t) and each firm (i), I regress IVs on deltas and days to maturity,

$$IV_{i,t,l} = a_{i,t} + b_{i,t} \cdot \Delta_{i,t,l} + c_{i,t} \cdot DTM_{i,t,l} + \epsilon_{i,t,l}, \quad (3.5)$$

¹OptionMetrics computes IV's based on a binomial tree model that accounts for the early exercise premium, and interpolates them to a fixed grid of maturities and option deltas. Delta serves as a measure of the options' moneyness. Calls (puts) with a delta of 0.5 (−0.5) are roughly at-the-money, whereas options with deltas less than 0.5 in absolute value are out-of-the-money.

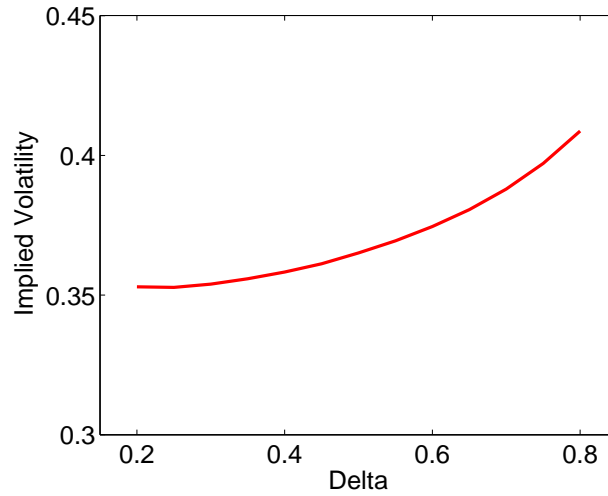


Figure 3.1: Implied Volatility as a Function of Delta, Intel Corp.

This figure shows average implied volatility over 1996-2012 as a function of option delta for Intel Corp. Implied volatilities are taken from OptionMetrics (they account for the early exercise premium), and they are based on out-of-the-money calls and puts with a maturity of 30 days.

where l denotes an option available for firm i on day t , Δ denotes the call-equivalent delta (delta for calls and one plus delta for puts), and DTM denotes days to maturity. I include all observations that are out-of-the-money and have less than 6 month to maturity. The measure of firm i 's smirk on day t is given by $b_{i,t}$, with larger values corresponding to a steeper curve. For the analysis in Section 3.4, I compute monthly smirks by averaging the daily values within each month. The same measure of the smirk has been used previously by Christoffersen, Fournier, and Jacobs [2013]. An alternative measure of the smirk would be the difference between the IV of an out-of-the-money put and the IV of an at-the-money option. The approach used in the present paper has the advantage that it is based on a large number of observations, which makes it more robust. It also avoids having to specify a particular moneyness level for the out-of-the-money option, which involves a very subjective choice. Figure 3.1 illustrates the mean IV as a function of Δ for Intel Corp., and Table 3.3.1 shows the average value of $b_{i,t}$ for all 53 firms. As previously documented by Bakshi, Kapadia, and Madan [2003], the average smirk on individual stocks is positive and shows large cross-sectional variation.

Measuring the variance premium (VP) requires both an estimate of the firm's realized variance and the corresponding variance swap rate. I estimate each firm's daily realized variance ($RV_{i,t}$) from five-minute returns based on national best bid and offer quotes, computed by examining all exchanges offering quotes on a given stock. Intra-daily quote data is taken from the TAQ database. I apply common filters for minimizing the effect of microstructure noise and recording errors. For the main analysis in Section 3.4, I further

Table 3.1: Option Characteristics

	Ticker	Company Name	b $\times 10$	RV $\times 100$	VSR $\times 100$	$\ln(\frac{RV}{VSR})$ $\times 100$
1	AA	Alcoa Inc.	0.84	16.52	16.86	-16.86
2	AEP	American Electric Power Co	0.90	7.14	6.43	-12.35
3	ALL	The Allstate Corp.	0.92	11.92	11.71	-10.06
4	AMGN	Amgen, Inc.	1.06	12.34	13.23	-19.81
5	AVP	Avon Products, Inc.	0.78	12.59	12.97	-21.32
6	AXP	American Express Co	1.24	14.46	14.16	-19.83
7	BA	The Boeing Co	0.89	10.69	10.55	-13.02
8	BAX	Baxter International Inc.	0.74	8.56	8.35	-18.05
9	BHI	Baker Hughes Inc.	0.95	20.00	19.11	-5.80
10	BMJ	Bristol-Myers Squibb Co	0.83	10.09	8.94	-8.90
11	CI	CIGNA Corp.	0.84	14.41	15.10	-27.28
12	CL	Colgate-Palmolive Co	0.76	6.88	6.50	-7.65
13	CPB	Campbell Soup Co	0.58	7.09	7.38	-19.25
14	CSC	Computer Sciences Corp.	0.94	14.27	15.81	-28.51
15	CSCO	Cisco Systems, Inc.	1.20	18.01	19.65	-20.75
16	DD	Du Pont De Nemours And Co	0.95	9.84	8.79	2.05
17	DIS	The Walt Disney Co	0.98	11.56	10.94	-17.26
18	DOW	Dow Chemical	1.09	12.37	13.09	-16.92
19	EMC	EMC Corp.	0.99	24.49	22.32	-5.50
20	ETR	Entergy Corp.	0.59	6.62	7.59	-25.11
21	F	Ford Motor Co	1.39	24.02	23.47	-15.66
22	FDX	FedEx Corp.	0.89	9.99	11.14	-21.36
23	GD	General Dynamics Corp.	0.83	7.61	8.07	-15.49
24	GE	General Electric Co	1.18	11.03	10.72	-13.49
25	HAL	Halliburton Co	0.99	21.40	20.09	-5.53
26	HD	The Home Depot, Inc.	1.08	12.27	11.69	-12.56
27	HPQ	Hewlett-Packard Co	0.94	16.86	15.74	-10.79
28	IBM	International Business Machines	0.95	9.02	9.48	-23.50
29	INTC	Intel Corp.	0.96	16.47	15.97	-12.79
30	IP	International Paper Co	0.96	14.40	14.03	-6.31
31	JNJ	Johnson & Johnson	0.88	5.46	5.43	-17.09
32	KO	The Coca-Cola Co	0.81	6.02	6.20	-13.41
33	LTD	Limited Brands Inc.	1.44	17.35	17.52	-11.40
34	MCD	McDonald's Corp.	0.84	7.70	7.41	-8.71
35	MMM	3M Co	0.89	7.00	6.83	-9.89
36	MO	Altria Group Inc.	0.92	8.06	8.97	-21.15
37	MRK	Merck & Co., Inc.	0.90	9.34	8.28	-7.61
38	MSFT	Microsoft Corp.	0.91	10.20	11.21	-20.09
39	NSC	Norfolk Southern Corp.	0.85	13.10	11.73	-0.98
40	PEP	PepsiCo, Inc.	0.79	7.02	6.17	-4.42
41	PFE	Pfizer Inc.	0.82	9.10	8.82	-12.49
42	PG	The Procter & Gamble Co	0.86	7.01	5.67	-7.59

Continued on next page

Table 3.1 – continued from previous page

	Ticker	Company Name	b $\times 10$	RV $\times 100$	VSR $\times 100$	$\ln(\frac{RV}{VSR})$ $\times 100$
43	RSH	RadioShack Corp.	1.14	25.19	24.21	-19.50
44	SLB	Schlumberger Limited	0.87	14.97	14.44	-8.18
45	SO	The Southern Co	0.69	5.33	5.59	-17.84
46	TXN	Texas Instruments Inc.	1.06	21.89	19.69	-2.80
47	UTX	United Technologies Corp.	0.98	8.62	8.44	-12.19
48	VZ	Verizon Communications Inc.	0.98	8.16	7.79	-8.77
49	WMB	Williams Companies, Inc.	1.02	33.33	24.11	-13.28
50	WMT	Wal-Mart Stores, Inc.	0.84	8.53	8.18	-7.99
51	WY	Weyerhaeuser Co	0.98	12.17	12.33	-12.04
52	XOM	Exxon Mobil Corp.	0.87	6.91	6.43	-7.19
53	XRX	Xerox Corp.	1.18	21.16	21.90	-9.44

This table shows mean option characteristics for the set of fifty three firms over 1996-2012. The slope of the implied volatility curve, measured via Equation 3.5, is denoted by b . The realized variance (RV) and the variance swap rate (VSR) are both expressed in annualized variance units. The variance premium is measured as the log of the realized variance over the month divided by the variance swap rate at the end of the previous month.

require monthly RV estimates, which I compute by adding the daily estimates within a given month.

Synthetic variance swap rates (VSR) are computed similar to the VIX index via a discretization of the formula

$$VSR_{t,T} = \frac{2}{T-t} \int_0^\infty \frac{\Theta_t(K,T)}{B_t(T)K^2} dK, \quad (3.6)$$

where $\Theta_t(K,T)$ denotes the time- t price of an out-of-the-money option with strike K and maturity T and $B_t(T)$ denotes the time- t price of a bond paying one dollar at T . I use IV surface data for the 30 day maturity. Following Carr and Wu [2009], the IVs reported by OptionMetrics are converted into option prices using the Black-Scholes model (rather than a binomial tree model) in order to strip option prices of the early exercise premium.² I use the extrapolation method of Jiang and Tian [2005] for evaluating the integral, i.e. I set implied volatilities outside of the observed strike range equal to the endpoint values of the observed range.

²All of my results are quantitatively similar if I instead use the option prices reported by OptionMetrics, which are computed from IVs based on a binomial model that incorporates the early exercise premium. The approach of Carr and Wu [2009] conforms more closely to the theory underlying the replication of variance swap rates, which is based on European options.

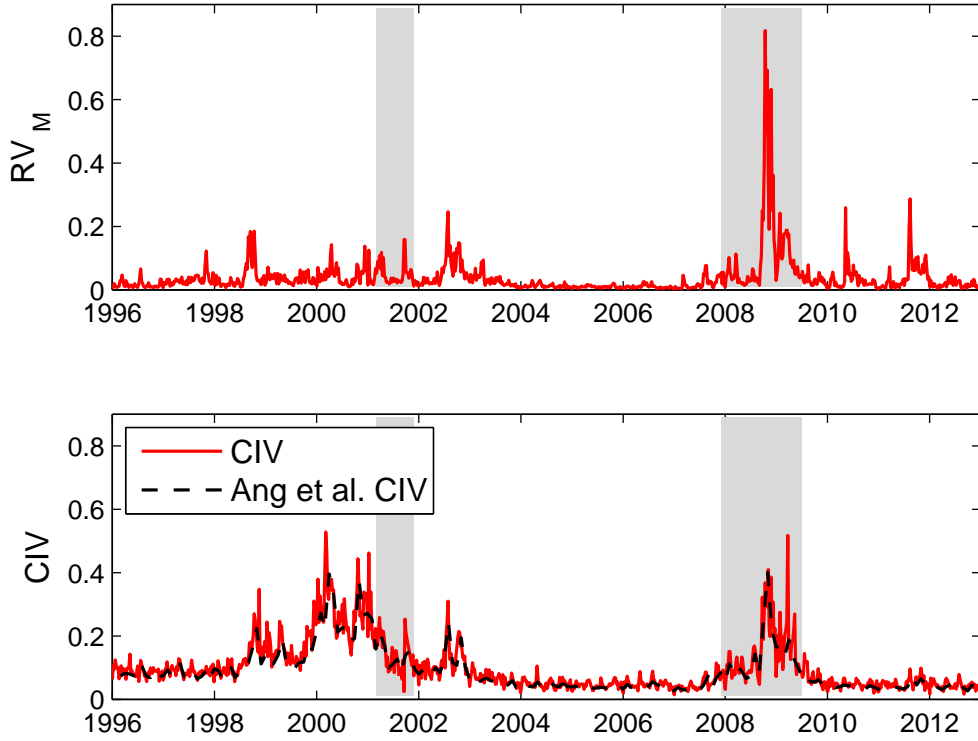


Figure 3.2: Systematic Variance Factors, 1996-2012

This figure shows weekly time series of the two variance factors. The top panel shows the realized variance of the market and the bottom panel shows the common idiosyncratic variance factor. Both series are expressed in annualized variance units. Shaded regions mark NBER recessions.

The (log) variance premium is measured as $\ln(RV_{t:t+21}/VSR_t) \times 100$, where VSR_t denotes the swap rate at the end of month t and $RV_{t:t+21}$ equals the RV over the following month. The log variance premium can be interpreted as the continuously compounded excess return (in percent) to going long the variance swap contract and holding it to maturity. This is the measure used for most of the analysis in Carr and Wu [2009], making my results comparable to theirs. Table 3.3.1 shows the mean annualized realized variances, VSR and the VP for all firms. With one exception, all of the variance premia are negative. This finding is in line with Carr and Wu [2009], who find the great majority of the stocks in their 1996-2003 sample to have a negative mean variance premium.

3.3.2 Estimating Exposure to Sources of Systematic Variance Risk

As discussed in Section 3.2, I consider two sources of undiversifiable variance risk, the common variance of idiosyncratic returns from a factor model and the variance of the market.

The daily common idiosyncratic variance (CIV) factor is computed as the value-weighted squared daily idiosyncratic return across all stocks in the CRSP universe. Specifically, on each day of the sample, I estimate the Fama-French model based on the most recent quarter (63 days) of daily data for each firm:³

$$r_{i,s} - r_s^f = b_{i,t}^0 + b_{i,t}^1 MKT_s + b_{i,t}^2 SMB_s + b_{i,t}^3 HML_s + e_{i,s} \quad \text{for } s \in \{t - 62, \dots, t\},$$

where the variable MKT represents the excess return on the market portfolio, SMB is the size factor, and HML is the value factor. Next, I compute the CIV as the cross-sectional value-weighted squared residual on the last day in the three month window,

$$CIV_t = \sum_{i=1}^{N_t} w_{i,t} e_{i,t}^2,$$

where N_t denotes the number of available CRSP firms on day t ,⁴ and $w_{i,t}$ denotes firm i 's market capitalization relative to that of all N_t firms. Value-weighted averages of idiosyncratic returns have been used previously as measures of CIV by [Campbell, Lettau, Malkiel, and Xu \[2001\]](#) and [Bekaert, Hodrick, and Zhang \[2012\]](#). Different from the previous studies, I use the squared daily residual as an estimate of firm i 's daily residual variance. Obviously, this estimate is very noisy because it is based on a single observation. Nevertheless, the law of large numbers ensures that the noise in individual firms' estimates becomes negligible when taking the cross-sectional average across a large number of firms.

To illustrate that CIV represents a sensible measure of the common variation in the variance of idiosyncratic returns, I compare it to a common idiosyncratic variance factor based on the monthly idiosyncratic variance measure of [Ang, Hodrick, Xing, and Zhang \[2006\]](#). In particular, I estimate the Fama-French model based on the daily observations within each calendar month and compute firm i 's monthly idiosyncratic return variance based on the sample variance of all daily residuals for the month. Next, I compute the monthly CIV factor as the cross-sectional average, weighted by the market weights at the end of the previous month (see also [Bekaert, Hodrick, and Zhang \[2012\]](#)). The resulting series has a correlation of 0.987 with the time-aggregated series of the daily CIV measure used in the present paper. The crucial difference of the daily measure proposed here is that it enables me to estimate loadings on the factor based on a short rolling window of daily observations.

³The subscript t on the coefficients denotes the fact that they are estimated on a rolling window that ends on day t .

⁴In order for a firm to be included in the analysis on day t , I require that a minimum of $57 \approx 0.9 \times 63$ daily return observations are available over the past 63 days. Small, infrequently traded stocks are therefore excluded from the sample.

The realized variance of the market ($RV_{M,t}$) is computed based on five-minute returns on S&P500 futures, which were obtained from TICKDATA. Figure 3.2 shows time-series for both the realized variance of the market (top panel) and the CIV factor (bottom panel). For better visibility, I aggregate both series to a weekly frequency. For comparison, I overlay the CIV^{Ang} factor in the bottom panel, which has a monthly frequency. It is clear that, apart from the different frequency, both series behave very similarly.

Having obtained time-series for each firm's realized variance as well the realized variance of the market and the CIV factor, I estimate each firm's exposure to the two sources of systematic variance risk from

$$RV_{i,s} = \beta_{i,t}^0 + \beta_{i,t}^M RV_{M,s} + \beta_{i,t}^{CIV} CIV_s + \epsilon_{i,s} \quad \text{for } s \in \{t - 62, \dots, t\}. \quad (3.7)$$

The regression is run at the end of each month based on daily data for the previous quarter, resulting in a monthly time series for $\beta_{i,t}^M$ and $\beta_{i,t}^{CIV}$. A 3-month window is appropriate because earnings announcements, which represent a mostly idiosyncratic event with a large effect on individual firms' variances, occur on a quarterly basis. The mean R^2 's of regression 3.7 for individual firms range from 9% to 36% with a cross-sectional median of 21%. This shows that a substantial part of the time-variation in individual firms' variances can be attributed to the two variance factors.

3.4 Results

In this section, I investigate the relationship between firms' loadings on the two undiversible variance factors and characteristics of their option prices. My main finding is that firms whose variance co-moves stronger with market variance have steeper implied volatility smirks and *larger* (less negative) variance premia. This pattern is illustrated with cross-sectional regressions as well as sorts based on the estimated loadings. It holds across different subsamples and it is robust to different approaches for estimating loadings. Exposure to common idiosyncratic variance impacts neither the variance premium nor the smirk in a robust fashion.

3.4.1 Fama-MacBeth Regressions

I cross-sectionally regress monthly option characteristics of each firm on its latest available risk loadings,

$$y_{i,t+1} = \lambda_{0,t+1} + \lambda_{1,t+1} \hat{\beta}_{i,t}^M + \lambda_{2,t+1} \hat{\beta}_{i,t}^{CIV} + e_{i,t+1}, \quad (3.8)$$

where $y_{i,t+1}$ denotes either the variance premium or the smirk in month $t+1$ and the loadings ($\hat{\beta}_{i,t}^M, \hat{\beta}_{i,t}^{CIV}$) are estimates based on data up to the end of month t from the first pass

Table 3.2: Fama-MacBeth Regressions

This table reports cross-sectional regressions of option characteristics on lagged estimated loadings on the two variance factors. Panel A shows results for the variance premium and panel B shows results for the implied volatility smirk. Loadings are obtained from 3-month rolling window time-series regressions of firm i 's realized variance on the realized variance of the market and the common idiosyncratic variance factor, using daily data (see Equation 3.7). I report time-series averages of the second-stage coefficients. t -statistics are reported in brackets and are based on Newey and West [1987] standard errors using 3 lags. Regression specifications I and II are univariate, whereas specification III uses both loadings as regressors. The table shows results for the full sample (1996-2012) as well as two subsamples (1996-2003 and 2004-2012).

	1996-2012			1996-2003			2004-2013		
	I	II	III	I	II	III	I	II	III
A: VP									
β^M	2.42 [4.79]		2.50 [4.69]	2.59 [3.74]		2.99 [4.17]	2.27 [3.11]		2.07 [2.68]
β^{CIV}		0.14 [0.26]	-0.58 [-1.04]		0.16 [0.20]	-1.45 [1.77]		0.11 [0.16]	0.19 [0.25]
B: Smirk									
β^M	0.08 [4.09]		0.09 [4.95]	0.04 [5.12]		0.05 [4.97]	0.12 [3.34]		0.13 [4.14]
β^{CIV}		0.03 [1.99]	0.02 [1.37]		0.01 [0.54]	0.00 [0.01]		0.05 [2.10]	0.05 [2.09]

regression (Equation 3.7). As explained in Section 3.3, the variance premium in month $t + 1$ is measured by the holding period return of a one-month variance swap purchased at the end of month t , and the smirk is measured by the average of daily slope estimates (from Equation 3.5) over month $t + 1$. The results of the Fama-MacBeth regressions for the full sample and two subsamples are presented in Table 3.2. Specifications I and II show the univariate effect of each loading separately, whereas specification III estimates the effects jointly.

The table shows that exposure to CIV is not related to the variance premium. The effect of β^{CIV} is insignificant for all samples and regression specifications, with the exception of the early sample, where the effect is marginally significant in the joint specification (with a t -statistic of 1.77). Furthermore, while exposure to CIV is significantly related to the smirk in the full sample (with a t -statistic of 1.99), the effect is not robust across subsamples and it becomes insignificant in the bivariate specification. Overall, the evidence in Table 3.2 therefore suggests that exposure to CIV does not play an important role for option prices.

Exposure to market variance, on the other hand, has a very significant positive effect on both the variance premium and the smirk. In the full sample, the coefficient on β^M has a t -statistic of 4.79 (4.69) in the univariate (bivariate) regression for the variance premium and a t -statistic of 4.09 (4.95) for the smirk. Furthermore, the effect remains significant in

both subsamples, both for the univariate and the bivariate regression specification. The positive association between market variance exposure and the slope of the smirk is consistent with the evidence in Christoffersen, Fournier, and Jacobs [2013], who show that unconditional estimates of market betas are significantly positively related to the average smirk among DJIA firms. The results in Table 3.2 show that their result continues to hold when one allows for time-variation in loadings. The positive association between market variance exposure and the variance premium implies that firms with larger loadings carry *larger* (less negative) variance premia. This is very surprising because it is well-known that market variance carries a negative price of risk. One would therefore expect firms whose variance co-moves stronger with the variance of the market to carry larger absolute variance premia.

An important concern about the above inference stems from the two-stage estimation procedure, which implies that regressors are measured with noise. While the reported t -statistics correct for autocorrelation and heteroscedasticity as in Newey and West [1987], they do not account for errors-in-variables. Unfortunately, appropriate adjustments are only known under restrictive distributional assumptions and are therefore not feasible in the present case. In the next section, I show that the same results arise for an inference procedure that produces conservative results in the presence of errors-in-variables, namely a simple sorting exercise based on the estimated loadings.

3.4.2 Sorts

At the end of each month, I use the most recent estimate of either β^M or β^{CIV} from regression 3.7 to sort firms into five groups, and I compute the average variance premium and the average smirk within each group. I then compute the time series average of the characteristics for each group, as well as for the difference in characteristics between groups five and one and the associated t -statistic. This procedure yields conservative results in the presence of errors in the sorting variable, because such errors cause some firms to be assigned to the wrong group in each period. An additional advantage relative to cross-sectional regressions lies in the fact that sorts are robust to outliers in the estimated loadings. The results of the sorting exercise are presented in Table 3.5, both for the full sample and two subsamples.

Panel A shows that both the variance premium and the smirk are positively related to β^M , confirming the result of the Fama-MacBeth regressions. For the full sample, the variance premium increases monotonically from -18.80 for stock with low β^M (group 1) to -9.72 for stocks with high β^M (group 5). The difference between groups five and one is highly statistically significant with a t -statistic of 5.47. It is also economically large, implying

Table 3.3: Option characteristics of firms sorted by variance loadings

This table shows average option characteristics of five groups of firms, sorted monthly by their loadings on the two variance factors. Loadings are obtained from 3-month rolling window time-series regressions of firm i 's realized variance on the realized variance of the market and the common idiosyncratic variance factor, using daily data (see Equation 3.7). I then sort firms into five groups based on the estimated β^M (Panel A) and β^I (Panel B) and determine the average characteristic within each groups over the following month. Groups one and five contain 10 firms each, whereas groups two through four contain 11 firms. For loadings measured up to the end of month t , the smirk and variance swap rates are also measured at the end of month t , whereas realized variance is computed over the subsequent month. t -statistics for the 5 – 1 difference are shown in brackets and are based on Newey and West [1987] standard errors using 3 lags.

	1996-2012			1996-2003			2004-2012		
	β	VP	smirk	β	VP	smirk	β	VP	smirk
A: Sort on β^M									
1 (Low)	-0.62	-18.80	0.83	-0.36	-19.58	0.70	-0.86	-18.11	0.93
2	0.43	-13.73	0.87	0.44	-11.95	0.79	0.42	-15.29	0.94
3	0.78	-12.17	0.91	0.78	-10.01	0.78	0.77	-14.07	1.03
4	1.24	-12.14	0.98	1.28	-10.44	0.82	1.20	-13.63	1.11
5 (High)	3.55	-9.72	1.13	4.13	-8.17	0.96	3.03	-11.08	1.27
5-1		9.08	0.30		11.40	0.26		7.03	0.34
$[t - stat]$		[5.47]	[5.97]		[4.28]	[6.08]		[3.52]	[3.92]
B: Sort on β^{CIV}									
1 (Low)	-0.25	-15.58	0.94	-0.28	-14.56	0.81	-0.23	-16.47	1.05
2	0.15	-12.92	0.86	0.14	-11.95	0.74	0.16	-13.78	0.96
3	0.34	-11.94	0.90	0.34	-10.04	0.78	0.35	-13.62	1.02
4	0.65	-11.28	0.96	0.64	-10.39	0.83	0.66	-12.07	1.08
5 (High)	2.78	-15.02	1.05	2.49	-13.22	0.91	3.04	-16.61	1.18
5-1		0.56	0.12		1.35	0.10		-0.14	0.13
$[t - stat]$		[0.43]	[2.95]		[0.81]	[1.67]		[-0.07]	[2.54]

that the average return of variance swaps in group one is twice as large as in group five. Similarly, the smirk increases monotonically from 0.83 in group one to 1.13 in group five, and the difference is highly significant with a t -statistic of 5.97. Lastly, note that the five minus one difference for both the variance premium and the smirk remains statistically significant at the 1% level in the two subsamples.

The above results show that firms with larger *historical* loadings on market variance have larger (less negative) future variance premia. Given the negative price of market variance risk, this represents a puzzle only to the extent that loadings are persistent, so that high loadings and large variance premia occur contemporaneously. To check whether this is indeed the case, I compute loadings from the daily realized variances over the post-formation month. Table 3.4 shows the results. While the spread in post-formation loadings (denoted by β_{post}^M) is less pronounced than the spread in historical loadings shown in table 3.5, the difference in loadings between group 5 (equal to 1.66) and group 1 (equal to 0.80) remains large. The table further shows that firms in group 5 have a substantially higher realized

Table 3.4: Characteristics of firms sorted by β^M

This table shows transition probabilities as well as different characteristics of firms sorted by β^M . β_{post}^M is measured from regression 3.7, using daily data over the post formation month. RV_{post} is measured from intra-daily data over the post formation month. The leverage ration (denoted by "Lev") is defined as book debt over book debt plus market equity. Data on book debt is from COMPUSTAT. t-statistics for the 5 – 1 difference are shown in brackets and are based on Newey and West [1987] standard errors using 3 lags.

	Prob(transition to Portfolio)					β_{post}^M	RV_{post} ×100	Lev
	1	2	3	4	5			
1 (Low)	0.61	0.21	0.08	0.06	0.04	0.80	10.61	0.38
2	0.19	0.48	0.20	0.08	0.04	0.85	9.03	0.34
3	0.08	0.21	0.45	0.21	0.05	0.75	10.33	0.33
4	0.05	0.09	0.22	0.48	0.17	0.94	12.77	0.42
5 (High)	0.04	0.04	0.06	0.20	0.67	1.66	20.70	0.72
5-1						0.86	10.09	0.34
[t – stat]						[4.05]	[4.90]	[3.11]

variance (denoted by RV_{post}) and a higher leverage ratio (denoted by "Lev") in the post-formation month. I also computed the mean firm size and the mean book-to-market ratio and found them to be very close to constant across the five groups (results not shown). Lastly, the transition probability matrix shows that firms in the extreme groups remain in the same group with a probability of approximately 2/3, which implies that loadings exhibit relatively high persistence. This suggests that extreme loadings are not typically the result of outlier observations in the firms' variance series.

Panel B of Table 3.5 presents results for sorts based on β^{CIV} . As in the Fama-MacBeth regressions, exposure to CIV has no detectable effect on the variance premium, with the 5 – 1 spread being insignificant in all samples. The effect on the smirk is not clear. While the 5 – 1 spread is at least marginally significant in all samples, the mean smirk is not monotone across the five groups.

3.4.3 Robustness: Alternative Loading Estimates

For the main analysis, I computed loadings based on a three-month window of daily data for firm level realized variances and the two variance factors (see Equation 3.7). In this section, I illustrate that the results are robust to estimating loadings (1) based on first-differenced variances, (2) based on log variances (3) based on a 12 month window of weekly variance data (4) based on a univariate regression that excludes CIV and (5) based on a 3 month window of daily returns, i.e. a loading estimate from the CAPM. Because sorts based on estimated loadings produce more robust results than cross-sectional regressions, I focus on the former to save space. Further, I show robustness results for sorts based on β^M only, because β^{CIV} did not result in consistent findings across cross-sectional regressions

Table 3.5: Option Characteristics of Firms Sorted by β^M : Alternative Loading Estimates

This table repeats the sorting analysis presented in Table 3.5 based on alternative estimates of β^M . Loadings are estimated based on alternate versions of regression 3.7. Panel A contains the benchmark results. In Panel B, loadings are estimated from a regression of $\Delta RV_{i,t}$ on $\Delta RV_{M,t}$ and ΔCIV_t . Panel C estimates regression 3.7 based on log variances. Panel D is based on a 1 year window of weekly variance series. Weekly variances are computed by summing the daily values within the week, both for firm level realized variances and for the two variance factors. Panel E contains results for univariate β_t^M estimates, i.e. estimates from a regression that excludes CIV_t . For Panel F, loadings are estimated from the CAPM, using a 3 month window of daily returns.

	A: Daily, levels			B: Daily, 1st differences			C: Daily, logs		
	β	VP	smirk	β	VP	smirk	β	VP	smirk
1 (Low)	-0.62	-18.80	0.83	-1.03	-17.55	0.86	0.15	-16.39	0.90
2	0.43	-13.73	0.87	0.29	-13.59	0.83	0.27	-12.07	0.90
3	0.78	-12.17	0.91	0.63	-12.67	0.93	0.34	-12.00	0.92
4	1.24	-12.14	0.98	1.09	-11.94	0.98	0.42	-13.09	0.97
5 (High)	3.55	-9.72	1.13	3.56	-10.78	1.11	0.53	-13.11	1.03
5-1		9.08	0.30		6.77	0.25		3.28	0.13
$[t - stat]$		[5.47]	[5.97]		[4.06]	[5.12]		[2.11]	[3.96]
	D: Weekly, levels			E: Daily, levels, univar.			F: Daily, returns		
	β	VP	smirk	β	VP	smirk	β	VP	smirk
1 (Low)	-0.27	-19.36	0.82	-0.23	-18.68	0.80	0.37	-17.12	0.77
2	0.76	-14.64	0.82	0.53	-13.62	0.86	0.64	-12.66	0.85
3	1.20	-11.03	0.93	0.89	-12.50	0.92	0.87	-12.17	0.91
4	1.81	-10.65	1.02	1.38	-11.47	0.99	1.12	-12.26	1.03
5 (High)	4.19	-11.07	1.13	3.90	-10.33	1.15	1.59	-12.44	1.15
5-1		8.29	0.31		8.35	0.35		4.67	0.38
$[t - stat]$		[5.14]	[7.10]		[5.54]	[6.24]		[3.03]	[6.74]

and sorts.

Table 3.5 shows the results. For comparison, the benchmark results are repeated in Panel A. Panel B shows that results do not change substantially when loadings are estimated based on the first differences of the variance series rather than their levels. For the results in Panel C, loadings are computed by running regression 3.7 in logs instead of levels, which has the effect of downweighting observations with large variance values in the loading estimation. To the extent that large variance values are caused by noisy observations, this approach may lead to more precise (and therefore more informative) loading estimates. However, it is also conceivable that large variance values are informative about important shocks, in which case it may be harmful to decrease the weight on these observations. The results show that the 5 – 1 spreads for both the variance premium and the smirk are reduced relative to the benchmark, which suggests that downweighting large observations may not be a desirable approach in this case. Regardless, both spreads remain positive and statistically significant. Panel D shows that results remain very similar to the benchmark when loadings are estimated based on weekly data and a 52-week rolling window. The 5 – 1 difference changes from 9.08 to 8.29 for the variance premium and from 0.30 to 0.31

for the smirk, and both spreads remain highly statistically significant. Furthermore, the mean characteristics continue to increase almost monotonically from group one to group 5. Similarly, estimating β^M univariately, i.e. by excluding CIV from regression 3.7, has a negligible effect on the results (Panel E). Lastly, Panel F shows the results of sorting based on CAPM betas, which equal $\sqrt{\beta^M}$ under certain conditions (see Section 3.2). While the 5 – 1 spread for the variance premium becomes somewhat smaller in this case, it remains positive and significant at the 1% level. The spread for the smirk remains close to the benchmark value.

3.4.4 Comparison with Carr and Wu [2009]

The positive association between loadings on market variance and the variance premium is surprising in light of the fact that the variance premium on the market is negative. Additionally, my result contradicts the findings of Carr and Wu [2009], who document a significantly negative relationship. In this section, I revisit their finding to understand the source of the difference in results.

There are several important differences between Carr and Wu’s approach and the one in the present paper. First, their sample spans 1996-2003 while mine spans 1996-2012. As I have documented in Sections 3.4.1 and 3.4.2 this difference has an immaterial effect on my result, i.e. the relationship between market variance exposure and firms’ variance premia is very similar in the earlier sample. Second, Carr and Wu consider a different set of asset, consisting of 35 firms and 5 stock indices, while I focus on 53 firms. In both papers, the set of firms is chosen to include only firms with a very liquid option market. I investigate the effect of including indices among the test assets below. Third, the authors estimate loadings from an unconditional regression of firm i ’s monthly log realized variance on the monthly log realized variance of the market. Monthly realized variances are computed based on daily data. In contrast, I allow for time-variation in loadings by estimating them based on rolling window regressions from daily realized variances, which I compute based on intra-daily return data. The use of intra-daily data results in more precise estimates of spot variances than daily data (see, e.g. Andersen, Bollerslev, Diebold, and Labys [2003]), which in turn allows me to capture time-variation in loadings in a precise fashion. Further, I have shown in Section 3.4.3 that my result is robust to measuring loadings based on logged variables rather than levels. Below, I examine the robustness of Carr and Wu’s approach to measuring loadings from variances expressed in levels. Fourth, Carr and Wu compute variance swap rates from actual option quotes, while I use OptionMetrics’s implied volatility surface data. I show below that my approach results in a stronger relationship between variance premia and loadings when applied to Carr and Wu’s sample.

Carr and Wu [2009] estimate the following relationship between firms' mean variance premia and their unconditional loadings on market variance (see their Equation 13)

$$\overline{VP}_i = 0.006 - 0.328 \beta_i^M + e_i, \quad R^2 = 18.4\%, \quad (3.9)$$

$\begin{smallmatrix} [0.09] \\ [-2.96] \end{smallmatrix}$

with t -statistics shown in brackets. I begin by replicating Carr and Wu's results with the exception that I continue to rely on IV surface data for computing synthetic variance swap rates and obtain

$$\overline{VP}_i = 0.112 - 0.324 \beta_i^M + e_i, \quad R^2 = 27.6\%. \quad (3.10)$$

$\begin{smallmatrix} [2.17] \\ [-3.81] \end{smallmatrix}$

While my regression yields a very similar *negative* slope coefficient, the use of variance swap rates computed based on IV surface data results in a somewhat higher R^2 and t -statistic on the slope coefficient.⁵ Because my interest lies in cross-sectional differences in equity options rather than index options, I exclude the 5 stock indices and re-run the regression based on the 35 stocks in Carr and Wu's sample,

$$\overline{VP}_i = -0.008 - 0.053 \beta_i^M + e_i, \quad R^2 = 1.3\%. \quad (3.11)$$

$\begin{smallmatrix} [-0.17] \\ [-0.65] \end{smallmatrix}$

Regression 3.11 shows that the strength of the previous result is driven almost entirely by the inclusion of the five stock indices. While the sign of the slope coefficient remains negative when excluding indices, it becomes insignificant and the R^2 drops from 27.6% to 1.3%. Next, I investigate the importance of measuring variance loadings based on log variances rather than levels. Continuing to focus on the set of 35 firms, I find⁶

$$\overline{VP}_i = -0.106 + 0.016 \beta_i^M + e_i, \quad R^2 = 29.2\%, \quad (3.12)$$

$\begin{smallmatrix} [-4.60] \\ [3.69] \end{smallmatrix}$

showing that Carr and Wu's finding is not robust to measuring variances in levels. Measuring loadings in levels instead results in a *positive* and significant coefficient estimate as well as a very high R^2 , mimicking the result of the present paper.

3.5 Conclusion

This paper investigates the relationship between cross-sectional differences in the variance premium and the implied volatility smirk and the underlying firms' exposure to market

⁵A potential explanation for this finding is that with raw data, there is a lot of cross-sectional variation in the range of strikes across firms, whereas the range is equal across firms when using the IV surface. The reason is that OptionMetrics interpolates and extrapolated the raw data to a fixed grid of option deltas to construct the surface.

⁶When I instead run this regression based on all of Carr and Wu's 40 assets (including the 5 stock indices), I obtain a slope coefficient of 0.026 with a t -statistic of 4.25 and an R^2 of 32.2%. This shows that both the inclusion of the stock indices and the measurement of loadings based on logged variances is necessary to obtain a significantly negative slope coefficient in Carr and Wu's sample.

variance risk and common idiosyncratic variance (CIV) risk. While I find no robust relationship between exposure to CIV and equity options, I document the puzzling fact that exposure to market variance risk is associated with a larger (less negative) variance premium. I show that this effect persists in sub-samples and that it is robust to numerous approaches for estimating loadings. The finding suggests that variance premia in equity options are inconsistent with a factor model for returns and a negative variance premium for the market.

Appendix A

Data

Filters applied to option data

Observations with the following characteristics were removed.

1. Non-standard expiration dates
2. PM-settled options
3. Options with less than a week to expiration
4. Observations with error codes 999 (for ask) and 998 (for bid)
5. Observations whose bid-ask spread exceeds 10 times the bid
6. Singles (a call without matching put or a put without matching call)
7. The option's mid quote violates simple no arbitrage bounds. I allow for a small margin of error to reflect the fact that the assumed risk-free rate may not exactly reflect the prevailing lending rate for option brokers.

I further manually remove a few observations with obvious data errors.

Computing synthetic variance swap rates

With two exceptions, I use the same procedure that the CBOE uses to compute the VIX in order to compute synthetic variance swap rates. While the VIX is based on maturities bracketing 30 calendar days, I apply the same approach to compute swap rates with maturities of 30, 60, ..., 360 days. The two exceptions are:

Steps for computing implied volatilities on a fixed grid

- On any day in the sample, I first compute the (Black-Scholes) IV and the standardized moneyness for all available options. To standardize moneyness, I use the previously computed variance swap rate with the same maturity as the option.
- I then use a Gaussian kernel to interpolate IV to a fixed grid of relative moneyness from -2 to 1 and maturities from 1 to 12 months. This is the same procedure used by OptionMetrics to compute its well-known implied volatility surface.² I use a kernel weight of 0.05 in the maturity dimension (measured as the log of days to maturity) and a weight of 0.005 in the moneyness dimension, both of which are similar to the values used by OptionMetrics.

Data for annual cash flows and basic asset prices

Data for annual cash flows and asset prices are equivalent to those in [Bansal, Kiku, and Yaron \[2012\]](#) and [Beeler and Campbell \[2012\]](#) – extended to the end of 2012 – with one exception: I add the four quarterly ex-ante estimates of the risk-free rate within each year to compute the annual risk-free rate instead of multiplying the first-quarter estimate by four. The alternative corresponds more closely to the model-equivalent, which is based on the sum of the risk-free rates within the year, both in my paper and in the above-cited papers.

²OptionMetrics expresses IV as a function of maturity and the option’s delta.

Appendix B

Model solution details

The model solution is characterized by the $N \times 1$ vectors

$$\lambda^V, \lambda^\mu, \lambda^d, \mathcal{B}(\tau), \lambda^c(\tau, K), \mathcal{V}(\tau),$$

for $\tau \in \mathbb{N}^+$ and $K \in \mathbb{R}^+$. Section 1.3.2 describes the general procedure of solving for these vectors. This appendix contains the algebraic details. In deriving the solutions, I consider the more general endowment

$$\begin{aligned}\Delta c_{t+1} &= \mu_t^c + \sigma_t^c \varepsilon_{t+1}^c \\ \Delta d_{t+1} &= \mu_t^d + \sigma_t^d \varepsilon_{t+1}^d,\end{aligned}$$

which allows for arbitrary Markov-switching processes for both the mean and the volatility of $(\Delta c, \Delta d)$. The model in the main text is a special case given by $\mu_t^c = \mu_t^d = \mu$, $\sigma_t^c = \sigma_t$, and $\sigma_t^d = \varphi \sigma_t$.

Notation

Throughout the appendix, denote the cumulative density function (cdf) of a standard normal by $\Phi(\cdot)$, and let the number of arguments indicate whether the cdf is univariate or bivariate. Let $\mathbf{1}\{\cdot\}$ denote the indicator function. Denote the Hadamard (element-wise) matrix product by \odot . Lastly, define

$$\begin{aligned}\mu_t^{cd} &\equiv (\alpha - 1)\mu_t^c + \mu_t^d \\ \sigma_t^{cd} &\equiv \frac{1}{2}(\alpha - 1)^2(\sigma_t^c)^2 + \frac{1}{2}(\sigma_t^d)^2 + (\alpha - 1)\sigma_t^c\sigma_t^d\end{aligned}$$

The derivations presented below makes extensive use of the the following Lemma, the proof of which is contained in Appendix C.

Lemma 1. Let x, y be standard normal with correlation ρ , and let a, b, r, s be constants. Then

(a)

$$E[e^{rx+sy}\mathbf{1}\{x \leq a\}] = e^{\frac{1}{2}(r^2+2\rho rs+s^2)}\Phi(a-r-\rho s)$$

(b)

$$E[e^{rx+sy}\mathbf{1}\{a \leq y\}] = e^{\frac{1}{2}(r^2+2\rho rs+s^2)} [1 - \Phi(a - \rho r - s)]$$

(c)

$$E[e^{rx+sy}\mathbf{1}\{x \leq a\}\mathbf{1}\{b \leq y\}] = e^{\frac{1}{2}(r^2+2\rho rs+s^2)} [\Phi(a-r-\rho s) - \Phi(a-r-\rho s, b-\rho r-s)]$$

(d)

$$E[e^{rx}y^2\mathbf{1}\{x \leq a\}] = e^{\frac{r^2}{2}}(1+r^2\rho^2)\Phi(a-r) - e^{\frac{2ra-a^2}{2}}\frac{(r+a)\rho^2}{\sqrt{2\pi}} \equiv \Omega(r, a)$$

(e)

$$E[e^{rx}y\mathbf{1}\{x \leq a\}] = \rho e^{\frac{r^2}{2}} \left(r\Phi(a-r) - \frac{1}{\sqrt{2\pi}}e^{-\frac{(a-r)^2}{2}} \right) \equiv \Gamma(r, a)$$

Solving for the Utility Ratios – λ^V and λ^μ

Using the law of iterated expectations, the expectation in the pricing kernel (Equation 1.7) can be written as $E_t[\mathbf{1}(V_{t+1} \leq \delta\mu_t)] = E_t[\Phi(\phi_{t+1}^c)]$. Dividing the value function in Equation 1.4 by C_t gives

$$\lambda_t^V = [(1 - \beta) + \beta(\lambda_t^\mu)^\rho]^\frac{1}{\rho}. \quad (\text{B.1})$$

Dividing the certainty equivalent in Equation 1.5 by C_t and re-arranging terms gives

$$\lambda_t^\mu = \begin{cases} E_t \left[e^{\alpha \Delta c_{t+1}} (\lambda_{t+1}^V)^\alpha \frac{1 + \theta \mathbf{1}\{\varepsilon_{t+1}^c \leq \phi_{t+1}^c\}}{1 + \theta \delta^\alpha E_t[\Phi(\phi_{t+1}^c)]} \right]^\frac{1}{\alpha}, & \text{for } \alpha \leq 1, \alpha \neq 0 \\ \exp \left(E_t \left[\frac{(\log(\lambda_{t+1}^V) + \Delta c_{t+1})(1 + \theta \mathbf{1}\{\varepsilon_{t+1}^c \leq \phi_{t+1}^c\}) - \theta \log(\delta) \mathbf{1}\{\varepsilon_{t+1}^c \leq \phi_{t+1}^c\}}{1 + \theta E_t[\Phi(\phi_{t+1}^c)]} \right] \right) & \text{for } \alpha = 0 \end{cases} \quad (\text{B.2})$$

The expectation over ε_{t+1}^c can be evaluated by using Lemma 1a. In the case $\alpha \leq 1, \alpha \neq 0$, the objects in the lemma are given by $r = \alpha \sigma_t^c$, $s = 0$, and $a = \phi_{t+1}^c$. To solve the case of $\alpha = 0$, note that for $\varepsilon \sim N(0, 1)$, $E[\varepsilon \mathbf{1}\{\varepsilon \leq a\}] = \int_{-\infty}^a \varepsilon f(\varepsilon) d\varepsilon = -\frac{1}{\sqrt{2\pi}} e^{-\frac{\varepsilon^2}{2}} \Big|_{-\infty}^a = -\Phi'(a)$. It follows that

$$\lambda_t^\mu = \begin{cases} E_t \left[\frac{(\lambda_{t+1}^V)^\alpha}{1 + \theta \delta^\alpha E_t[\Phi(\phi_{t+1}^c)]} e^{\alpha \mu_t^c + \frac{1}{2} \alpha^2 (\sigma_t^c)^2} \left(1 + \theta \Phi(\phi_{t+1}^c - \alpha \sigma_t^c) \right) \right]^\frac{1}{\alpha}, & \text{for } \alpha \leq 1, \alpha \neq 0 \\ \exp \left(E_t \left[\frac{(\log(\lambda_{t+1}^V) + \mu_t^c)(1 + \theta \Phi(\phi_{t+1}^c)) - \sigma_t^c \theta \Phi'(\phi_{t+1}^c) - \theta \log(\delta) \Phi(\phi_{t+1}^c)}{1 + \theta E_t[\Phi(\phi_{t+1}^c)]} \right] \right) & \text{for } \alpha = 0 \end{cases} \quad (\text{B.3})$$

Given a guess for λ^V and λ^μ , the remaining expectation in equation B.3 can be evaluated as a matrix product. The system of equations in B.1 and B.3 has to be solved numerically.

Solving for Bond Prices – $\mathcal{B}(\tau)$

The price of a one-period bond equals

$$\begin{aligned}
\mathcal{B}_t(1) &= E_t[M_{t+1}] \\
&= E_t \left[\beta e^{(\alpha-1)\Delta c_{t+1}} \left(\frac{\lambda_{t+1}^V}{\lambda_t^\mu} \right)^{\alpha-\rho} \left(\frac{1 + \theta \mathbf{1}\{\varepsilon_{t+1}^c \leq \phi_{t+1}^c\}}{1 + \delta^\alpha \theta E_t[\Phi(\phi_{t+1}^c)]} \right) \right] \\
&= E_t \left[\beta e^{(\alpha-1)\mu_t^c + \frac{1}{2}(\alpha-1)^2(\sigma_t^c)^2} \left(\frac{\lambda_{t+1}^V}{\lambda_t^\mu} \right)^{\alpha-\rho} \left(\frac{1 + \theta \Phi(\phi_{t+1}^c - (\alpha-1)\sigma_t^c)}{1 + \delta^\alpha \theta E_t[\Phi(\phi_{t+1}^c)]} \right) \right],
\end{aligned} \tag{B.4}$$

where the last equality uses the law of iterated expectations and Lemma 1a with $r = (\alpha-1)\sigma_t^c$, $s = 0$, and $a = \phi_{t+1}^c$. Prices of multi-period bonds can be expressed recursively as

$$\mathcal{B}_t(\tau) \equiv E_t[M_{t:t+\tau}] = E_t \left[\prod_{h=1}^{\tau} M_{t+h} \right] = E_t \left[\left(\prod_{h=1}^{\tau-1} M_{t+h} \right) E_{t+\tau-1}[M_{t+\tau}] \right]$$

To evaluate the remaining expectations, denote the term in equation B.4 inside the expectation by a_{ij}^b when the Markov chain is in state i at time t in in state j at time $t+1$. Collect the terms a_{ij}^b in a matrix A^b . Then bond prices can be written in matrix form as

$$\begin{aligned}
\mathcal{B}(1) &= (P \odot A^b) \cdot \iota_N \\
\mathcal{B}(\tau) &= (P \odot A^b) \cdot \mathcal{B}(\tau-1)
\end{aligned}$$

Solving for the Price-Dividend Ratio – λ^d

After dividing by D_t , the Euler equation for the dividend claim is given by

$$\begin{aligned}
\lambda_t^d &\equiv \frac{S_t}{D_t} = E_t \left[M_{t+1} \frac{S_{t+1} + D_{t+1}}{D_t} \right] \\
&= E_t \left[\beta \left(\frac{\lambda_{t+1}^V}{\lambda_t^\mu} \right)^{\alpha-\rho} \left(\frac{1 + \theta \mathbf{1}\{\varepsilon_{t+1}^c \leq \phi_{t+1}^c\}}{1 + \delta^\alpha \theta E_t[\Phi(\phi_{t+1}^c)]} \right) e^{(\alpha-1)\Delta c_{t+1} + \Delta d_{t+1}} (\lambda_{t+1}^d + 1) \right]
\end{aligned}$$

One can integrate out $(\varepsilon_{t+1}^c, \varepsilon_{t+1}^d)$ by using the law of iterated expectations. Applying Lemma 1a with $r = (\alpha-1)\sigma_t^c$, $s = \sigma_t^d$, and $a = \phi_{t+1}^c$ yields

$$\lambda_t^d = E_t \left[\underbrace{\beta \left(\frac{\lambda_{t+1}^V}{\lambda_t^\mu} \right)^{\alpha-\rho} \left(\frac{1 + \theta \Phi(\phi_{t+1}^c - (\alpha-1)\sigma_t^c - \varrho \sigma_t^d)}{1 + \delta^\alpha \theta E_t[\Phi(\phi_{t+1}^c)]} \right) e^{\mu_t^{cd} + \sigma_t^{cd}}}_{\equiv a_{ij}^d} (\lambda_{t+1}^d + 1) \right],$$

where μ_t^{cd} and σ_t^{cd} were defined under "Notation". To evaluate the remaining expectation and to solve for λ^d , denote the term pre-multiplying $(\lambda_{t+1}^d + 1)$ inside the expectation by a_{ij}^d when the Markov chain is in state i at time t in in state j at time $t+1$. Collect the

terms a_{ij}^d in a matrix A^d . Then the expectation can be evaluated in matrix form as

$$\begin{aligned}
 \lambda^d &= [P \odot A^d \odot (\mathbf{1}_N + \iota_N(\lambda^d)')] \iota_N \\
 &= [P \odot A^d] \iota_N + [(P \odot A^d) \odot (\iota_N(\lambda^d)')] \iota_N \\
 &= [P \odot A^d] \iota_N + (P \odot A^d) \lambda^d \\
 \Leftrightarrow \lambda^d &= (I_N - P \odot A^d)^{-1} [P \odot A^d] \iota_N
 \end{aligned}$$

Solving for One-Period Call Prices – $\mathcal{C}(1, K)$

The (relative) price of a 1-period call with moneyness K equals

$$\mathcal{C}_t(1, K) \equiv E_t \left[M_{t+1} \max \left(0, \frac{S_{t+1}}{S_t} - K \right) \right],$$

The call payoff is triggered if

$$\frac{S_{t+1}}{S_t} > K \Leftrightarrow \frac{\lambda_{t+1}^d}{\lambda_t^d} e^{\Delta d_{t+1}} > K \Leftrightarrow \varepsilon_{t+1}^d > \frac{\log \left(K \frac{\lambda_t^d}{\lambda_{t+1}^d} \right) - \mu_t^d}{\sigma_t^d} \equiv \phi_{t+1}^d(K),$$

where I have defined the payoff threshold $\phi_{t+1}^d(K)$. The call price can now be written as

$$\begin{aligned} \mathcal{C}_t(1, K) &= E_t \left[M_{t+1} \left(\frac{\lambda_{t+1}^d}{\lambda_t^d} e^{\Delta d_{t+1}} - K \right) \mathbf{1} \left\{ \phi_{t+1}^d(K) < \varepsilon_{t+1}^d \right\} \right] \\ &= E_t \left[\beta e^{(\alpha-1)\Delta c_{t+1}} \left(\frac{\lambda_{t+1}^V}{\lambda_t^\mu} \right)^{\alpha-\rho} \left(\frac{1 + \theta \mathbf{1} \{ \varepsilon_{t+1}^c \leq \phi_{t+1}^c \}}{1 + \delta^\alpha \theta E_t[\Phi(\phi_{t+1}^c)]} \right) \left(\frac{\lambda_{t+1}^d}{\lambda_t^d} e^{\Delta d_{t+1}} - K \right) \mathbf{1} \left\{ \phi_{t+1}^d(K) < \varepsilon_{t+1}^d \right\} \right] \end{aligned}$$

To integrate out $(\varepsilon_{t+1}^c, \varepsilon_{t+1}^d)$, one has to use the law of iterated expectations in combination with Lemma 1 several times. Specifically, the above expression contains four additive parts containing normal innovations. To keep notation manageable, I first integrate over the normal terms in each of these four expressions separately.

$$\begin{aligned} E_t \left[e^{(\alpha-1)\Delta c_{t+1} + \Delta d_{t+1}} \mathbf{1} \left\{ \phi_{t+1}^d(K) < \varepsilon_{t+1}^d \right\} \right] &= E_t \left[\underbrace{e^{\mu_t^{cd} + \sigma_t^{cd}} (1 - \Phi(\phi_{t+1}^d(K) - (\alpha-1)\varrho\sigma_t^c - \sigma_t^d))}_{\equiv \chi_{t+1}^1} \right] \\ E_t \left[e^{(\alpha-1)\Delta c_{t+1}} \mathbf{1} \left\{ \phi_{t+1}^d(K) < \varepsilon_{t+1}^d \right\} \right] &= E_t \left[\underbrace{e^{(\alpha-1)\mu_t^c + \frac{1}{2}(\alpha-1)^2(\sigma_t^c)^2} (1 - \Phi(\phi_{t+1}^d(K) - (\alpha-1)\varrho\sigma_t^c))}_{\equiv \chi_{t+1}^2} \right] \\ E_t \left[e^{(\alpha-1)\Delta c_{t+1} + \Delta d_{t+1}} \mathbf{1} \{ \varepsilon_{t+1}^c \leq \phi_{t+1}^c \} \mathbf{1} \left\{ \phi_{t+1}^d(K) < \varepsilon_{t+1}^d \right\} \right] &= E_t \left[\underbrace{e^{\mu_t^{cd} + \sigma_t^{cd}} \left(\Phi(\phi_{t+1}^c - (\alpha-1)\sigma_t^c - \varrho\sigma_t^d) - \Phi(\phi_{t+1}^c - (\alpha-1)\sigma_t^c - \varrho\sigma_t^d, \phi_{t+1}^d(K) + \gamma\rho\sigma_t^c - \sigma_t^d) \right)}_{\equiv \chi_{t+1}^3} \right] \\ E_t \left[e^{(\alpha-1)\Delta c_{t+1}} \mathbf{1} \{ \varepsilon_{t+1}^c \leq \phi_{t+1}^c \} \mathbf{1} \left(\phi_{t+1}^d(K) < \varepsilon_{t+1}^d \right) \right] &= E_t \left[\underbrace{e^{(\alpha-1)\mu_t^c + \frac{1}{2}(\alpha-1)^2(\sigma_t^c)^2} \left(\Phi(\phi_{t+1}^c - (\alpha-1)\sigma_t^c) - \Phi(\phi_{t+1}^c - (\alpha-1)\sigma_t^c, \phi_{t+1}^d(K) - (\alpha-1)\varrho\sigma_t^c) \right)}_{\equiv \chi_{t+1}^4} \right] \end{aligned}$$

Using these terms, the call price can be written as

$$\mathcal{C}_t(1, K) = E_t \left[\frac{\beta}{1 + \delta^\alpha \theta E_t[\Phi(\phi_{t+1}^c)]} \left(\frac{\lambda_{t+1}^V}{\lambda_t^\mu} \right)^{\alpha-\rho} \times \left(\frac{\lambda_{t+1}^d}{\lambda_t^d} (\chi_{t+1}^1 + \theta \chi_{t+1}^3) - K (\chi_{t+1}^2 + \theta \chi_{t+1}^4) \right) \right]$$

and using similar notation as above, it can be evaluated for each K as

$$\mathcal{C}(1, K) = (P \odot A^c(K)) \cdot \iota_N$$

Solving for Variance Swap Rates – $\mathcal{V}(\tau)$

The τ -period variance swap rate is given by

$$\begin{aligned} \mathcal{V}_t(\tau) &= E_t^Q \left[\sum_{h=1}^{\tau} r_{t+h}^2 \right] = E_t [M_{t:t+\tau}]^{-1} \times E_t \left[M_{t:t+\tau} \sum_{h=1}^{\tau} r_{t+h}^2 \right] \\ &= \mathcal{B}_t(\tau)^{-1} \times \sum_{h=1}^{\tau} E_t [M_{t:t+h} M_{t+h:t+\tau} r_{t+h}^2] \\ &= \mathcal{B}_t(\tau)^{-1} \times \sum_{h=1}^{\tau} E_t [M_{t:t+h} r_{t+h}^2 E_{t+h} [M_{t+h:t+\tau}]] \\ &= \mathcal{B}_t(\tau)^{-1} \times \sum_{h=1}^{\tau} E_t \underbrace{\left[M_{t:t+h} r_{t+h}^2 \lambda_{t+h}^b(\tau - h) \right]}_{\equiv \mathcal{V}_t(h, \tau)} \end{aligned}$$

The terms $\mathcal{V}_t(h, \tau)$, for $h \leq \tau$ and $h, \tau \geq 2$, can be computed recursively as

$$\mathcal{V}_t(h, \tau) = E_t [M_{t+1} \mathcal{V}_{t+1}(h-1, \tau-1)],$$

and evaluated in matrix form as

$$\mathcal{V}(h, \tau) = (P \odot A^b) \cdot \mathcal{V}(h-1, \tau-1)$$

where the matrix A^b was defined under "Solving for Bond Prices". The recursion begins with the terms $\mathcal{V}_t(1, \kappa)$ for $\kappa = 1, \dots, \tau$, which can be computed as

$$\begin{aligned} \mathcal{V}_t(1, \kappa) &= E_t [M_{t+1} r_{t+1}^2 \mathcal{B}_{t+1}(\kappa-1)] \\ &= E_t \left[\beta e^{(\alpha-1)\Delta c_{t+1}} \left(\frac{\lambda_{t+1}^V}{\lambda_t^\mu} \right)^{\alpha-\rho} \left(\frac{1 + \theta \mathbf{1}\{\varepsilon_{t+1}^c \leq \phi_{t+1}^c\}}{1 + \delta^\alpha \theta E_t[\Phi(\phi_{t+1}^c)]} \right) \times \mathcal{B}_{t+1}(\kappa-1) \right. \\ &\quad \left. \times \left(\log \left(\frac{\lambda_{t+1}^d}{\lambda_t^d} \right)^2 + (\mu_t^d)^2 + (\sigma_t^d)^2 (\varepsilon_{t+1}^d)^2 + 2\mu_t^d \sigma_t^d \varepsilon_{t+1}^d + 2 \log \left(\frac{\lambda_{t+1}^d}{\lambda_t^d} \right) (\mu_t^d + \sigma_t^d \varepsilon_{t+1}^d) \right) \right], \end{aligned}$$

where $\mathcal{B}_{t+1}(0) = 1$. To integrate out $(\varepsilon_{t+1}^c, \varepsilon_{t+1}^d)$, one has to use the law of iterated expectations in combination with Lemma 1 several times. For notational convenience, I first integrate over the normal terms in parts of the above expression individually, and I

subsequently combine terms. First, using Lemma 1d with $r = (\alpha - 1)\sigma_t^c$ and $a = \infty$,

$$E_t \left[e^{(\alpha-1)\Delta c_{t+1}} (\varepsilon_{t+1}^d)^2 \right] = \underbrace{e^{(\alpha-1)\mu_t} \Omega((\alpha-1)\sigma_t^c, \infty)}_{\equiv \xi_{1,t+1}},$$

where $\Omega(\cdot, \cdot)$ was defined in Lemma 1d. Note that $\Omega(r, \infty) = e^{\frac{r^2}{2}} (1 + r^2 \rho^2)$.¹ Second, using Lemma 1d with $r = (\alpha - 1)\sigma_t^c$ and $a = \phi_{t+1}^c$,

$$E_t \left[e^{(\alpha-1)\Delta c_{t+1}} \mathbf{1}\{\varepsilon_{t+1}^c \leq \phi_{t+1}^c\} (\varepsilon_{t+1}^d)^2 \right] = E_t \left[\underbrace{e^{(\alpha-1)\mu_t} \Omega((\alpha-1)\sigma_t^c, \phi_{t+1}^c)}_{\equiv \xi_{2,t+1}} \right].$$

Third, using Lemma 1e with $r = (\alpha - 1)\sigma_t^c$ and $a = \infty$,

$$E_t \left[e^{(\alpha-1)\Delta c_{t+1}} \varepsilon_{t+1}^d \right] = \underbrace{e^{(\alpha-1)\mu_t} \Gamma((\alpha-1)\sigma_t^c, \infty)}_{\equiv \xi_{3,t+1}}.$$

Note that $\Gamma(r, \infty) = r \rho e^{\frac{r^2}{2}}$. Forth, using Lemma 1e with $r = (\alpha - 1)\sigma_t^c$ and $a = \phi_{t+1}^c$,

$$E_t \left[e^{(\alpha-1)\Delta c_{t+1}} \mathbf{1}\{\varepsilon_{t+1}^c \leq \phi_{t+1}^c\} \varepsilon_{t+1}^d \right] = E_t \left[\underbrace{e^{(\alpha-1)\mu_t} \Gamma((\alpha-1)\sigma_t^c, \phi_{t+1}^c)}_{\equiv \xi_{4,t+1}} \right],$$

Lastly, using Lemma 1a with $r = (\alpha - 1)\sigma_t^c$, $s = 0$, and $a = \phi_{t+1}^c$,

$$E_t \left[e^{(\alpha-1)\Delta c_{t+1}} \mathbf{1}\{\varepsilon_{t+1}^c \leq \phi_{t+1}^c\} \right] = E_t \left[e^{(\alpha-1)\mu_t + \frac{1}{2}(\alpha-1)^2(\sigma_t^c)^2} \Phi(\phi_{t+1}^c - (\alpha-1)\sigma_t^c) \right].$$

Using this last result as well as the ξ -terms, $\mathcal{V}_t(1, \kappa)$ can be written as

$$\begin{aligned} \mathcal{V}_t(1, \kappa) = & E_t \left[\mathcal{B}_{t+1}(\kappa - 1) \times \left\{ \beta e^{(\alpha-1)\mu_t + \frac{1}{2}(\alpha-1)^2(\sigma_t^c)^2} \left(\frac{\lambda_{t+1}^V}{\lambda_t^\mu} \right)^{\alpha-\rho} \left(\frac{1 + \theta \Phi(\phi_{t+1}^c - (\alpha-1)\sigma_t^c)}{1 + \delta^\alpha \theta E_t[\Phi(\phi_{t+1}^c)]} \right) \right. \right. \\ & \times \left(\log \left(\frac{\lambda_{t+1}^d}{\lambda_t^d} \right)^2 + (\mu_t^d)^2 + 2 \log \left(\frac{\lambda_{t+1}^d}{\lambda_t^d} \right) \mu_t^d \right) \\ & + \left(\frac{\beta}{1 + \delta^\alpha \theta E_t[\Phi(\phi_{t+1}^c)]} \right) \left(\frac{\lambda_{t+1}^V}{\lambda_t^\mu} \right)^{\alpha-\rho} \\ & \times \left((\sigma_t^d)^2 (\xi_{1,t+1} + \theta \xi_{2,t+1}) + \left[2\mu_t^d \sigma_t^d + 2 \log \left(\frac{\lambda_{t+1}^d}{\lambda_t^d} \right) \sigma_t^d \right] (\xi_{3,t+1} + \theta \xi_{4,t+1}) \right) \left. \right\} \right] \end{aligned}$$

To evaluate the remaining expectation, denote the term in the curly brackets by a_{ij}^ν when the Markov chain is in state i at time t in in state j at time $t + 1$. Collect the terms a_{ij}^ν

¹This holds because in the second term of Ω , the exponential factor goes to zero faster than the latter factor goes to infinity.

in a matrix A^ν . Then the expectation can be evaluated in matrix form as

$$\mathcal{V}(1, \kappa) = (P \odot A^\nu) \cdot \mathcal{B}(\kappa - 1)$$

At this point one can apply the above recursion to compute $\mathcal{V}(h, \kappa)$ for $h > 1$. Lastly, variance swap rates can be computed by summing appropriate terms.

Appendix C

Proof of Lemma 1

Proof, parts a-c. All three results are special cases of the following more general result

$$E[e^{rx+sy}\mathbf{1}\{a \leq x \leq b\}\mathbf{1}\{c \leq y \leq d\}] = e^{\frac{1}{2}(r^2+2\rho rs+s^2)} [\Phi(b^*, d^*) + \Phi(a^*, c^*) - \Phi(a^*, d^*) - \Phi(c^*, b^*)],$$

where $a^* = a - r - \rho s$, $b^* = b - r - \rho s$, $c^* = c - \rho r - s$, and $d^* = d - \rho r - s$. In what follows, I prove this more general case.

$$E[e^{rx+sy}\mathbf{1}\{a \leq x \leq b\}\mathbf{1}\{c \leq y \leq d\}] = \frac{1}{2\pi\sqrt{1-\rho^2}} \int_a^b \int_c^d e^{rx+sy-\frac{x^2-2\rho xy+y^2}{2(1-\rho^2)}} dydx$$

I next re-write the exponent. This is easier in matrix notation. Define $t = [r \ s]'$, $z = [x \ y]'$,

$$\Sigma \equiv \begin{bmatrix} 1 & \rho \\ \rho & 1 \end{bmatrix}, \text{ and } \varphi \equiv \Sigma t = \begin{bmatrix} r + s\rho \\ s + r\rho \end{bmatrix}. \text{ Then}$$

$$\begin{aligned} rx + sy - \frac{x^2 - 2\rho xy + y^2}{2(1 - \rho^2)} &= t'z - \frac{1}{2}z'\Sigma^{-1}z \\ &= \frac{1}{2}(z't + t'z - z'\Sigma^{-1}z) \\ &= \frac{1}{2}(z'\Sigma^{-1}\varphi + \varphi'\Sigma^{-1}z - z'\Sigma^{-1}z) \\ &= \frac{1}{2}(z'\Sigma^{-1}\varphi - (z - \varphi)'\Sigma^{-1}z) \\ &= \frac{1}{2}(\varphi'\Sigma^{-1}\varphi + (z - \varphi)'\Sigma^{-1}\varphi - (z - \varphi)'\Sigma^{-1}z) \\ &= \frac{1}{2}(\varphi'\Sigma^{-1}\varphi - (z - \varphi)'\Sigma^{-1}(z - \varphi)) \\ &= \frac{1}{2}t'\Sigma t - \frac{1}{2}(z - \varphi)'\Sigma^{-1}(z - \varphi) \end{aligned}$$

Note that $t'\Sigma t = r^2 + 2\rho rs + s^2$. Let $v = z_1 - \varphi_1 = x - r - s\rho$ and $w = z_2 - \varphi_2 = y - s - r\rho$ so that $dv = dx$ and $dw = dy$. Plugging back the re-written exponent along with this

change of variables yields the result:

$$E[e^{rx+sy} \mathbf{1}\{a \leq x \leq b\} \mathbf{1}\{c \leq y \leq d\}] = e^{\frac{1}{2}(r^2+2\rho rs+s^2)} \frac{1}{2\pi|\Sigma|^{1/2}} \int_{a-r-s\rho}^{b-r-s\rho} \int_{c-s-r\rho}^{d-s-r\rho} e^{\frac{v^2-2\rho vw+w^2}{2(1-\rho^2)}} dw dv$$

The special cases are obtained by noting that

1. $\Phi(-\infty, x) = \Phi(x, -\infty) = 0$
2. $\Phi(\infty, x) = \Phi(x, \infty) = \Phi(x)$

■

Proof, part d.

$$E [e^{rx} y^2 \mathbf{1}\{x \leq a\}] = \int_{-\infty}^a \int_{-\infty}^{\infty} e^{rx} y^2 \frac{1}{2\pi\sqrt{1-\rho^2}} e^{-\frac{x^2-2\rho xy+y^2}{2(1-\rho^2)}} dy dx$$

The exponent can be written as

$$\begin{aligned} rx - \frac{x^2 - 2\rho xy + y^2}{2(1-\rho^2)} &= rx - \frac{x^2(1-\rho^2) + \rho^2 x^2 - 2\rho xy + y^2}{2(1-\rho^2)} \\ &= -\frac{x^2 - 2rx}{2} - \frac{y^2 - 2(\rho x)y + (\rho x)^2}{2(1-\rho^2)} \\ &= \frac{r^2}{2} - \frac{(x-r)^2}{2} - \frac{(y-\rho x)^2}{2(1-\rho^2)} \end{aligned}$$

Let $z = \frac{y-\rho x}{\sqrt{1-\rho^2}}$, which implies $dz = \frac{dy}{\sqrt{1-\rho^2}}$ and $y^2 = z^2(1-\rho^2) + 2\rho\sqrt{1-\rho^2}xz + \rho^2 x^2$.

Substituting the re-written exponent along with the change of variables gives

$$\begin{aligned} E [e^{rx} y^2 \mathbf{1}\{x \leq a\}] &= \int_{-\infty}^a \int_{-\infty}^{\infty} \left(z^2(1-\rho^2) + 2\rho\sqrt{1-\rho^2}xz + \rho^2 x^2 \right) \frac{1}{2\pi} e^{\frac{r^2}{2} - \frac{(x-r)^2}{2} - \frac{z^2}{2}} dz dx \\ &= e^{\frac{r^2}{2}} \int_{-\infty}^a e^{-\frac{(x-r)^2}{2}} \frac{1}{\sqrt{2\pi}} \left(\int_{-\infty}^{\infty} \left(z^2(1-\rho^2) + 2\rho\sqrt{1-\rho^2}xz + \rho^2 x^2 \right) \frac{1}{\sqrt{2\pi}} e^{-\frac{z^2}{2}} dz \right) dx \\ &= e^{\frac{r^2}{2}} \frac{1}{\sqrt{2\pi}} \int_{-\infty}^a e^{-\frac{(x-r)^2}{2}} (1-\rho^2 + \rho^2 x^2) dx, \end{aligned}$$

where the last equality used the fact that $z \sim N(0, 1)$. Now let $w = x - r$, which implies $dw = dx$ and $x^2 = w^2 + 2wr + r^2$, so that

$$\begin{aligned} E [e^{rx} y^2 \mathbf{1}\{x \leq a\}] &= e^{\frac{r^2}{2}} \frac{1}{\sqrt{2\pi}} \int_{-\infty}^{a-r} e^{-\frac{w^2}{2}} (1-\rho^2 + \rho^2(w^2 + 2wr + r^2)) dw \\ &= e^{\frac{r^2}{2}} \left((1-\rho^2 + \rho^2 r^2) \Phi(a-r) + \rho^2 \int_{-\infty}^{a-r} w^2 \frac{1}{\sqrt{2\pi}} e^{-\frac{w^2}{2}} dw + 2\rho^2 r \int_{-\infty}^{a-r} w \frac{1}{\sqrt{2\pi}} e^{-\frac{w^2}{2}} dw \right) \\ &= e^{\frac{r^2}{2}} \left((1-\rho^2 + \rho^2 r^2) \Phi(a-r) + \rho^2 \int_{-\infty}^{a-r} w^2 \frac{1}{\sqrt{2\pi}} e^{-\frac{w^2}{2}} dw - 2\rho^2 r e^{-\frac{(a-r)^2}{2}} \right) \end{aligned}$$

The remaining integral can be evaluated using integration by parts.

$$\frac{1}{\sqrt{2\pi}} \int_{-\infty}^{a-r} \underbrace{(-w)}_{\equiv u} \underbrace{(-we^{-\frac{w^2}{2}})}_{\equiv dv} dw = -\frac{1}{\sqrt{2\pi}} we^{-\frac{w^2}{2}} \Big|_{-\infty}^{a-r} + \int_{-\infty}^{a-r} \frac{1}{\sqrt{2\pi}} e^{-\frac{w^2}{2}} dw = \frac{a-r}{\sqrt{2\pi}} e^{-\frac{(a-r)^2}{2}} + \Phi(a-r)$$

Substituting this back in and combining terms gives the result.

■

Proof, part e.

$$E[e^{rx}y\mathbf{1}\{x \leq a\}] = \int_{-\infty}^a \int_{-\infty}^{\infty} e^{rx}y \frac{1}{2\pi\sqrt{1-\rho^2}} e^{-\frac{x^2-2\rho xy+y^2}{2(1-\rho^2)}} dy dx$$

The exponent can be written as

$$\begin{aligned} rx - \frac{x^2 - 2\rho xy + y^2}{2(1-\rho^2)} &= rx - \frac{x^2(1-\rho^2) + \rho^2 x^2 - 2\rho xy + y^2}{2(1-\rho^2)} \\ &= -\frac{x^2 - 2rx}{2} - \frac{y^2 - 2(\rho x)y + (\rho x)^2}{2(1-\rho^2)} \\ &= \frac{r^2}{2} - \frac{(x-r)^2}{2} - \frac{(y-\rho x)^2}{2(1-\rho^2)} \end{aligned}$$

Let $z = \frac{y-\rho x}{\sqrt{1-\rho^2}}$, which implies $dz = \frac{dy}{\sqrt{1-\rho^2}}$ and $y = z\sqrt{1-\rho^2} + \rho x$. Substituting the re-written exponent along with the change of variables gives

$$\begin{aligned} E[e^{rx}y\mathbf{1}\{x \leq a\}] &= \int_{-\infty}^a \int_{-\infty}^{\infty} \left(z\sqrt{1-\rho^2} + \rho x\right) \frac{1}{2\pi} e^{\frac{r^2}{2} - \frac{(x-r)^2}{2} - \frac{z^2}{2}} dz dx \\ &= e^{\frac{r^2}{2}} \int_{-\infty}^a e^{-\frac{(x-r)^2}{2}} \frac{1}{\sqrt{2\pi}} \left(\int_{-\infty}^{\infty} \left(z\sqrt{1-\rho^2} + \rho x\right) \frac{1}{\sqrt{2\pi}} e^{-\frac{z^2}{2}} dz \right) dx \\ &= \rho e^{\frac{r^2}{2}} \frac{1}{\sqrt{2\pi}} \int_{-\infty}^a x e^{-\frac{(x-r)^2}{2}} dx, \end{aligned}$$

where the last equality used the fact that $z \sim N(0, 1)$. Now let $w = x - r$, which implies $dw = dx$, so that

$$\begin{aligned} E[e^{rx}y\mathbf{1}\{x \leq a\}] &= \rho e^{\frac{r^2}{2}} \frac{1}{\sqrt{2\pi}} \int_{-\infty}^{a-r} (r+w) e^{-\frac{w^2}{2}} dw \\ &= \rho e^{\frac{r^2}{2}} \left(r\Phi(a-r) + \frac{1}{\sqrt{2\pi}} \int_{-\infty}^{a-r} w e^{-\frac{w^2}{2}} dw \right) \\ &= \rho e^{\frac{r^2}{2}} \left(r\Phi(a-r) - \frac{1}{\sqrt{2\pi}} e^{-\frac{(a-r)^2}{2}} \right) \end{aligned}$$

■

Bibliography

- ANDERSEN, T. G., T. BOLLERSLEV, F. X. DIEBOLD, AND H. EBENS (2001): “The distribution of realized stock return volatility,” *Journal of Financial Economics*, 61, 43–76.
- ANDERSEN, T. G., T. BOLLERSLEV, F. X. DIEBOLD, AND P. LABYS (2003): “Modeling and Forecasting Realized Volatility,” *Econometrica*, 71(2), 579–625.
- ANDERSEN, T. G., O. BONDARENKO, AND M. T. GANZALEZ-PEREZ (2012): “Uncovering Novel Features of Equity-Index Return Dynamics via Corridor Implied Volatility,” Working Paper.
- ANG, A., R. J. HODRICK, Y. XING, AND X. ZHANG (2006): “The Cross-Section of Volatility and Expected Returns,” *Journal of Finance*, 61(1), 259–299.
- (2009): “High Idiosyncratic Volatility and Low Returns: International and Further U.S. Evidence,” *Journal of Financial Economics*, 91, 1–23.
- BACKUS, D., M. CHERNOV, AND I. MARTIN (2011): “Disasters Implied by Equity Index Options,” *Journal of Finance*, 66(6), 1969–2012.
- BAKSHI, G., AND N. KAPADIA (2003): “Delta-Hedged Gains and the Negative Market Volatility Risk Premium,” *Review of Financial Studies*, 16(2), 527–566.
- BAKSHI, G., N. KAPADIA, AND D. MADAN (2003): “Stock Return Characteristics, Skew Laws, and the Differential Pricing of Individual Equity Options,” *Review of Financial Studies*, 16(1), 101–143.
- BANSAL, R., D. KIKU, AND A. YARON (2012): “An Empirical Evaluation of the Long-Run Risks Model for Asset Prices,” *Critical Finance Review*, 1(1), 183–221.
- BANSAL, R., AND A. YARON (2004): “Risks for the Long Run: A Potential Resolution of Asset Pricing Puzzles,” *Journal of Finance*, 57(4), 1481–1509.
- BARNDORFF-NIELSEN, O. E., P. R. HANSEN, A. LUNDE, AND N. SHEPHARD (2008): “Designing Realized Kernels to Measure the Ex Post Variation of Equity Prices in the Presence of Noise,” *Econometrica*, 76(6), 1481–1536.

- BARRO, R. J. (2006): "Rare disasters and asset markets in the twentieth century," *Quarterly Journal of Economics*, 121(3), 823–866.
- BARRO, R. J., AND J. F. URSUA (2008): "Macroeconomic crises since 1870," *Brookings Papers on Economic Activity*, p. 255–335.
- BEELER, J., AND J. Y. CAMPBELL (2012): "The Long-Run Risks Model and Aggregate Asset Prices: An Empirical Assessment," *Critical Finance Review*, 1(1), 141–182.
- BEKAERT, G., R. J. HODRICK, AND X. ZHANG (2012): "Aggregate Idiosyncratic Volatility," *Journal of Financial and Quantitative Analysis*, 47(6), 1155–1185.
- BENZONI, L., P. COLLIN-DUFRESNE, AND R. S. GOLDSTEIN (2007): "Portfolio Choice over the Life-Cycle When the Stock and Labor Markets are Cointegrated," *Journal of Finance*, 62(5), 2123–2167.
- (2011): "Explaining Asset Pricing Puzzles Associated with the 1987 Market Crash," *Journal of Financial Economics*, 101, 552–573.
- BLACK, F. (1976): "Studies in Stock Price Volatility Changes," *Proceedings of the 1976 Business Meeting of the Business and Economics Statistics Section, American Statistical Association*, pp. 177 – 181.
- BOGUTH, O., AND L.-A. KUEHN (2013): "Consumption Volatility Risk," *Journal of Finance*, forthcoming.
- BOLLERSLEV, T., G. TAUCHEN, AND H. ZHOU (2009): "Expected Stock Returns and Variance Risk Premia," *Review of Financial Studies*, (11), 4464–4492.
- BOLLERSLEV, T., AND V. TODOROV (2011): "Tails, Fears, and Risk Premia," *Journal of Finance*, 66(6), 2165–2211.
- BONOMO, M., R. GARCIA, N. MEDDAHI, AND R. TEDONGAP (2011): "Generalized Disappointment Aversion, Long-run Volatility Risk, and Asset Prices," *Review of Financial Studies*, 24(1), 82–122.
- BRANDT, M. W., A. BRAV, J. R. GRAHAM, AND A. KUMAR (2009): "The Idiosyncratic Volatility Puzzle: Time Trend or Speculative Episodes?," *Review of Financial Studies*, 23(2), 863–899.
- BREEDEN, D., AND R. H. LITZENBERGER (1978): "State Contingent Prices Implicit in option Prices," *Journal of Business*, 51(4), 3–24.
- BRITTEN-JONES, M., AND A. NEUBERGER (2000): "Option Prices, Implied Price Processes, and Stochastic Volatility," *Journal of Finance*, 55(2), 839–866.
- CALVET, L. E., AND A. J. FISHER (2001): "Forecasting Multifractal Volatility," *Journal of Financial Econometrics*, 105, 27–58.

- (2004): “How to Forecast Long-Run Volatility: Regime Switching and the Estimation of Multifractal Processes,” *Journal of Financial Econometrics*, 2(1), 49–83.
- (2007): “Multifrequency News and Stock Returns,” *Journal of Financial Economics*, 86, 178–212.
- CAMPANALE, C., R. CASTRO, AND G. L. CLEMENTI (2010): “Asset Pricing in a Production Economy with Chew-Dekel Preferences,” *Review of Economic Dynamics*, 13, 379–402.
- CAMPBELL, J. Y., J. F. COCCO, F. J. GOMES, AND P. J. MAENHOUT (2001): “Investing Retirement Wealth: A Life-Cycle Model,” in *Risk Aspects of Investment-Based Social Security Reform*, ed. by J. F. Campbell, and M. Feldstein. University of Chicago Press.
- CAMPBELL, J. Y., AND L. HENTSCHEL (1992): “No News is Good News: An Asymmetric Model of Changing Volatility in Stock Returns,” *Journal of Financial Economics*, 31(3), 281 – 318.
- CAMPBELL, J. Y., M. LETTAU, B. G. MALKIEL, AND Y. XU (2001): “Have Individual Stocks Become More Volatile? An Empirical Exploration of Idiosyncratic Risk,” *Journal of Finance*, 56(1), 1–43.
- CAO, J., AND B. HAN (2013): “Cross Section of Option Returns and Idiosyncratic Stock Volatility,” *Journal of Financial Economics*, 108, 231–249.
- CARR, P., AND L. WU (2003): “The Finite Moment Log Stable Process and Option Pricing,” *Journal of Finance*, 58(2), 753–777.
- (2009): “Variance Risk Premiums,” *Review of Financial Studies*, 22, 1311–1341.
- CHACKO, G., AND L. M. VICEIRA (2005): “Dynamic Consumption and Portfolio Choice with Stochastic Volatility in Incomplete Markets,” *Review of Financial Studies*, 18(4), 1369–1402.
- CHRISTOFFERSEN, P., B. FEUNOU, K. JACOBS, AND N. MEDDAHI (2013): “The Economic Value of Realized Volatility: Using High-Frequency Returns for Option Valuation,” *Journal of Financial and Quantitative Analysis*, forthcoming.
- CHRISTOFFERSEN, P., M. FOURNIER, AND K. JACOBS (2013): “The Factor Structure in Equity Options,” Working Paper.
- COCCO, J. F., F. J. GOMES, AND P. J. MAENHOUT (2005): “Consumption and Portfolio Choice over the Life Cycle,” *Review of Financial Studies*, 18(2), 491–533.
- COCHRANE, J. (2011): “Presidential Address: Discount Rates,” *Journal of Finance*, 66(4), 1047–1108.

- COVAL, J. D., AND T. SHUMWAY (2001): "Expected Option Returns," *Journal of Finance*, 56(3), 983–1009.
- DAVIS, S. J., AND P. WILLEN (2000a): "Occupation-level income shocks and asset returns: their covariance and implications for portfolio choice," *NBER Working Paper*.
- (2000b): "Using Financial Assets to Hedge Labor Income Risk: Estimating the Benefits," *Working Paper*.
- DEW-BECKER, I., S. GIGLIO, A. LE, AND M. RODRIQUEZ (2013): "The Term Structure of the Variance Risk Premium and Investor Preferences," *Working Paper*.
- DING, Z., C. W. J. GRANGER, AND F. ENGLE, ROBERT (1993): "A Long Memory Property of Stock Market Returns and a New Model," *Journal of Empirical Finance*, 1.
- DRECHSLER, I. (2013): "Uncertainty, Time-Varying Fear, and Asset Prices," *Journal of Finance*, forthcoming.
- DRECHSLER, I., AND A. YARON (2011): "What's Vol Got to Do with It," *Review of Financial Studies*, 24.
- DRIESSEN, J., P. J. MAENHOUT, AND G. VILKOV (2009): "The Price of Correlation Risk: Evidence from Equity Options," *Journal of Finance*, 64(3), 1377–1406.
- DU, D. (2011): "General Equilibrium Pricing of Options with Habit Formation and Event Risks," *Journal of Financial Economics*, 99, 400–426.
- DUAN, J.-C., AND J. WEI (2008): "Systematic Risk and the Price Structure of Individual Equity Options," *Review of Financial Studies*, 22(5), 1981–2006.
- EPSTEIN, L. G., AND S. E. ZIN (1989): "Substitution, Risk Aversion, and the Temporal Behavior of Consumption and Asset Returns: A Theoretical Framework," *Econometrica*, 57(4), 937–969.
- (2001): "The Independence Axiom and Asset Returns," *Journal of Empirical Finance*, 8, 537–572.
- FAMA, E. F., AND K. R. FRENCH (1993): "Common Risk Factors in the Returns on Stocks and Bonds," *Journal of Financial Economics*, 33(1), 3–56.
- FLEMING, J., C. KIRBY, AND B. OSTDIEK (2001): "The Economic Value of Volatility Timing," *Journal of Finance*, 56(1), 329 – 352.
- (2003): "The Economic Value of Volatility Timing Using "Realized" Volatility," *Journal of Financial Economics*, 67(3), 473 – 509.
- FORESI, S., AND L. WU (2005): "Crash-O-Phobia: A Domestic Fear or a Worldwide Concern?," *Journal of Derivatives*, pp. 8–21.

- FRENCH, K. R., W. G. SCHWERT, AND R. F. STAMBAUGH (1987): “Expected Stock Returns and Volatility,” *Journal of Financial Economics*, 19, 3 – 29.
- FU, F. (2009): “Idiosyncratic Risk and the Cross-Section of Expected Stock Returns,” *Journal of Financial Economics*, 91, 24–37.
- GOMES, F. J., AND A. MICHAELIDES (2005): “Optimal Life-cycle Asset Allocation: Understanding the Empirical Evidence,” *Journal of Finance*, 60(2), 869–904.
- GOURINCHAS, P.-O., AND J. A. PARKER (2002): “Consumption over the Life Cycle,” *Econometrica*, 70(1), 47–89.
- GOYAL, A., AND A. SARETTO (2009): “Cross-Section of Pption Returns and Volatility,” *Journal of Financial Economics*, 94, 310–326.
- GUL, F. (1991): “A Theory of Disappointment Aversion,” *Econometrica*, 59(3), 667–686.
- GUVENEN, F., S. OZKAN, AND J. SONG (2013): “The Nature of Countercyclical Income Risk,” *Working Paper*.
- HANSEN, P. R., Z. HUANG, AND H. SHEK, HOWARD (2012): “Reaalized GARCH: A Joint Model for Returns and Realized Measures of Volatility,” *Journal of Applied Econometrics*, 27, 877–906.
- HERSKOVIC, B., B. KELLY, H. LUSTIG, AND S. VAN NIEUWERBURGH (2014): “The Common Factor in Idiosyncratic Volatility,” *Working Paper*.
- JIANG, G., AND Y. TIAN (2005): “The Model-Free Implied Volatility and Its Information Content,” *Review of Financial Studies*, 18, 1305–1342.
- KOIJEN, R. S. J., T. E. NIJMAN, AND B. J. M. WERKER (2010): “When Can Life Cycle Investors Benefit from Time-Varying Bond Risk Premia?,” *Review of Financial Studies*, 23(2), 741–780.
- KOOPMAN, S. J., AND M. SCHARTH (2013): “The Analysis of Stochastic Volatility in the Presence of Daily Realized Measures,” *Journal of Financial Econometrics*, 11(1), 76–115.
- LETTAU, M., AND S. LUDVIGSON (2001): “Consumption, Aggregate Wealth, and Expected Stock Returns,” *Journal of Finance*, 56(3), 815–849.
- LIU, J. (2007): “Portfolio Selection in Stochastic Environments,” *Review of Financial Studies*, 20(1), 1–39.
- LUCAS, R. E. J. (1987): *Models of Business Cycles*. Basil Blackwell, New York.
- LYNCH, A. W., AND S. TAN (2011): “Labor Income Dynamics at Business-Cycle Frequencies: Implications for Portfolio Choice,” *Journal of Financial Economics*, 101(2), 333 – 359.

- MARTIN, I. (2013): “Simple Variance Swaps,” Working Paper.
- NAKAMURA, E., D. SERGEYEV, AND J. STEINSSON (2012): “Growth-rate and Uncertainty Shocks in Consumption: Cross-Country Evidence,” Working Paper.
- NEWBY, W. K., AND K. D. WEST (1987): “A Simple, Positive Semi-definite, Heteroskedasticity and Autocorrelation Consistent Covariance Matrix,” *Econometrica*, 55(3), 703–708.
- RIETZ, T. A. (1988): “The Equity Risk Premium: A Solution,” *Journal of Monetary Economics*, 22, 117–131.
- ROUTLEDGE, B. R., AND S. E. ZIN (2010): “Generalized Disappointment Aversion and Asset Prices,” *Journal of Finance*, 65(4), 1303–1332.
- ROUWENHORST, K. G. (1995): “Asset Pricing Implications of Equilibrium Business Cycle Models,” in *Frontiers of Business Cycle Research*, ed. by T. F. Cooley, pp. 294–330. Princeton University Press, Princeton, NJ.
- SCHREINDORFER, D. (2013): “Tails, Fears, and Equilibrium Option Prices,” Working Paper.
- SEO, S. B., AND J. A. WACHTER (2013): “Option Prices in a Model with Stochastic Disaster Risk,” Working Paper.
- SHALIASTOVICH, I. (2009): “Learning, Confidence, and Option prices,” Working Paper.
- TAMONI, A. (2011): “The Multi-horizon Dynamics of Risk and Return,” Working Paper.
- VICEIRA, L. M. (2001): “Optimal portfolio choice for long-horizon investors with non-tradable labor income,” *Journal of Finance*, 56(2), 433–470.
- WACHTER, J. A., AND M. YOGO (2010): “Why Do Household Portfolio Shares Rise in Wealth?,” *Review of Financial Studies*, 23(11), 3929–3965.
- WORKING, H. (1960): “Note on the Correlation of First Differences of Aggregates in a Random Chain,” *Econometrica*, 28, 916–918.